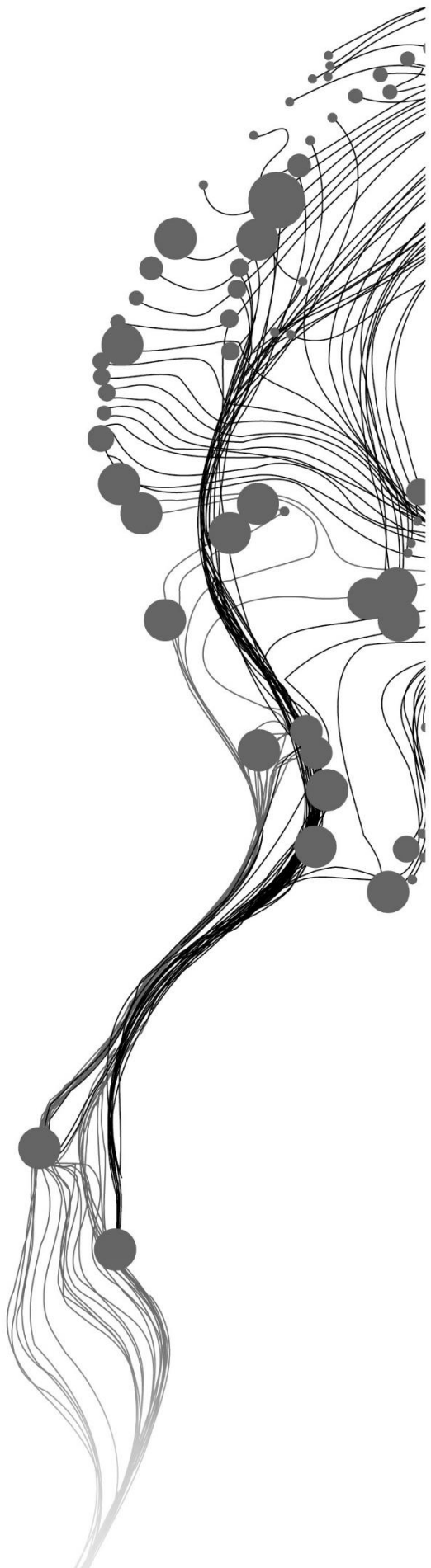


ANALYSING CHANGING MULTI- HAZARD RISK TO FLOW-LIKE PHENOMENA FOR URBAN PLANNING

FELIPE AUGUSTO FONSECA AREVALO
February, 2019

SUPERVISORS:
Dr, C.V, Westen
Drs, N.C, Kingma



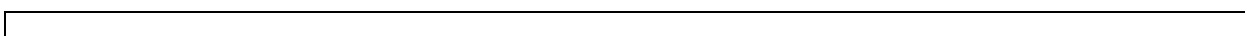
ANALYSING CHANGING MULTI- HAZARD RISK ASSOCIATED TO FLOW-LIKE PHENOMENA FOR URBAN PLANNING

FELIPE AUGUSTO FONSECA AREVALO
Enschede, The Netherlands, February, 2019

Thesis submitted to the Faculty of Geo-Information Science and Earth Observation of the University of Twente in partial fulfilment of the requirements for the degree of Master of Science in Geo-information Science and Earth Observation.
Specialization: Applied Earth Sciences

SUPERVISORS:
Dr, C.V, Westen
Drs, N.C, Kingma

THESIS ASSESSMENT BOARD:
Prof. Dr, V.G, Jetten (Chair]
Dr, Rens van Beek (External Examiner, Utrecht University)



DISCLAIMER

This document describes work undertaken as part of a programme of study at the Faculty of Geo-Information Science and Earth Observation of the University of Twente. All views and opinions expressed therein remain the sole responsibility of the author and do not necessarily represent those of the Faculty.

ABSTRACT

Static behaviour is not a common characteristic of society and nature. Society expands, contracts or migrates, interacting with a highly dynamic natural environment. In many occasions, these interactions help communities to thrive, but others can bring adverse outcomes. One of these outcomes is the exposure to natural hazards and the potential of loss of human life and societal assets. This potential of loss or risk as well changes as human development continues and as the natural environment changes due to the intense human intervention which leads to an intensification of the hazards.

Different works have been undertaken that try to understand and quantify the consequences of the occurrence of natural hazards on exposed communities. Some of these works aim to characterise each of the intervening risk components, which are the hazard, the vulnerability and the amount of exposed elements-at-risk. Others analyse the present risk for individual hazards or multiple hazards. However, few integrative studies analyse the variation of risk in time as a function of the societal transformations and the environmental changes related to climate change in the generation of hazards.

The objective of this research was to study how the risk to floods and debris flows might change in future due to climate change and urban growth in the urban area of Envigado, part of the Aburra Valley in Colombia. The economic risk to buildings was calculated for the present situation and for two future scenarios for the year 2050. Also, several risk reduction alternatives were evaluated and their behaviour under the various scenarios was compared, in order to determine the most change-proof alternative. This significance of this work lies on the supply to decision makers of information about the future consequences related to current decision options, and their economic feasibility.

To undertake this work a methodology was developed that consisted of a number of components. First, the flood and debris flow hazard were modelled, using the innovative multi-hazard tool OpenLISEM, which required extensive parametrization and calibration. Flood and debris flow depth maps were simulated for four return periods. Building footprints were characterized according to use, value, number of floors and people. Absolute physical vulnerability curves were generated for flood and debris flows, using content damage, structural damage, clean-up costs and damage to underground garages. The hazard intensities, the exposed building footprints and their vulnerabilities were integrated with an automated script in GIS to obtain losses for each return period and hazard type. The risk was subsequently calculated by integrating losses for all hazard types and return periods.

To capture the possible future conditions produced by urban growth and climate change two future scenarios were developed, and the changes in building location, building characteristics, and vulnerability were modelled. Climate change projections were used to generate new IDF curves, which served as input for the hazard modelling of the future scenarios. The consequences of these scenarios were determined and planning alternatives were proposed for the risk mitigation. Finally, the changes in future risk were analysed presenting some indicators to help decision-makers to visualise which alternatives offered the highest mitigation for a critical scenario of climate change and rapid population growth.

The results indicated that for the particular conditions of the study area, a mountainous environment in Colombia, the highest risk reduction is provided by hazard and vulnerability countermeasures. However, the best performing and economically feasible alternative might be the intervention of the vulnerability if preliminary economic evaluations are taken into account. Measures for hazard reduction showed less significant benefits in the mitigation of the consequences and if they are applied individually might not be cost-effective. However, the proposed alternative is not a final decision, as more emphasis should be given to addressing and quantifying the uncertainties in the process of risk calculation.

Future work needs to focus on the quantification and possible reduction of the epistemic uncertainty during the components of the risk and integrate the results inside a Spatial Decision Support Systems to support better decision making on risk reduction alternatives.

Keywords: multi-hazard; risk; flooding; debris flow; scenarios; risk reduction; alternatives

ACKNOWLEDGEMENTS

Challenges are something that one person undertakes but that cannot be accomplished without the support of many people behind.

First, I would like to thank my parents and brother. Their love and encouragement are my engines.

I would like to thank my supervisors Cees Van Westen and Nanette Kingma for all the knowledge, disposition, time, warmth etc., shared during my whole study period in ITC and during the development of this thesis. I feel privileged to be able to discuss with you whenever it was possible, I have grown a lot by listening to you. As well, I want to thank you in the name of my colleagues and friends of AES. You were atypical always watching for the wellbeing of the students. This attitude helped us to continue in the hard moments and after all, are the ones that remain in memory.

I would like to extend my thanks to the National University of Colombia and the Faculty of Mines-Medellin to support me during the fieldwork in Colombia. Especially to the professor Edier Aristizabal, Maria Isabel Arango, Sandra Lopez and the whole research group of Geohazards your help and willingness to share knowledge made possible to accomplish my work. I had so much fun with you while sharing cycling adventures, speaking about food, Avenidas torrenciales and OpenLisem. Marcius, Fangyu, and my own stay in Medellin was productive for your help.

I want to express my gratitude to Bastian van den Bout for sharing his knowledge and guiding me in the modelling process undertook in this study.

My gratitude to ITC and Colfuturo for sponsoring my studies in the Netherlands.

As well my thankfulness to the professor Manuel Garcia Lopez, Jose Vicente Amortegui and IGL, I enjoy studying natural hazards for your influence.

To my friends of AES Marcius Isip, Mishi Gogo, Vincent Katonda, Mulugueta Dibaba, Ayu Justicea, Kasimir Orłowski, Lilian Kato, Aaron Orr, Jacob and Fernando Brenner I am so thankful with you, we faced together many challenges and most importantly we shared each other view.

Finally, I want to give special thanks to Aiman Shahpurwala, Venus Rodriguez, Gerardo Macedo, Ricardo Morales and Oscar Bautista you have understood, helped and made thrive my work and activities. My stay in ITC has been so pleasant because of your care.

TABLE OF CONTENTS

1.	INTRODUCTION	1
1.1.	Background.....	1
1.2.	Literature review	1
1.3.	Challenges and recent approaches in the study of changing multi-hazard risk	3
1.4.	Research problem and scientific significance	4
1.5.	Objectives	4
1.6.	General methodology	5
2.	STUDY AREA AND DATA COLLECTION.....	7
2.1.	General context.....	7
2.2.	Study area – Municipality of Envigado and the Ayura Catchment (AC)	7
2.3.	The debris flow event of 1988	10
2.4.	Hazard modelling of flow-like phenomena AMVA(2018)	10
2.5.	Available information	10
3.	MULTI-HAZARD MODELLING	12
3.1.	Elaboration of input maps for the multi-hazard model OpenLISEM	12
3.2.	Summary of input maps for OPENLISEM	18
3.3.	Modelling flow-like phenomena (flooding and debris flow) for the present situation	19
3.4.	Modelling Results	20
3.5.	Discussion about hazard modelling	21
4.	ELEMENTS AT RISK AND VULNERABILITY ASSESSMENT	23
4.1.	Elements at risk characterisation	23
4.2.	Attributes of Final EaR database.....	26
4.3.	Characterisation of physical vulnerability of buildings	26
4.4.	Vulnerability results: absolute vulnerability curves.....	30
4.5.	Discussion on the generation of elements at risk and vulnerability data	31
5.	ESTIMATION OF PRESENT RISK	33
5.1.	Methodological approach.....	33
5.2.	Loss assessment and Risk analysis results	35
5.3.	Discussion.....	37
6.	FUTURE SCENARIOS AND PLANNING ALTERNATIVES.....	38
6.1.	Scenario 1 (S1): Rapid population growth and low climate change	39
6.2.	Scenario 2 (S2): Rapid population growth and climate change	41
6.3.	Alternative 0 (A0): No alternative	42
6.4.	Alternative 1 (A1) : Channel intervention.....	42
6.5.	Alternative 2 (A2): Solid load retention measures and slope stability measures	44
6.6.	Alternative 3 (A3): Risk reduction measures – Hydraulic protection for parking places	44
6.7.	Integration of possible future scenarios and planning alternatives	45
6.8.	Discussion.....	45
7.	ANALYSING CHANGING RISK	47
7.1.	Changes in losses for the influence of the scenarios of population growth and climate change	47
7.2.	Changes in risk for the implementation of alternatives	48
7.3.	Loss changes for the influence of the scenarios of population growth and climate change	49
7.4.	The behaviour of alternatives – Risk changes between scenarios	50
7.5.	Best performing alternative for risk reduction in the Ayura catchment (AC).....	51
7.6.	Discussions	51

8. DISCUSSION AND CONCLUSIONS	53
8.1. General discussion on the estimation of risk changes	53
8.2. Conclusions and future work	55
List of references	58

LIST OF FIGURES

Figure 1-1. Methodological flow chart	6
Figure 2-1. Aburra Valley and Municipality of Envigado.....	8
Figure 2-2. Growth of the urban area of Envigado between 1943-2016	8
Figure 2-3. Delimitation of the Ayura catchment (AC) and slope map.....	9
Figure 2-4. Flow-like phenomena for a precipitation of 500 years return period AMVA(2018).	10
Figure 2-5. 3D View of the Ayura catchment.	11
Figure 3-1. Obstruction caused by the presence of a concrete slab under bridges inside the channel of the Ayura stream....	12
Figure 3-2. Soil depths models produced by AMVA(2018) (left) and the present research (right).....	15
Figure 3-3. Compound DTM and Lisem channel	17
Figure 3-4. IDF curves for the Ayura catchment for the present situation for different return periods (Left) and an example of a synthetic rain event with 100 years return period (right).....	17
Figure 3-5. Pseudo ground water modelled to calculate initial soil moisture.	18
Figure 3-6. Modelled debris flow depth for an event with a Return Period of 25 years in the area of Rosellon.....	20
Figure 3-7. Hazard footprint in the urban area of the AC. (Left) water/ sediment height for return period of 25 years. (Right) water/ sediment height for the return period of 200 years.	21
Figure 3-8 Comparison of flooding footprints by AMVA(2018) (Left) and OpenLISEM (right) for the return period of 25 years. In the red circles are some of the points that were used in the attempt to calibrate the OpenLISEM model.....	22
Figure 4-1 Schematic representation of the building types and the reasons for their classification in relation to the risk assessment of floods and debris flows.	24
Figure 4-2 Final EaR database configuration.....	26
Figure 4-3. Relative vulnerability curves for flooding for residential use and other building uses.....	28
Figure 4-4. Typical material deposited in the Event of 1988 - Source: (AMVA, 2018).....	28
Figure 4-5. Vulnerability curves for buildings between for low-rise buildings (Ciurean et al., 2017).....	28
Figure 4-6. Graphical representation of the absolute vulnerability curve for medium-rise commercial buildings.....	30
Figure 5-1 Flowchart process implemented to calculate losses and risk for multi-hazards	34
Figure 5-2. Losses in the area of the hospital of Envigado for flow-like phenomena in the return periods of 25 and 200 years. The	35
Figure 5-3. Risk curves for flow-like phenomena in the present situation.....	36
Figure 5-4. Losses for flood and debris flood occurring simultaneously for the present situation in the return period 25 and 200 years.....	36
Figure 6-1. Scenarios and planning alternatives for risk reduction.....	38
Figure 6-2 Interaction between global scenarios and alternatives in the change of future impacts	39
Figure 6-3 Precipitation trend graph produced by climate change by AMVA(2018).....	41
Figure 6-4 IDF curve produced for climate change in the AC.....	41
Figure 6-5 (left) Percentage of change in flow height between 2018 and 2050 for the action of climate change.....	42
Figure 6-6 Channel improvement in the area of the Hospital of Envigado.	43
Figure 6-7 Flow depth reduction rate for the implementation for channel improvement. Return period of hazard: 25 years under climate change.....	43
Figure 6-8 Example of retention structures. Retention net of high resistance for the capture of solid load.....	44
Figure 6-9. Example of protection system to seal off underground garage entrance to avoid flooding.....	44
Figure 6-10. Debris flow height before and after the implementation the sediment retention structure.....	46
Figure 7-1. Loss curve for the present situation (S0) and for future scenarios: population growth and low climate change(S1) and for population growth and climate change (S2).....	47
Figure 7-2. Risk reduction of risk reduction measures in present scenario(2018)	48

Figure 7-3. Risk reduction of risk reduction measures for population growth and low climate change (2050)	48
Figure 7-4 Risk reduction of risk reduction measures for population growth and climate change (2050).....	49
Figure 7-5. Reduction of the losses in the scenarios(S0) and the future scenario with climate change (S2) for the implementation of planning alternatives.	49
Figure 7-6 Loss reduction (change) for the introduction of the combination of alternatives in the scenario of climate change and return period of 25 years.	50
Figure 7-7 Changing in the behaviour of the alternatives by scenario	51
Figure 8-1. Conceptualisation of the integration of the risk results inside Spatial Decision Support systems	57

LIST OF TABLES

Table 2-1. Data collected during fieldwork.....	11
Table 3-1. Geotechnical parameter of soils in the Ayura catchment	13
Table 3-2. Final soil parameters considered in this research	14
Table 3-3. Main Input maps for OPENLISEM used to model the multi-hazard condition in the Ayura Catchment...	19
Table 3-4. Discharges from AMVA(2018) and probable discharges of OPENLISEM	20
Table 4-1. Estimation of the number of people per building type (assuming they are in buildings with Residential or Heath land use type) for a night-time scenario in the present situation.	25
Table 4-3. Possible damage to contents by water-debris heights in residential areas.....	27
Table 4-2. Assumed average content for a residence of 100 m ²	27
Table 4-4. Example of absolute vulnerability curve for medium-rise commercial buildings and its parameters.....	30
Table 5-1. Potential losses in the present situation in the Ayura Catchment for flow-like phenomena	35
Table 6-1. Combination of scenarios and alternatives for the AC.....	45
Table 7-1. Average of Annual risk of present and future scenarios in the AC	47
Table 8-1. Summary of main assumptions in the research and their probable effects on risk.	54

LIST OF ANNEXES

<i>Annex 1. Map indicating the possible footprint for the event of 1988 in The Ayura catchment</i>	65
<i>Annex 2. Anaglyph map of the Ayura catchment with detail in of new and old fan</i>	66
<i>Annex 3. Monthly multi-year precipitation of the Ayura Catchment</i>	67
<i>Annex 4. OpenLISEM Script used to model antecedent rainfall in the Ayura catchment</i>	68
<i>Annex 5 Overview of Hazard maps obtained for different scenarios and alternatives</i>	69
<i>Annex 6. Interface of POP GIS- Micro-spatial tool to distribute population in municipality units to building footprints.</i>	70
<i>Annex 7. Absolute vulnerability tables</i>	71
<i>Annex 8. ILWIS Script for loss calculation in the Ayura catchment</i>	76
<i>Annex 9. ILWIS Script to calculate the risk (Area under the risk curve)</i>	78
<i>Annex 10. Map indicating possible areas that have changed for scenario 1, including densification area and urban expansion areas.</i>	79
<i>Annex 11. Map indicating the channel intervention</i>	80
<i>Annex 12. Maps indicating changes in losses between scenarios(S0,S1,S2) for the occurrence of multi-hazards in the return period of 25 years and aggregated by administrative units</i>	81
<i>Annex 13. Cost-Benefit Analysis</i>	82

1. INTRODUCTION

1.1. Background

Natural hazards often do not occur in isolation; they are part of the same overall natural system (or geosystem) in which interactions between the hazards are the rule and not the exception (Kappes et al., 2010). In mountainous environments, various hydro-meteorological hazards can be simultaneously triggered by extreme rainfall (Chen et al., 2016). Landslides and flooding can combine generating higher destruction than when they occur independently. This is the case in Latin America where the high mortality risk for multiple hazards is a trend (Dilley et al., 2005; Shi et al., 2016), e.g. as evidenced by the 2017 Mocoa disaster, and the 2019 Brumadinho dam failure in Brazil that killed hundreds of people.

Population and economic risks will increase based on factors such as climate change and urban expansion (Newman et al., 2017). Climate change will affect the frequency, magnitude and spatial extent of hazards (Gallina et al., 2016; Schmidt-Thomé, 2006), while urban developments will increase the exposure of goods and people, which in turn affects the hazard levels (linked to modifications of land cover).

To address these growing risk scenarios, one of the aims of the Sendai Framework is to improve the understanding of the risk with a multi-hazard approach (UNISDR, 2015). As mentioned by the ADB (Asian Development Bank) (2018), extensive knowledge of disaster risk is crucial to its treatment. For example, the awareness that risk is not static, neither temporally nor spatially, will allow to scientist and decision makers to plan and prepare better for future challenges.

The risk management cycle is a comprehensive tool to contribute to Sendai's aim. This cycle allows to methodically characterize and treat the risk by following different stages: 1) Risk analysis, used to estimate the overall risk by identifying and characterizing the hazards, the elements at risk (EaR) and vulnerabilities; 2) Risk assessment, used in the evaluation of risk tolerability; and 3) Risk management, intended to propose actions (structural and non-structural) in case the risk is not tolerable (Australian Geomechanics Society, 2000 and Fell et al., 2008). As a result, improved mitigation, preparation and response before the occurrence of a hazardous event is promoted (Greiving & Fleischhauer, 2006).

Focusing on the first stage, the Risk Analysis (either quantitative or qualitative) provides an idea of potential losses for the impact of hazards allowing to act before. To achieve this, methods such as Quantitative Risk Assessment (QRA) are generally used. QRA quantitatively characterizes and connects hazards, vulnerabilities and elements at risks (EaR) to obtain the consequences related to an event exposure (Fell et al., 2005).

Corominas et al., (2014) state that one of the key characteristics of the QRA is that it expresses the risk in common units, generally monetary values, casualties etc. This provides the QRA with an important coherency because it facilitates the reproducibility of the analysis by another scientist and the comparability of the results. For example, by using Geographic information systems (GIS) it is possible to locally calculate the risk of different scenarios and alternatives, which can be used to prioritize or to allocate resources to for consequence reduction in specific areas (Ferlisi, De Chiara & Cascini, 2016). Therefore QRAs can be guides of decision making. Planners can use the QRA to evaluate the risk of possible future planning alternatives such as land use modifications and/or implementation of risk reduction measures (a concept coined by Greiving & Fleischhauer, 2006). Moreover, the results of the QRA can be used as indicators inside spatial decision support systems (SDSS). The number of casualties and the number of losses from QRA can be incorporated in SDSSs to evaluate the trade-offs of different planning alternatives in future (Krol, et al., 2016). In this way, more cost-effective solutions can be proposed and implemented.

1.2. Literature review

To make use of the QRA and SDSS in the evaluation of risk, it is necessary to deepen in the concept of multi-hazards itself. A better understanding of multi-hazards will help to visualize the changes in risk that

will be increased for more dynamic interactions related to the effects of climate change and population growth.

1.2.1. Multi-hazard risk concept

With a few publications on this topic before 2000, the study of multi-hazard (MH) is still in its early stages, the reason for which different definitions have been proposed (Liu, Ling, & Gordon, 2017). In an initial stage, the definition of MH followed the conception of Hewitt and Burton (1971), that is to say, all hazards affecting one place. This derived, according to Gill & Malamud (2014) and (Kappes et al., 2012), in the understanding of MH as the independent analysis of spatially coincident hazards in one area, as known as multi-layer single hazard.

However, given that hazard interactions, as mentioned by Kappes et al., (2012), can lead to unexpected behaviours and intensified consequences, a more comprehensive and holistic approaches are necessary. In this way, a so-called multi-hazard risk (MHR) concept appears, as a second stage in the treatment and understanding of hazards. This emphasises in the importance to analyse hazards under a risk perspective with the aim to make comparable the effects of different phenomena that interrelate and interact dynamically.

Some examples of developments that have tried to approach the concept MHR are the multi-risk tools. Among representative ones, one can find HAZUS, CAPRA, RiskScape, ARMAGEDDON (van Westen, 2016). For instance, the CAPRA tool uses separate modules to calculate the hazards (e.g. landslides, earthquake, hurricanes, flooding and others) whose maps are combined, subsequently, in a stand-alone GIS platform. Then a probabilistic risk analysis is performed obtaining annual economic loss and maximum probabilistic loss (Universidad de los Andes, 2018).

In general, the problem of these multi-risk tools is that although they obtain a combined risk, the hazard is still analysed with a multi-layer approach or only one hazard interaction as the domino effect (Gallina et al., 2016; Liu et al., 2017). The former two points are bottlenecks that are related to the multiple interpretations that MHR has received (Gill & Malamud, 2014) and the complexity of modelling different multi-hazard interactions (Chen et al., 2016).

To enhance the understanding of the concept of MHR (third stage), Gill & Malamud (2014; 2017), took the initial concepts of MH and the challenges for the study of MHR expressed by Kappes et al., (2012) to propose a framework that made a transition between multi-layer hazard to fully assess MHR. This framework requires accomplishment of the following 4 components: 1) the identification of all individual hazards in an area; 2) the identification of all possible interactions; 3) the study of the temporal and spatial coincidence of different hazards in terms of the possible enhanced hazard impacts 4) the consideration of in terms of vulnerability variation after a multi-hazard shock.

Focusing on these interacting components, different authors proposed distinct classifications (Gill & Malamud, 2016; Liu et al., 2017; van Westen et al., 2014). From these some important interactions can be highlighted: 1) *Independent relationship*: hazards are triggered by a not apparent common factor (e.g. storm and earthquake) and do not have spatial or temporal interactions 2) *Triggering relationship (coupled/parallel events)*: different hazards are triggered by the same event and these induced hazards can combine (e.g. high precipitation generating landslides and flooding, which can combine in debris flow); 3) *Interactions where probability of hazards is either decreased or increased*: the occurrence of a primary hazard can alter the frequency of occurrence of a secondary hazard or modify the environmental conditions that will trigger a secondary hazard (e.g. the fire-flood cycle in debris and flash flood production according to Cannon & DeGraff (2009)). 4) *Chain or domino interactions*: one hazard triggers the others in sequence (e.g. an earthquake triggering landslides which can dam rivers with a possible formation of avalanches or debris flows if the dam breaks).

1.2.2. Example of coupled events: flow-like phenomena

Multi-hazards examples with coupled interactions are the so-called flow-like phenomena. They can be interpreted in different ways. One of the most accepted understandings is that when soil masses move rapidly flow-like behaviours can be classified as a landslide (e.g. Varnes, 1978; Cruden & Varnes, 1996; Hutchinson, 1988). However, as mentioned by Hungr et al., (2001) different ambiguities appear in the use of the term “flow-like” to try to describe different processes (e.g. creep, earth flows). As consequence, complications occur at the level of decision making: should flow-like phenomena managed as landslides, as water flow or a combination of both?

To help in the understanding of the concept of flow-like phenomena, considering the scale might be an alternative tool. While at very site-specific scale classic classifications can give a good characterization for a mass movement, at the level of the catchment some mass movements can be understood as coupled events (e.g. debris flow). In this way, flow-like phenomena can be seen as soil moving mass and high flowing water, triggered by the same precipitation event, that can combine in different proportions in a channel to the extent that the behaviour of each other changes into as a viscous mass.

One classification for flow-like phenomena that suits the above definition was proposed by Costa (1988) and used by De Chiara (2013). This classification considered rheological, geomorphological and sedimentological factors. 3 categories can be defined: water flood, hyperconcentrated flows and debris flows.

According to De Chiara (2013), based on Coussot & Meunier (1996), hyperconcentrated flows are two-phase flows of water and sediments produced mostly from the erosion of hillslopes and channels. The solid concentration ranges from 20-47% and the behaviour is controlled by the fine material. When the concentration of sediment is low the flow is Newtonian, and the phenomena can be considered a water flow (Costa, 1988). Hyper-concentrated flows usually occur during intense rainstorms. One type of hyperconcentrated flows is also known as debris flood, which transport massively sediments (O. Hungr et al., 2001). On the other hand, as mentioned by Hungr et al., (2015), debris flows are considered as rapid pulsing surges of heavily charged debris that travel long distances in a viscous water mass. Although, debris flows can occur simultaneously with floods, the proportion of debris (from clay to boulders) can reach 70-90% of the concentration (Costa, 1988). In many occasions, the initial soil volume in the source areas (generally from clusters of shallow landslides) is immensely surpassed by the material entrained during the displacement of a debris flows and deposited on fans. In other occasions, because of natural slope changes, debris flows can deposit a considerable part of the solid fraction along the path. In this occasion, the remaining loaded fluid continues as a debris flood (O. Hungr et al., 2001).

1.2.3. Modelling multi-hazards interactions

As already mentioned, one of the bottlenecks in the evaluation of hazard interactions is the complexity of their modelling. This has diffculted the evaluation of the multi-hazard risk in an area because of the possible enhanced intensities and the spatial hazards extents that interaction can produce (van Westen et al., 2014).

Some advances have been done in the physical modelling of coupled hazards in mountainous environments. Most of these advances are related to the use of analytical models, based on hydromechanics, for the simulation of the run-out of processes such as debris flow. This run-out can be used to evaluate the spatial extent of interacting hazards for the application of QRA (Quan et al., 2014).

Nonetheless, one inconvenient of the run-out models is that they do not simulate simultaneously the hydrological processes and the occurrence of landslides, being solids integrated as an input in later stages. To overcome this problem, Bout et al., (2018) proposed an integrated model capable of modelling rainfall triggered shallow landslides and flooding forming debris flow at catchment level, this based on the generalised two-phase model for debris flow of Pudasaini (1952) and a modified infinite slope model by Bout et al., (2018). This model is known as OPENLISEM for hydrometeorological hazards.

1.3. Challenges and recent approaches in the study of changing multi-hazard risk

According to Newman et al., (2017), most of the risk assessments and SDSSs use the analysis of a single hazard in present situations to propose planning alternatives for risk reduction. In other words, the formulation of solutions, generally, does not consider that the risk changes because the dynamic character of the hazard, of the vulnerability and of the elements at risk. For example, in hazards, external factors such as climate change can increase the frequency and intensity of triggering phenomena as precipitation. This alteration can raise the probability of occurrence of interacting hazards, leading to unexpected and destructive outcomes that the proposed planning alternatives, probably, will not be able to cope with.

For the aforementioned issue, there is a need to produce more quantitative approaches to characterise multi-hazard phenomena (Gill & Malamud, 2016). Some studies that have tried to respond to that need can be found Bell & Glade (2004) and Ferlisi et al., (2016). They used the QRA for the estimation of population risk associated to debris and hyper-concentrated flows using run-out analysis (Quan Luna et al., 2012). Similarly, studies for the definition of planning alternatives in multi-hazard environments such as Narasimhan et al., (2016) and Linnerooth-Bayer et al., (2016) can be a good starting point.

In terms of the study of changes in risk, Newman et al., (2017) highlighted that research is even more limited. One of the few examples was undertaken under a project called CHANGES of the 7th framework programme FP7 of the European Union (CHANGES, 2014). This project focused on the analysis of the variation of the spatial-temporal patterns of hydrometeorological hazards produced by climate and socio-economic changes (van Westen et al., 2014).

Perhaps one of the few comprehensive procedures to address changing multi-hazard risk and planning alternatives is proposed by van Westen & Greiving (2017) this will be a reference for the present research.

1.4. Research problem and scientific significance

Risk changes are a permanent condition of human development produced by variations in the hazard, vulnerability and elements-at-risk. Given that climate change is an imminent threat, and that our society will continue growing economically and spatially, the economic losses and casualties for the occurrence of hazards will rise as well. This will require that society responds with the aim to prevent, mitigate and recover from disasters.

However, on different occasions, the response does not integrate the risk knowledge into planning as a guiding criterion or does not consider that risk is not static. As a result, different solutions either do not maximise the risk reduction or they easily become obsolete in time. Even in some occasions if solutions are not well tailored to the phenomena, they can produce an increase in the risk.

Another problematic, that affects the response, is the potential changing nature of the hazard, In many environments, as in mountainous settings, hazards do not occur in isolation. They can interact changing their basic nature and producing enhanced destruction if they enter in contact with populated areas.

For all the above mentioned, this research presented a QRA for a mountainous urban setting in Latin America. This analysis took into account the changing multi-hazard nature of risk for factors as climate change and population growth and the performance of different alternatives.

This study is significant responds to the need for more quantitative approaches that analyse multi-hazard risk, and provides an approach to evaluate the risk reduction under changing environments. The results of this study can enrich the decision-making process because they aim to go beyond the static risk quantification. Instead they open the window to know how this risk behaves in time. As a consequence, evidence-based decisions can lead to higher benefit.

1.5. Objectives

The aim of the research is to model the dynamic multi-hazard risk within an urbanized watershed using a physically based model for different future scenarios and risk reduction planning alternatives.

Objective 1: To model with a physically-based model the current multi-hazard situation for flow-type phenomena

- How can the model be parametrized to represent the current multi-hazard situation?
- How to develop precipitation scenarios to model the current multi-hazard situation?
- To what extent is it possible to calibrate and validate the model with the available data?

Objective 2: To quantify the economic risk for the current situation

How to characterize the elements at risk for the current situation?

- How to analyse physical vulnerability in a complex urban setting?

Objective 3: To define future changes in the study area and the resulting changes in risk.

- Which possible scenarios of climate change, population change and land use change can be considered for the urban case study area?
- Which future years should be taken to evaluate the changes?
- How to translate the scenarios into changing risk components related to hazards, elements-at-risk and vulnerabilities?

Objective 4: To define possible planning alternatives for risk reduction

- Which type of planning alternatives can be considered and implemented for the particular conditions of the study area?

- How to translate the alternative into changing risk components related to hazards, elements-at-risk and vulnerabilities?

Objective 5: To quantify the risk reduction of planning alternatives

- How does the risk vary between current and future situations using different planning alternatives?

Objective 6: To evaluate the performance of planning alternatives under different future scenarios

- What is the planning alternative with the highest risk reduction?
- Which planning alternatives behaves best under the various future scenarios?
- To what extent the different planning alternatives can be implemented?

1.6. General methodology

The general directions taken for the present work to give an answer to the research questions are illustrated in the methodological flow chart of Figure 1-1. The main goal of this methodology was to study the changes in multi-hazard risk related to 2 components: the effect of different future scenarios (that are not controllable) and of different planning alternatives (which can be selected by the urban authorities). Once these two components were characterised, an evaluation about what alternative reduces the most the risk was done. Additionally, in a preliminary manner the best performing alternatives were evaluated to define which alternative is more economically feasible.

To develop the methodological framework presented in Figure 1-1 the methodology to analyse changing multi-hazard risk by van Westen & Greiving (2017) was adapted. This methodology was further developed in the chapters of this study listed below:

- Chapter 2 presents an overview of the study area with information about its physical and social characteristics.
- Chapter 3 contains the parametrization and calibration of the OpenLISEM model that will be used to evaluate the spatial extent and intensity of the multi-hazards considered for the study area. The chapter also presents a summary of the results for the present situation in the catchment.
- Chapter 4 presents how the information collected in the field was translated into a usable database of elements-at-risk (EaR) with corresponding vulnerabilities for the development of QRA.
- Chapter 5 summarises the procedure and considerations to execute the QRA for multi-hazards for the present situation. Two products are presented and discussed: the losses for the multi-hazard situation for different return periods and the total average annual risk for the study area.
- Chapter 6 contains a description of how future scenarios were constructed and the implementation of planning alternatives for risk reduction in the study area. Their effects in terms of the hazard, the EaR and their vulnerabilities were as well part of the discussion.
- Chapter 7 presents the estimation of risk changes between the present and the future in function of the different scenarios and planning alternatives. Additionally in the annexes, the alternatives with the highest risk reduction were evaluated to define the investment required to guarantee their feasibility using cost-benefit analysis. Further discussions about how to use the risk analysis results and the influence of uncertainty in the estimation of risk were raised.
- Chapter 8. Contains the conclusions and a general discussion of the drawbacks encountered in the study. Recommendations for future work are exposed.

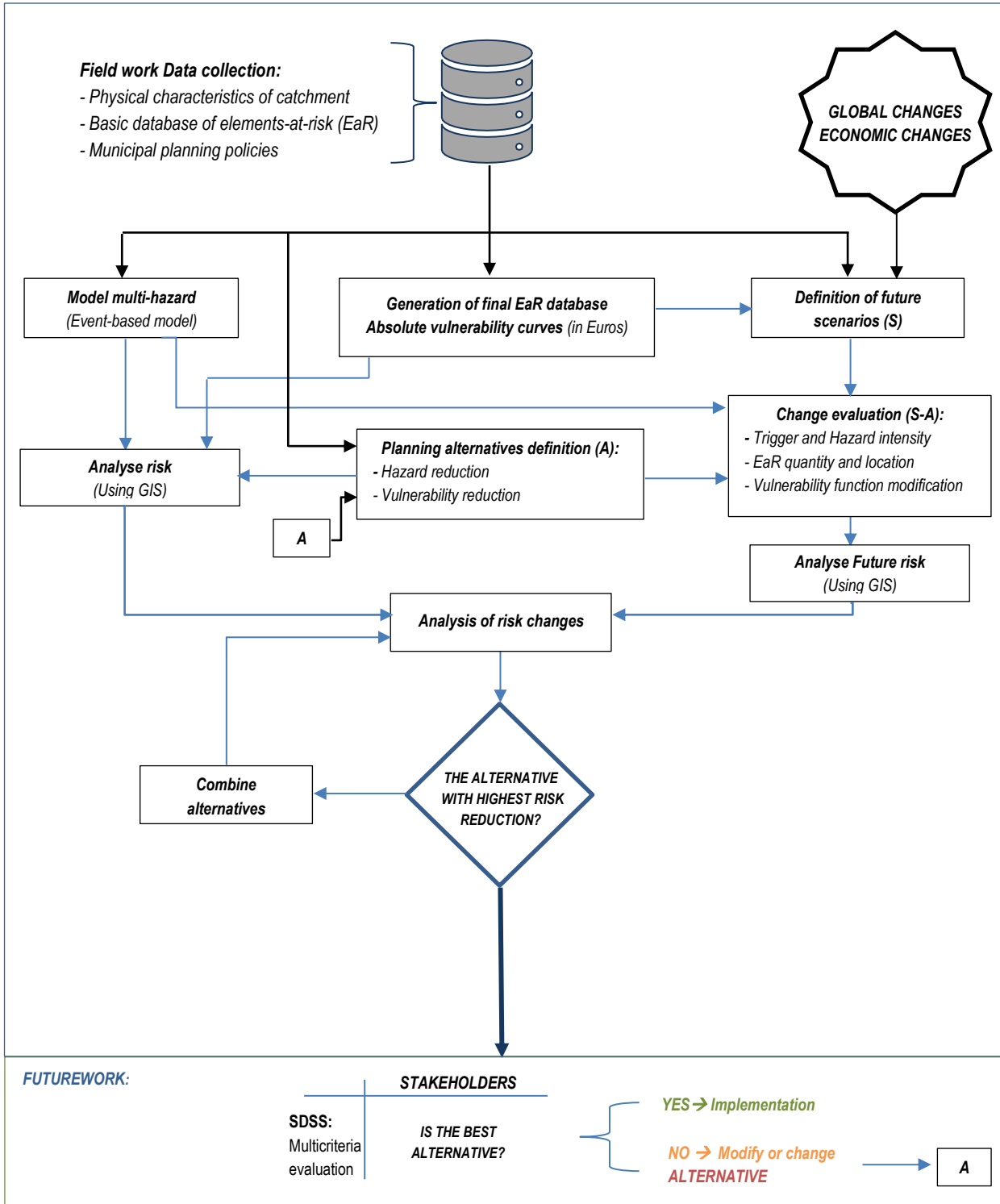


Figure 1-1. Methodological flow chart

2. STUDY AREA AND DATA COLLECTION

In this chapter, the general characteristics of the study area are presented as well as the data collected during the fieldwork. Before introducing the specific study area, the regional setting is discussed. This setting has an important influence in the physical configuration of the catchment analysed and likewise as on the social development issues.

2.1. General context

The study area is located within one of the most populated valleys in Colombia, the so-called Aburra Valley (AV). As stated by Hermelin (2007) and Restrepo (1981), the AV (see Figure 2-1) is a regional river basin with a length of 64 km and a variable width with an average of approximately 9 km. Its lowest point is around 1400 m.a.s.l. and its highest point reaches 3000 m.a.s.l. The mean temperature in the region ranges from 13 to 22°C (depending on the height), and the precipitations vary from 1400 mm/year in the North to 3000 mm/year in the South.

One of the most important characteristics of the AV is that it is surrounded by mountains with complex geology that makes the valley highly prone to mass movements. A wide diversity of geologic units are found such as schist, gneisses, amphibolite, dunites and migmatites (Henaó & Monsalve, 2018), which have been altered by past tectonic activity, weathering and erosive processes producing very extensive slope deposits (Hermelin, 1984; Garcia, 2006). In terms of landslide activity, based on Shlemon (1979), Garcia (2006) pointed out that old mass movement processes might be related to earthquakes, while for recent landslides rainfall and hydrology are the predominant cause.

Different studies have been undertaken in the AV to establish the relation between rainfall and earthquakes with landslides in slope deposits and residual soils. Several studies about the influence of precipitation on landslide occurrence are available. Some examples are Aristizábal, Velez & Martinez (2016) who analysed antecedent rainfall for landslide occurrence, and Aristizabal et al., (2011) who carried out an analysis of rainfall thresholds among others.

Regarding to landslides triggered by earthquakes, the number of studies is limited. This topic is gaining more attention because, although no recent earthquakes are recorded, the AV is inside an intermediate seismic zone. Even the region is located close active fault called the Romeral fault whose activity is linked to the earthquakes of Popayan in 1983 and Armenia in 1999 which are cities located approximately 300km away of the AV.

Because of the setting of the AV, the National University of Colombia, the local government of AV and initiatives as 100 Resilient cities (2016) have collaborated to characterise the potential hazards that can affect the different municipalities of the region. Recently results of this collaboration are the called “Basic hazard studies” for mass movements, flooding and other flow-like phenomena for the different municipalities of the AV (AMVA, 2018). This study not only characterised recurrent hazards like landslides and flooding but as well as interacting hazards such as flow-like phenomena. These interacting phenomena have gained importance because most of the municipalities of the AV have developed on alluvial fan areas of torrential origin, which makes them prone to this kind of events.

2.2. Study area – Municipality of Envigado and the Ayura Catchment (AC)

The AV has 10 municipalities, of which the municipality of Envigado (see Figure 2-1) was selected as a study area for two reasons: 1) the availability of information to undertake physical modelling for multi-hazards and risk and 2) Envigado has the highest population growth rate in the AV (Horbath, 2016).

Although the number of disastrous events involving flow-like phenomena in Envigado is more reduced compared to other municipalities, there is historical evidence of debris flows (e.g. in the year 1988). In addition to that, there is a rapid population growth in this municipality that might lead to high losses in the case extreme events occur. Figure 2-2 gives an impression of the rapid transformation that this area underwent from being a series of rural land parcels in 1943 to a densely occupied area in 2016 that continues growing rapidly.

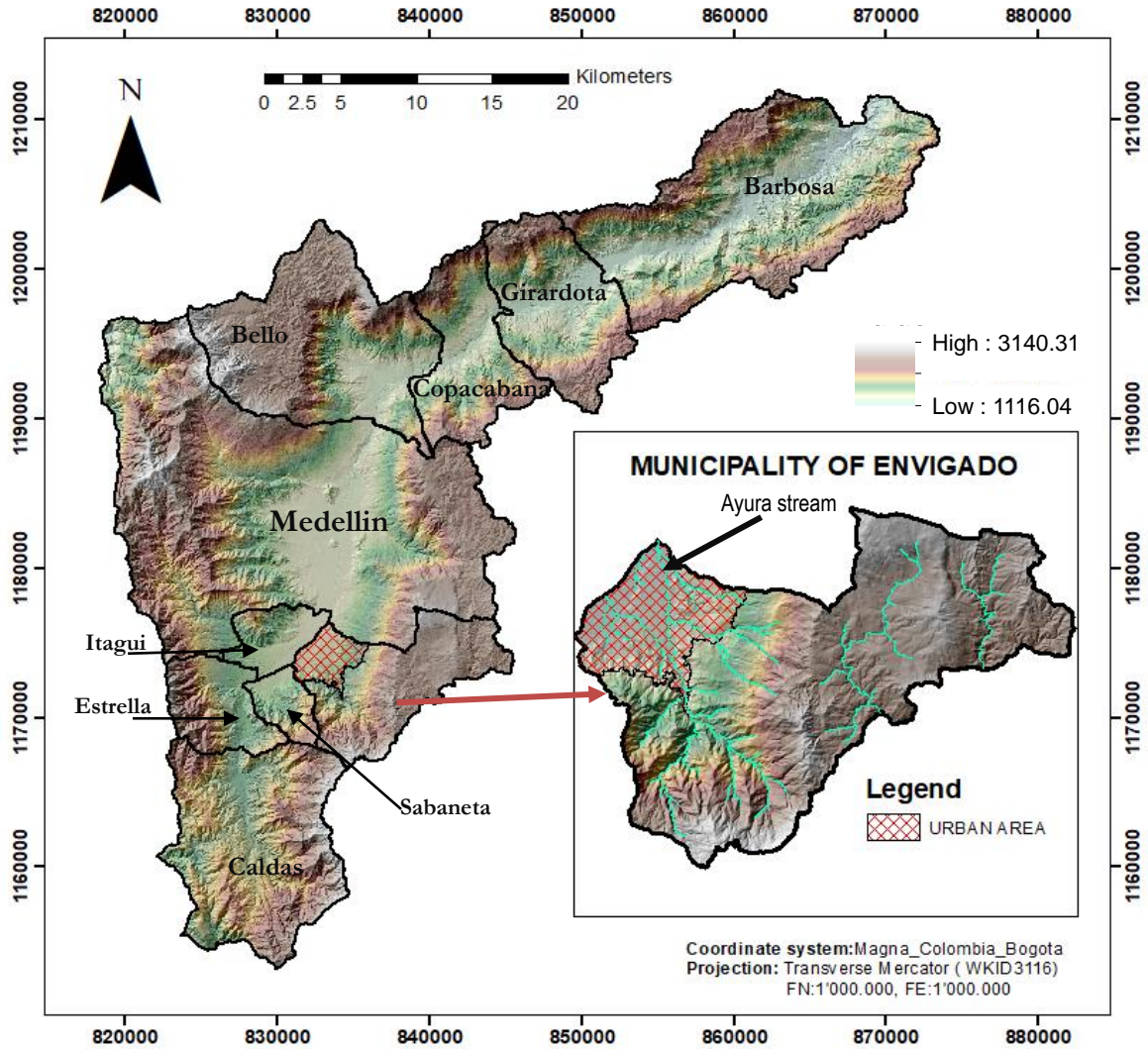


Figure 2-1. Aburra Valley and Municipality of Envigado. In the left a view of the AV with the different municipalities. In the right the municipality of Envigado. Inside Envigado hatched in red colour is presented the urban area.

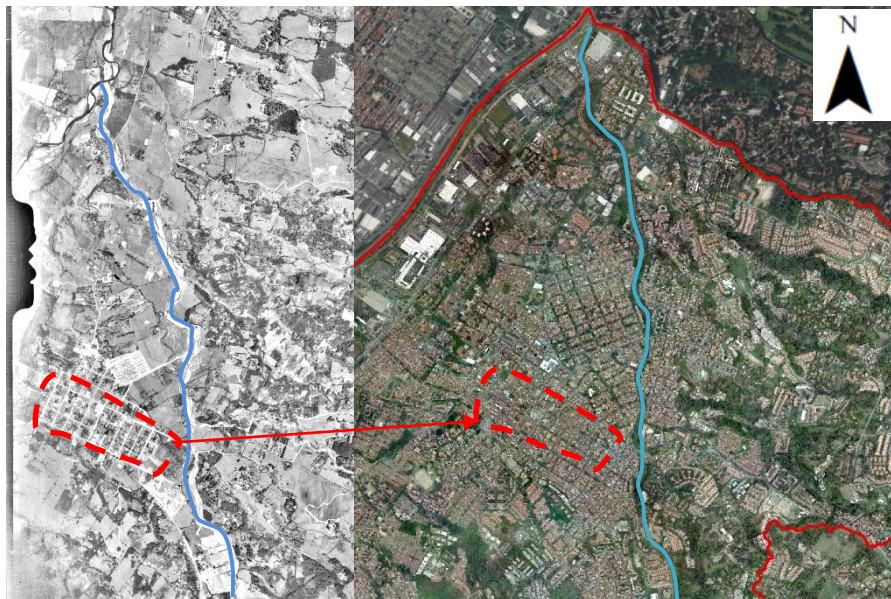


Figure 2-2. Growth of the urban area of Envigado between 1943-2016. In blue the main stream of Envigado the Ayura stream. In red the reference point of expansion

Envigado is connected to the main municipality of the AV called Medellin, the second largest city in Colombia. Located in the south-east of the AV, the municipality has an area of approximately 79 km² with the lowest point at 1550 m.a.s.l. and highest point at 2900 m.a.s.l. (Alcaldía de Envigado, 2018b). The urban centre is located in the lowest zone and has an area 12.2 Km² and an estimated population for 2016 of 219.991 inhabitants (Alcaldía de Envigado, 2018a). The annual precipitation is approximately 2107 mm with important peaks in the months of April to May and October to November.

According to AMVA (2018), these precipitation months are highly correlated to hazard occurrences such as landslides (38% of the events), flooding (60% of the events) and flow-like events (2%). Specifically for landslides, they occur in the steep areas of the municipality (43.5% of the territory) and eventually can trigger flow-like events in the municipality. AMVA(2018) reported extreme events of flood/debris flow occurrences in the years 1938, 1944, 1950 and 1988. There is very limited information available about the impacted area and causal factors available. However, based on the last event from 1988 (Caballero, 1988 and Florez & Parra, 1988), flow-like phenomena, and specifically a debris flow, could have occurred in past due to the formation of clustered shallow landslides that combined with the stream flow of the main drainage of the city, the *Ayura stream*. The above matches with the geomorphological setting of the area. The municipality is on a depositional environment of torrential origin, where the urban area was developed on different torrential fans (AMVA, 2018).

This kind of multi-hazard events seem to occur every 25 years according to AMVA (2018). It is very important to know how a new event would affect the city, which is now much larger than in 1988 when the last event occurred. As a result, different hazard analysis projects have been performed. The most recent one, carried out by AMVA(2018), showed the hazard extent and intensity in the main catchment of Envigado, the Ayura catchment (AC). The hazard footprint obtained by AMVA in the urban area is presented in section 2.4.

Although there are various other small watersheds in Envigado, only the Ayura catchment (AC) was selected to model the multi-hazard risk of one part the urban area of Envigado, which is located inside this catchment. The Ayura catchment (AC) has an area of 40 km², a length of 10 km and a maximum width of 5.5 km. The area contains numerous colluvial deposits and weathered metamorphic soils on slopes that may reach 45 degrees. Figure 2-3 shows the Ayura catchment.

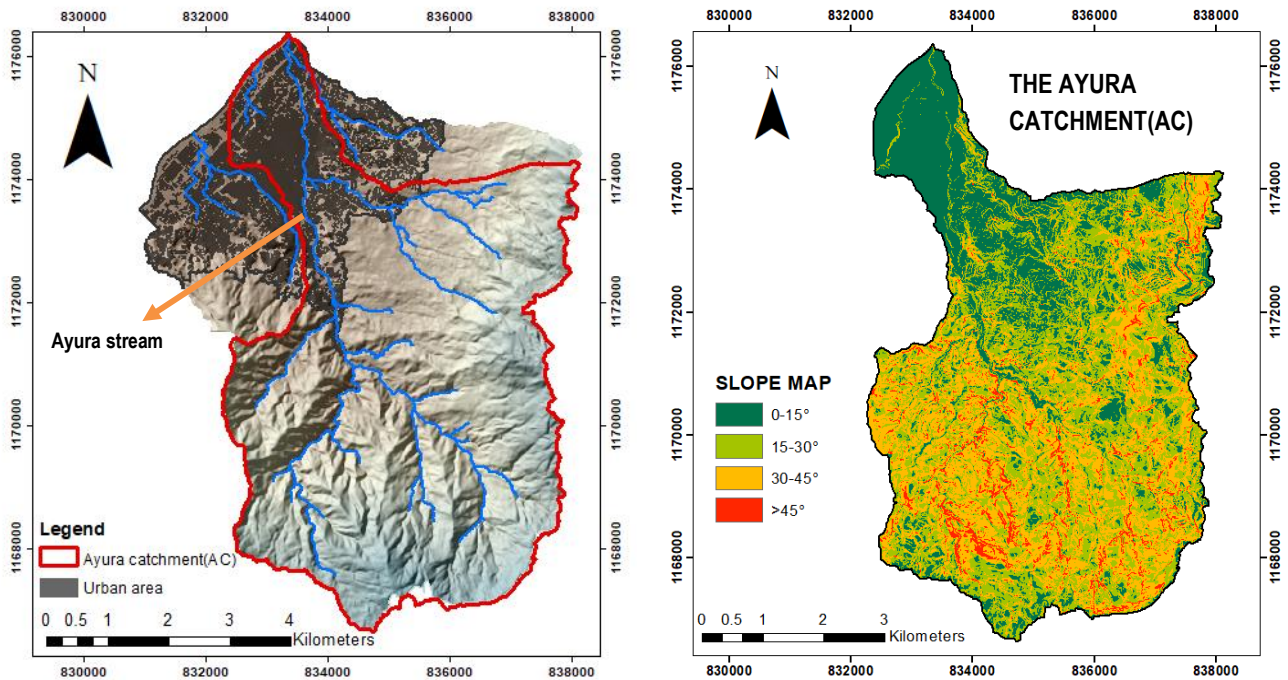


Figure 2-3. Delimitation of the Ayura catchment (AC) and slope map

2.3. The debris flow event of 1988

As stated by Caballero(1988) and Florez & Parra(1988), on 14 April 1988 a debris flow reached the urban area of Envigado. This flow was triggered 45 minutes after precipitation of only 6 to 8 mm with a duration of 30 minutes. As it was reported by these authors, the precipitation was not particularly extreme for this period of the year. Possible causes might be related to the effect of antecedent rainfall, changes in the land cover in the upper part of the catchment, precipitation not recorded in the upper part of the AC or even the destruction of a natural dam. However, with the data available, this could not be evaluated.

As mentioned by Caballero(1988) and Florez & Parra(1988) this event has been the largest in the last 70 years. According to them, water and debris reached the upper part of the urban area located 1 to 3 km downstream of the transition between the very steep slopes and the start of the deposition in the AC. According to the inhabitants of the area the debris flow reached 2 to 3m above the margins of the river. The event affected 48 persons, destroyed 10 house, and affected the aqueduct (AMVA, 2018). Annex 1 shows the possible footprint of the event. This was reconstructed from the reports of Caballero(1988) and Florez & Parra(1988).

2.4. Hazard modelling of flow-like phenomena AMVA(2018)

Similar events as 1988 are expected to occur again in the AC. For this reason, AMVA (2018) modelled the hazard for flooding and flow-like phenomena under extreme rainfall. These models were undertaken for return periods (RP) of 25,50, 100 years for flooding (using HEC-RAS) and 500 for flow-like phenomena, using the software IBER 2D (University of da Coruna, 2019).

To model the flow-like phenomena for the 500 years RP, the discharge was increased by 40% to represent the possible incoming sediments from shallow landslides. Also, the rugosity of the channels was increased to simulate energy losses related to turbulent flow (AMVA, 2018). Finally, the model was calibrated using the level of the Medellin river (called as well Aburra River) in the discharge points (e.g. Ayura stream) for return periods of 25 years. Figure 2-4 presents the hazard footprint for flow-like phenomena corresponding to the water/solids height for 500 years return period. In Figure 2-4 only the urban area of the AC is displayed, this area was the focus of the research.

2.5. Available information

For this study, with the support of the Faculty of Mines of the National University of Colombia (UNAL), fieldwork was carried out in October 2018. It was possible to collect secondary information about the AC, its hazards and the elements at risk (EaR) of Envigado. In terms of the hazard, the main source of information was the hazard study of AMVA (2018) about landslides, flooding and flow-like phenomena in the municipalities of the AV, which was developed by UNAL and the Government of the Metropolitan areas of the AV. With regard to the EaR, the databases of the Master Plan of Envigado (POT, 2011) were provided by the Planning Department of Envigado. The data is summarised in

Table 2-1.

A 3D view of the study area is presented in Figure 2-5 to help to visualise the local setting.

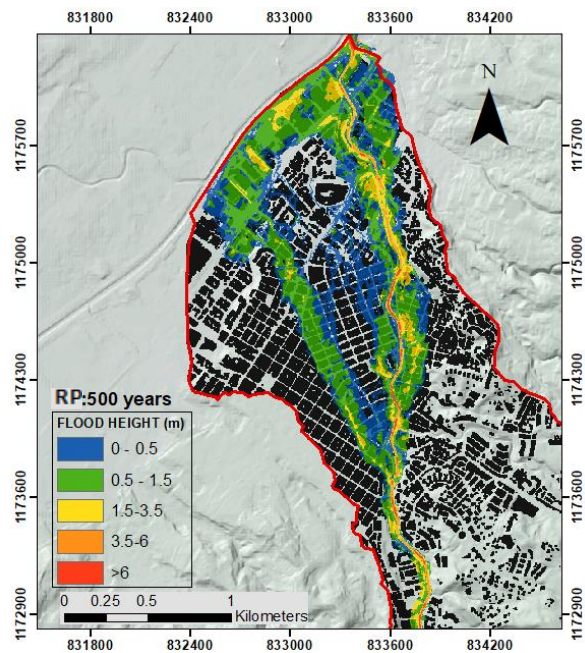


Figure 2-4. Flow-like phenomena for a precipitation of 500 years return period AMVA(2018).

Table 2-1. Data collected during fieldwork

	Type	Source	Date	Description
Hazard	Lithology	AMVA(2018)	2018	Compilation of rock and soil parameters from different municipalities of the AV-and summary of parameters for the AC
	DTM	Instituto Geografico Agustin Codazzi	2014	Elevation model with a resolution of 2m. Produced from the elevation model for the rural area of Envigado (scale 1:5000) and of the urban area of Envigado (scale 1:2000)
	Event Inventory	DesInventar	2018	- Natural hazard inventory used in the region. - Reports hazard events with damages
	Landcover	AMVA(2018)	2018	From the aerial image of 2016. Method used: semiautomatic classification. Following Corine Land cover classes
	Rainfall information	AMVA(2018)	2018	IDF curves adapted to climate change Produced from precipitation records in the Ayura station: - 1948 -1996: hourly data - 1996- present: 15 minutes
	Hazard information	AMVA(2018)	2018	Hazard footprints produced by AMVA with IBER 2D software (RP=500years) and HEC-RAS (RP=25,50,100 years)
	Seismic information	Universidad de los Andes, 2015	2016	Peak ground acceleration map 10% exceedance probability in 475 years
EaR	Land use	Master plan Envigado (POT,2011)	2011	Shapefiles aggregated level (neighbourhood).
	Building footprint	Master plan Envigado (POT,2011)	2017	Shapefile from 2011 but updated for 2017
	Road Footprint	Master plan Envigado (POT,2011)	2011	Shape file
	Population data	No data	-	No data could be obtained during fieldwork
Vulnerability	Value of buildings	AMVA(2006)	2006	General valuation of structures by building use
	Vulnerability curves	Not available from AMVA(2018)	-	Obtained from literature Ciurean et al., (2017) and CAPRA.

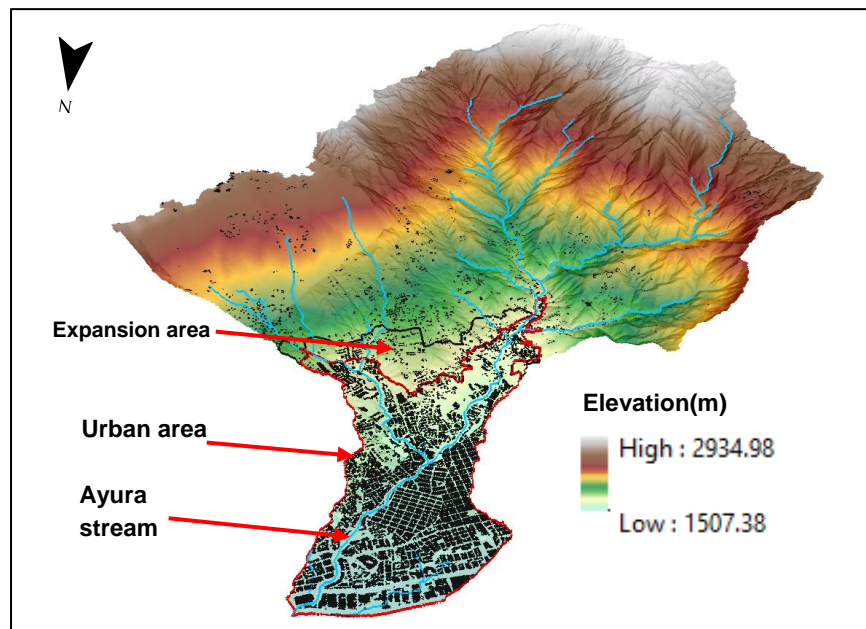


Figure 2-5. 3D View of the Ayura catchment.

3. MULTI-HAZARD MODELLING

This chapter presents an overview of the main steps to translate the collected data into usable input maps for physical modelling of the multi-hazard processes within the AC. To perform this modelling the software OpenLISEM-Hazard was selected for its capacity to simulate two-phase (solid-liquid) equations that allow representing the behaviour of interacting hazards such as flow-like phenomena. Hazard maps for flooding and debris flow/hyper-concentrated flows were produced for the present situation of the AC.

3.1. Elaboration of input maps for the multi-hazard model OpenLISEM

OpenLISEM is a model that requires an extensive number of parameters in the form of raster maps and tables (Bout et al., 2018). To produce them the collected field data was processed with the aim of representing the site conditions. Once this was done, the tables and raster maps were produced using PCRaster, an open-source GIS aimed at modelling. In the following sections, some of the main parameters for OpenLISEM are presented and discussed.

3.1.1. Digital Terrain Model (DTM)

The elevation model provided by AMVA (2018) was a DTM with filtered structures. As it was shown in section 2.5, this DTM was produced from two sources with different spatial resolutions. As a consequence, the urban areas were better defined than rural areas (in the middle and upper part of the AC). However, the consequences for modelling were considered marginal because the streams and slopes kept a good definition in the rural area. Another issue in the DTM was the presence of artefacts nearby to some streams, but they were not removed because there were few and subtracting them would imply as well to affect areas without problems.

Subsequently, the DTM was resampled to 5 meters using the nearest neighbourhood algorithm. This resolution was selected to be able to represent as much as possible the obstructions in the channel. It was found during fieldwork, that some bridges had very low slabs inside the river channel resulting in a reduction of the hydraulic capacity of the Ayura stream. Thus, to represent this effect, on relevant locations the channel depth was uplifted. The selected points were the bridges whose slabs were significantly inside the channel reducing the water flow under flooding conditions (see Figure 3-1). The additional elevation assigned was considered as the thickness of the bridge slab.

Similarly two bridge piles with a height of 10m and a cross section around 5 m (1 pixel) were included as flow obstacles. The reason to include them was that AMVA (2018) reported they have high influence in the hydraulic capacity of the stream.



Figure 3-1. Obstruction caused by the presence of a concrete slab under bridges inside the channel of the Ayura stream.

3.1.2. Catchment boundary

The watershed of the AC, was shown in Figure 2-3, was delineated using ArcGIS and PCRaster based on the DTM features. Interestingly, in the lower part of the AC (or urban area) both software produced a very narrow delimitation very close to the stream. As a consequence, the deposition materials from the flooding and debris flow would not be able to spread in the whole deposition area. For this reason, based on the geomorphological descriptions of AMVA (2018), the visualisation of the relief using anaglyph (see Annex 2) and the observations during the fieldwork, a manual reshaping of the catchment boundaries was made. This reshaping included a wider deposition area which was limited by a probable uplifted old alluvial fan.

3.1.3. Soil properties

Before making use of the soil data provided by AMVA (2018), a revision was done to verify their representativity for the area. It was found that the soil properties were extracted from secondary data, mainly engineering studies developed along the AV. Specific soil data for Envigado corresponded to perforations and soil tests in the lower part of the municipality (or urban area). Unfortunately, soil information for the middle and high parts of the AC was scarce. For this reason, missing soil data was extrapolated by AMVA (2018) using the information available from soils in the AV with similar parental rocks. However, these extrapolations have limitations. As observed in AMVA (2018) and during the fieldwork, although the rocks and formation conditions might be similar along the AV, each individual sub-catchment in the AV is exposed to different rainfall conditions, slopes, rock intercalations, etc. This might imply that soil types vary in space. As a consequence, it can be considered that soil characteristics are a large source of uncertainty.

AMVA (2018) represented the variability of the properties of the soil units in the AC using the standard deviation (see Table 3-1). The parameters evaluated were cohesion(c'), internal friction angle (ϕ') and density(γ). Notice the highest standard deviations in the table.

Table 3-1. Geotechnical parameter of soils in the Ayura catchment

Geotechnical unit	Soil type (USCS)	Friction Angle (degrees)		Cohesion (kPa)		Unitary weight (KN/m ³)	
		μ	σ	μ	σ	μ	σ
Amphibolite of Medellin	CL	30	3	10	4	18	2.26
Alluvial Deposit	GM	22.5	2.27	5	2	19	3.21
Torrential deposit	GM	32	3.23	5	2	19	2.9
Recent landslide deposit	CL o ML	31.18	3.12	15	5	15.4	3.5
Deposit I	ML	22.5	2.27	15	5	19.5	2.6
Deposit II	ML	22.5	2.27	15	5	19.5	2.56
Deposit III	ML	17.5	1.77	20	5	20.5	2.56
Deposit IV	ML	30	3.03	7.9	3.16	19.4	2.56
Deposit V	ML	22.5	2.27	15	5	19.5	2.56
Dunnites of Medellin	ML	22	2.22	10	4	19	3.9
Schist of Cajamarca	ML	18.5	1.87	20	8	18.17	0.8
Anthropic fillings	SM o GM	30	3.03	7.9	3.16	19	3.5

Other studies such as Vega (2013), Valencia et al., (2005) and Parra & Hidalgo (2015) that characterised the materials of the AV showed similar variability in soil characteristics. Parra & Hidalgo (2015), for example, remarked that in the East of the AV, a source of uncertainty was the difficulty to make a differentiation between soil deposits, residual soil and weathered rock. Therefore, in the absence of detailed data for the AC, the values proposed by AMVA(2018) in Table 3-1, were used as the main source for this research.

Other important parameters to model hydrometeorological hazards using OpenLISEM-Hazard such as hydraulic conductivity (ksat), medium grain size (D50), porosity (θ_s), initial moisture content (θ_i), residual moisture content (θ_r), and average suction at the wetting front (psi) were estimated using literature and reports from earlier studies in Envigado. Ksat and θ_s were estimated using a compendium of soil properties developed by Koliji (2008) that are based on standard values proposed by the Association of Swiss Road and Traffic Engineers and other authors. To retrieve these parameters the USCS soil classification of each geotechnical unit presented in Table 3-1 was used as a key. It is worthy to mention,

that given the high variability of the values presented by Koliji (2008), the upper extreme value of k_{sat} for each soil was selected. The reason for this was that even if clays can be found in the AC the proportion of materials with bigger size soil grain are as well important. As consequence, more infiltration would be expected and with a better response of landslide behaviour in the model. D_{50} was assigned a low value equal to the value of the amphibolites of Medellin (see Table 3-2). At the beginning, a higher value was considered based on 4 validation samples taken in the field. However, because of the limited number of samples, a lower value was preferred based on the geological description of the unit (schist of Cajamarca) by AMVA(2018). Another reason to select low values of D_{50} , and not the ones measured from the 4 samples (75% sand with a size of 1750 microns), was that the collected materials could correspond to intercalations of granite in the area, which are not frequent. However, it is advisable in future to check the parameter with a more comprehensive sampling scheme.

Residual moisture (θ_r) and ψ_i , were defined using soil retention curves and the Green-Ampt wetting front graph (Rawls et al., 1989) Given that these graphs required the soil texture in order to retrieve the parameters, it was necessary to use an equivalence between the USCS and USDA soil classification systems. The proposed equivalence was developed by US CORP OF ENGINEERS (García-Gaines & Frankenstein, 2015). Although this equivalence does fully not translate USCS into USDA systems, they can be very useful when only USCS classification is available (as frequently occurs in Engineering studies that use the USCS system) and grain size distribution for fine material is absent.

Table 3-2 presents a summary of the final parameters adopted for the research. Some units from AMVA(2018) were merged because they were considered as similar. For instance, the deposits I to V. In the table, different footnotes indicate the source and additional commentaries about the parameters.

Table 3-2. Final soil parameters considered in this research

Soil unit	Cohesion (kPa) ¹	D50 (um)	Soil density ¹ (kg/m ³)	phi ¹ (°)	k_{sat} ² (mm/h)	Porosity ² θ_s	Initial moisture ⁹ θ_i	Residual moisture ^{3,4} θ_r	ψ_i ^{4,5} (cm)
Dunnite	10	40 ⁶	1900	22	24	0.67	0.4	0.21	30
Debris flow deposit	5	42.5 ⁶	1900	32	50	0.36	0.28	0.15	10
Alluvial deposit	5	40 ⁷	1900	22.5	180	0.36	0.27	0.15	10
Deposit vert	14.7	40 ⁶	1965	22.9	24	0.4	28	0.29	30
Anthropic filling	7.9	100 ⁶	1900	30	30	0.4	0.2	0.2	10
Migmatite	17	45 ⁸	1740	27.5	44	0.58	0.4	0.15	40
Landslide Deposit	15	40 ⁶	1540	31.18	24	0.5	0.2	0.3	30
Amphibolite of Medellin	10 ⁹	40 ⁶	1800	30	24	0.67	0.4 ⁸	0.35	30
Schist of Cajamarca	6 ⁹	40 ^{6,10}	1820	24 ⁹	45	0.5	0.23 ⁹	0.25	30

3.1.4. Soil depth estimation

As mentioned by Bout et al., (2018), soil depth is a parameter with enormous influence on physical modelling with OpenLISEM. This is because the model uses a variation on the infinite slope model, that depends on

¹ From AMVA(2018)

² From Koliji(2008)

³ From soil retention curves

⁴ Translation between soil classification system USCS and USDA (García-Gaines & Frankenstein, 2015).

⁵ Green-Ampt wetting front graph by Rawls et al., (1989)

⁶ From drilling and test developed in different geologic units in the Aburra Valley by (AMVA, 2006)

⁷ Assumed equal as dunnite values

⁸ From (Valencia, 2005)

⁹ From (Risk Office of Envigado, 2010)

¹⁰ Sampling during field work materials were 1750 microns but for lack of extensive sampling they were not used.

the soil depth, to estimate the safety factor (FOS) of slopes. The influence of soil depth on FOS can be seen in a basic formulation of the infinite slope model presented by Griffiths, Huang, & Fenton, (2011) shown below.

$$FOS = \frac{(Z\gamma \cos^2 \beta - u)\tan\phi' + c'}{Z\gamma \sin\beta \cos\beta} \quad [1]$$

Where:

γ is the total unit weight, β is the slope inclination, u pore pressure at the base of the slice, ϕ' is the effective friction angle at the base of the slice and c' the effective cohesion at the base of the slide.

As it can be seen the safety factor varies inversely to the soil depth (z); thus, in the light of the equation, it is expected that higher soil depths produce smaller FOS or more slope instability.

In absence of representative spatial data to make an estimation of soil depth two approaches were considered. First, AMVA (2018) proposed a soil depth map based on Catani et al., (2010) that used topographical factors to estimate the parameter. Second, a soil depth map was produced that used the average values resulting from the approach of Kuriakose et al., (2009) and Von Ruetten et al., (2013). While Kuriakose et al., (2009) used topographical factors to define soil depth, Von Ruetten et al., (2013) used soil production and transport balance assuming that topography is at steady-state. For the implementation of the two models, two scripts adapting the proposed models by Kuriakose et al., (2009) and Von Ruetten et al., (2013) were developed by Bout et al., (2018) using PcRaster. The soil depth maps produced by AMVA (2018) and in this research are shown below.

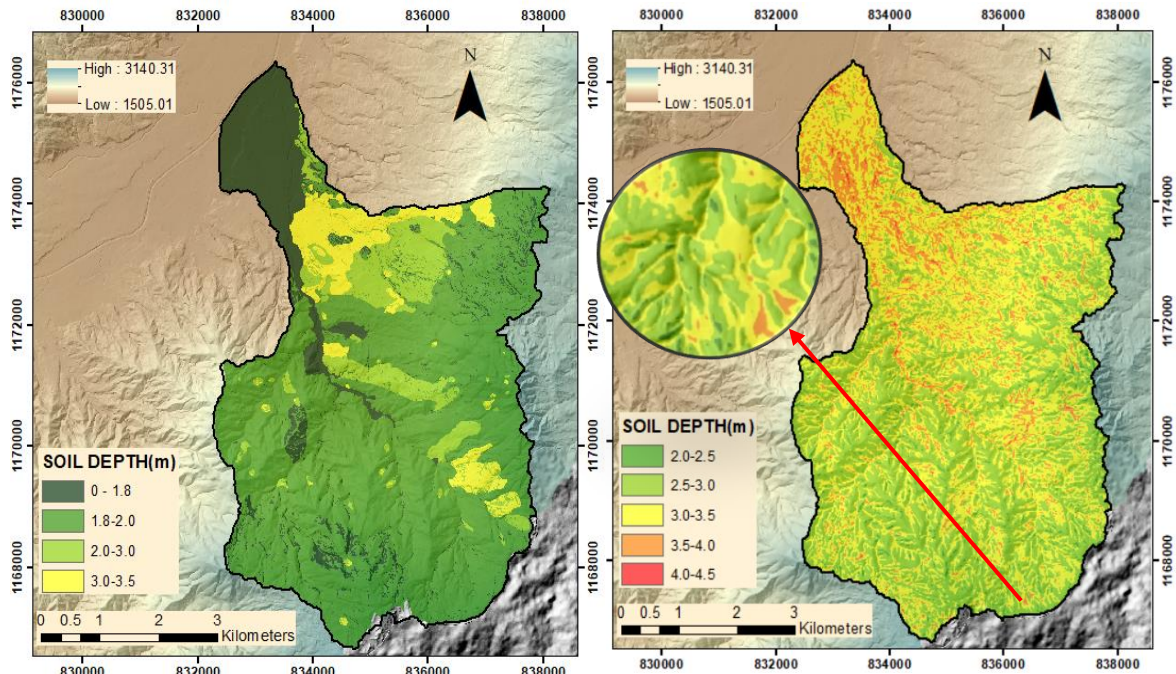


Figure 3-2. Soil depths models produced by AMVA(2018) (left) and the present research (right)

After comparing the map produced by AMVA(2018) and the map produced in this research, it was noticed that with the later, deeper soils were modelled. It was also noticed that the soil map that we produced tended to better represent the variation of soil depth according to the different features of the terrain. This means that ridges were calculated with less deep soils and concavities with deeper soils. Conversely, the soil map of AMVA (2018) showed to be less reactive to the terrain variations. Therefore, the soil depth produced in this research was selected. However, soil depths were not further calibrated because during the field work it was noticed that soil depths could reach 4 m in the upper part of the AC. In Figure 3-2, highlighted in the detail, shows one location where it could be noticed in the field that soil depths can reach 4 m. These depths were also reported in a geotechnical report elaborated in the area by the Risk Office of Envigado (2010).

However, further validation is necessary to be carried out in different points to assess the necessity of calibration.

3.1.5. Analysis of land cover and catchment rugosity

After a visual comparison between satellite images and the land cover map provided by AMVA(2018), one problem was found. Some areas in the upper part of the AC corresponding to the vegetation in 2017 were inaccurately classified as bare soil. It was found that the reason for this was that the image used for the classification was from a past year (probably 1 or 2 years) in which logging activities took place. Therefore, manual correction was performed.

The reason to make this modification was the extension and location of the problem: an approximate area of 0.5 Km² on steep slopes (20 to 50 degrees). The presence of bare soil in these conditions can induce additional and stronger erosion not evidenced in fieldwork, in an area located in a very hazard-prone zone, according to Florez & Parra (1988). However, logging activities can take place again and produce unfavourable conditions but this was not considered in the model.

Linked to land cover is the surface roughness which varies in the catchment. Given that no information was obtained on this during the fieldwork, rugosities- in terms of the number of Manning's n- were adopted for each land cover class based on Bout et al., (2018). In particular, for the land cover named as "water" that corresponds to the stream of the AC, the Manning number used was the average for the Ayura stream, equal to 0.05. This was calculated by AMVA(2018) by analysing channel photos following the methodologies, for example, proposed by Barnes (1967) and Arcement & Schneider (1989). Although the present research only considered average Manning values for the principal stream of the AC, it is recommendable to assign in future the individual values for secondary streams. Variations in Manning's n have a direct effect on water and debris flow. These can result in lower hazard intensities than in reality, if n is reduced.

Root cohesion, a factor linked to land cover as the added cohesion for roots, was not considered in the modelling of interacting multi-hazards of this research. Including this factor can reduce the occurrence of triggered landslides especially for short return period precipitations.

3.1.6. Maximum plant storage and plant cover

One important parameter for interception modelling in OpenLISEM is the maximum canopy storage (S_{max}). This was calculated using different expressions for S_{max} for different types of vegetation (Jong & Jetten, 2007): Pines and eucalyptus in the upper part of the AC and in the urban area; pines and crops in the medium and high part, and clumped grass distributed along the whole catchment (following the land cover). The vegetation type was selected according to the fieldwork and a land cover study developed by UNAL (2014) in Envigado.

S_{max} for different vegetation types is a function of the NDVI and the Leaf Area Index(LAI). The former was calculated by processing a Sentinel-2 satellite image of August 23rd of 2018. The latter was calculated using the equations [2,3] (Bout, et al., 2018):

$$Cover = 1 - e^{-2*NDVI/(1-NDVI)}; LAI = \frac{\ln(1-cover)}{-0.4} \quad [2,3]$$

3.1.7. OpenLisem channel: An issue between channel flow and overland flow

According to Bout et al., (2018), water flow in OpenLisem is divided into overland flow, channel flow and flooding which are coupled using an artificial channel. When overland flow reaches the channel and this completes its capacity, water transforms in flooding. Some advantages of the introduction of this artificial channel are that it allows spreading the infiltration in the width of the channel, and routing the flow not only in the size of one raster cell but in the complete width of the real channel. The later facilitating the calibration based on the channel runoff rather than in the surface runoff (Bout, et al., 2018; Starkloff & Stolte, 2014).

The above approach is useful when the DEMs have a coarse resolution and rivers are not well defined. These rivers can be filled up and replaced for the channel of OpenLisem. However, this was not the case in the AC. The DTM had an acceptable quality and the irregular river shapes were considered important in the behaviour of water and debris flow. For this reason, an alternative approach was taken. The OpenLISEM channel was placed under the river bottom of the original DTM. However, instead of

using the real depth of the channel, a depth of 20 cm was used. In the case of channel width, the real measures of the channel were used (15 m). With this mixed approach it was expected to keep, to a certain extent, the numerical solutions and the water routing of the OpenLISEM channel while including the irregularities and obstacles of the original river (from the DTM). Given the small depth of the LISEM channel implemented, it was not expected to have a representative influence on the water height once the model was run. An idealised visualization of the procedure is illustrated in Figure 3-3.

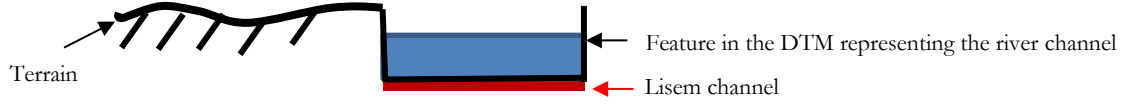


Figure 3-3. Compound DTM and Lisem channel

Based on the above figure, it was expected that once the OpenLISEM channel was overflowed the water in the river DTM channel would be treated as surface flow. This might produce differences in the water-debris height results because flow equations for both channels are treated differently (Bout et al., 2018; Starkloff & Stolte, 2014). The extent of these differences were not evaluated in this research, however, it is necessary for the future to compare the differences in water height produced by a compound channel and a OpenLISEM channel.

Alternatively, since high-resolution DEM are increasingly available, the uncertainty and errors would be reduced by integrating the actual DEM channel as an OpenLISEM channel, or implementing a module to discretise efficiently channel sections.

3.1.8. Precipitation input for the AC

As already stated, rainfall is one of the main causal factors of hydrometeorological hazards in mountainous areas (Chen et al., 2016). As mentioned by Jayawardena, (2015), flow-like phenomena such as debris flows can occur when displaced soil masses combine with the flowing water of streams, which is the case in AV.

In the Abura Valley, most of the landslide processes occur in high precipitation periods influenced by antecedent rainfall (Aristizábal & Gómez, 2007). For this reason, during these precipitation periods, it is more probable that landslide and flowing water combine leading to the formation of processes with different concentration of solids (e.g debris flow). For this reason, different rainfall events were designed to evaluate the response of the AC. These events were for rainfall with 25, 50,100, and 200 years return period.

These precipitation events were constructed using the IDF curves produced by AMVA(2018) who used the data of one station in the area. These IDF curves were developed using a Gumbel analysis with data from the year 1996 to 2016. Although in this station the information was from the 80s, AMVA (2018) only considered the data between 1996 to 2016, which had high resolution (with records each 15minutes). The IDF equation [4] produced by AMVA(2018) for the current situation was:

$$I = \frac{534 * t^{0.23}}{(d+0.25)^{0.77}} \quad [4]$$

Graphically, the mentioned return periods, are represented in Figure 3-4.

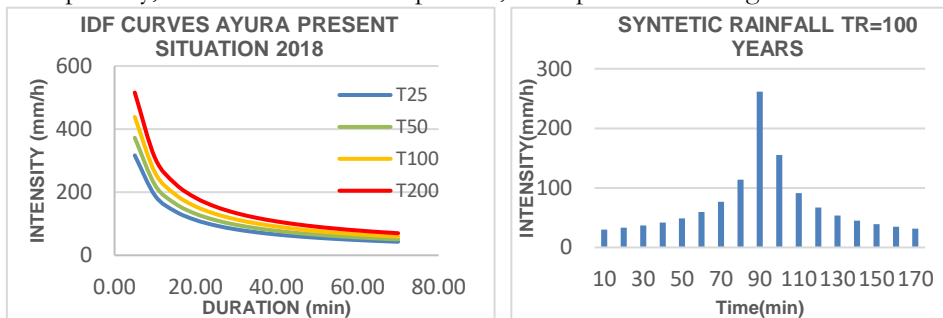


Figure 3-4. IDF curves for the Ayura catchment for the present situation for different return periods (Left) and an example of a synthetic rain event with 100 years return period (right).

From the IDF curves, synthetic rainfall events were created for their use in OpenLISEM. These syntenic events were constructed for a time of 170 mins which correspond to the concentration-time of the AC calculated by AMVA (2018). The concentration-time was used because this time gives the maximum

discharge in the catchment. The alternating block method was the method used to distribute the rain in time. One example is shown alongside the IDF curves in Figure 3-4.

3.1.9. Antecedent rainfall and its effect on the initial soil moisture

OpenLISEM is an event-based model which implies that it can represent the behaviour of the catchment as a response to a particular rainfall event. However, this entails that in principle OpenLISEM is limited in the simulation of antecedent conditions such as groundwater variations (Ma, 2018) and antecedent rainfall. This is especially important for the AV and the AC where antecedent rainfall plays an important role in the generation of shallow landslides (AMVA, 2018; Aristizábal et al., 2016).

As mentioned in section 2.3 during the event of April 14th 1988 the daily precipitation was not particularly abnormal. For this reason in the absence of earthquake conditions the event might have been linked to 1) a non-registered intense rain in the upper part of the AC, or 2) antecedent rainfall conditions, or 3) to a landslide dam break (which cannot be modelled in the current context).

By observing the monthly multiyear precipitation from 1972 to 2006 (see Annex 3), it could be noticed that 1988 was one of the years with more registered precipitation in the month of April. It is possible that most of the precipitation in that month had occurred previous to the day of the event, making possible the hypothesis of antecedent rainfall influence. However, this fact could not be confirmed because more detailed information about rainfall was not possible to be acquired.

One approach to simulate the antecedent rainfall in the OpenLISEM model was to increase the initial soil moisture (θ_i). To do this, a script presented in Bout et al., (2018) and shown in Annex 4 was applied. The input data to run this script was the DTM, the soil depth, θ_s , θ_i , θ_r , K_{sat} and a time step corresponding to a number of days after the rain. This script simulates how water fills the empty spaces of

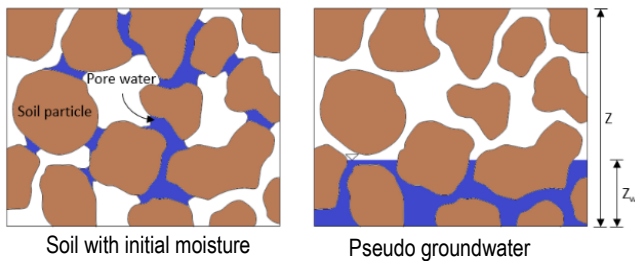


Figure 3-5. Pseudo ground water modelled to calculate initial soil moisture. Source: Ma(2018).

the soil, after a precipitation period, at a rate equivalent to the hydraulic conductivity of the soil resulting in an increase of groundwater depth. To do this instead to consider the water distributed in the pores, it is assumed that the pore water is in the bottom of the soil layer, which starts rising once the wetting front reaches the water level and stops when the room in the pores is finished. This water level is considered as a pseudo-groundwater. The graphical representation of the mentioned assumption is shown in Figure 3-5 taken from

Ma(2018).

After that the pseudo groundwater starts increasing, the moisture varies linearly according to the equation[5] (Bout et al., 2018; Ma, 2018).

$$Z_w = \left(\frac{\theta_i - \theta_r}{\theta_s - \theta_r} \right) * Z \tag{5}$$

Where Z is the soil depth, θ_s the porosity and θ_r the residual moisture (moisture at field capacity).

As a result of applying this script, a 7% increase of moisture was calculated overall for all the AC. However, locally in areas nearby to river sources (upper AC) moisture increased with values that surpassed the 50% with regard to θ_i . This is because water accumulates by gravity action in concave shapes (between ridges) where deeper soils are present (according to the modelled soil depth in previous chapters).

3.2. Summary of input maps for OPENLISEM

Four types of input data are required to run OpenLISEM: Topography, Land use, Soil types and Rainfall. These data types were presented in the previous sections and summarized in Table 3-3. Raster maps and tables to run OpenLISEM were produced using GIS software (ArcGIS) and PCRaster.

Table 3-3. Main Input maps for OPENLISEM used to model the multi-hazard condition in the Ayura Catchment

CATEGORY	INPUT MAP	COMMENTARY
Topography related	DTM	Elevation model with a resolution of 5m
	Gradient(or Slope)	-
	Water Flow maps	Related maps: local drain direction map(Idd) for the catchment and Dimension channel Ayura stream: 0.2 m depth, 15m width.
	LISEM Channels	Channel dimension of other streams:0.2 depth, ranging 3-15 m according to stream order in function of accumulated flowing material
	Stream obstructions	Pixels with a higher value than the DTM
Rainfall	ASCII file	Tables with precipitation for return periods:25,50,100,200 years
Soil surface	Manning map (n)	Manning for each land unit
	Random roughness	Not described in this research- based on Jetten & Bout (2018). Ranging from 0.5cm for urban areas to 2cm for the forest.
Surface cover	Cover	Produced by the land unit. Each pixel has one only cover
	Leaf Area Index	-
	Maximum canopy storage	-
	Vegetation height	Estimated for land unit. In forested areas in the upper AC, an average height of 15m was selected
	House cover	Each pixel was assumed fully occupied if there was a building.
	Roads	Roads with a width of 5 m
Erosion	Cohesion	-
	Median grain diameter (D50)	-
	Aggregate stability	Assumed value 20. High uncertainty value
Slope stability	Material density	-
	Phi	-
	Root cohesion	Not included for the presence of high-intensity precipitations (see Kuriakose et al., 2006)
	Peak ground acceleration	Maps with 0.15-0.2g (gravitational force)- Partially used. Future work needs to see their influence
Infiltration maps	Ksat	-
	Psi	-
	Initial soil moisture content	Initial moisture content based on antecedent rainfall
	Residual moisture content	-
	Porosity	Equal to the saturation ratio of each soil
	Soil depth	-

Note: Other maps can be included such as typical rock size. However, in the field, this information was not retrieved.

3.3. Modelling flow-like phenomena (flooding and debris flow) for the present situation

3.3.1. Calibration and of the hazard model

The use of extensive and continuous records (e.g water discharge in the outlet and landslide inventories) in-situ are necessary for a correct calibration of the hazard models (Jayawardena, 2015). However, this was not possible for this research. Rainfall records with their associated discharge (or water height) were not available. As well, landslide inventories could not be used because the landslide locations were not systematically recorded with their specific rainfall events, especially in the upper parts of the catchment because the inventory used only records with population directly affected. For this reason, during the fieldwork it was observed that shallow landslides might be triggered in the upper part of the catchment and that most might have a depth of 1 m (Caballero, 1988). We tried to replicate this in the calibration process. To guarantee that flow results were close to the reality the following approaches were taken:

- 1) Calibration based on the flooding results of AMVA (2018) for the return period of 25 years. Different calibration combinations were used until flooding depths were in the same order of magnitude as the modelling results of AMVA(2018).
- 2) Calibration using the discharges calculated by AMVA (2018) for the AC. Given that the channel of OpenLISEM was not defined with the real dimensions of the Ayura stream (See section 3.1.7), it was not possible to calculate de total discharge in the channel, but only the one corresponding to the channel cross-section of 15 m x 0.2 m. However, by applying a geometrical relation between the section of the OpenLISEM channel and the average cross section of the real channel (15 m x 5 m), it was

found that although the relation might not be perfect, the discharges of OpenLISEM were close to those of AMVA(2018). The relation applied was the following:

$$Q_{channel_litem} = V \times A_{channel_litem} \tag{6}$$

$$Q_{total_probable} = V \times A_{average_channel} \tag{7}$$

Assuming a constant velocity:

$$Q_{Total_probable} = Q_{channel_litem} * (A_{average_channel}/A_{channel_litem}) \tag{8}$$

The probable OpenLISEM discharges for the various return periods are presented in Table 3-4.

Table 3-4 Discharges from AMVA(2018) and probable discharges of OPENLISEM

Return Period	Discharge Q by AMVA (2018) (m³/s)	Discharge Q (Total probable) by OpenLISEM (m³/s)
25	373	347
50	452	448
100	548	570

Note: The discharges of the channel of OpenLISEM implemented in this research were obtained from a modelling without sediments as it was done by AMVA(2018) for the return periods shown in the table.

3.3.2. Model validation

The lack of extensive data about past multi-hazard events in terms of their intensity (height) and extent, along with the lack of information about landslide occurrence in the in the upper part of the AC, made it very difficult to carry out a proper validation.

One indicator that might confirm that the model is capable of reproducing the multi-hazard events of the AC is the behaviour of the debris flow in a point known by the Envigado community as “Rosellon” (see Figure 3-6). According to the available historical records (Caballero Acosta, 2011; Florez & Parra, 1988), this point was impacted by the event of 1988. Few details are known, but according to Florez & Parra (1988) during the episode, the water in the main channel reached a height of at least the 3 m and flooded the area with 1 to 2 meters, which correspond to the OpenLISEM results. In the area, some protection walls and water intake were reported as damaged during the event of 1988. According to the model, as highlighted by the red circle the flow has the tendency to create a shortcut overflowing the area. The buildings located nowadays in the Rosellon area are a mix of industrial and residential use.

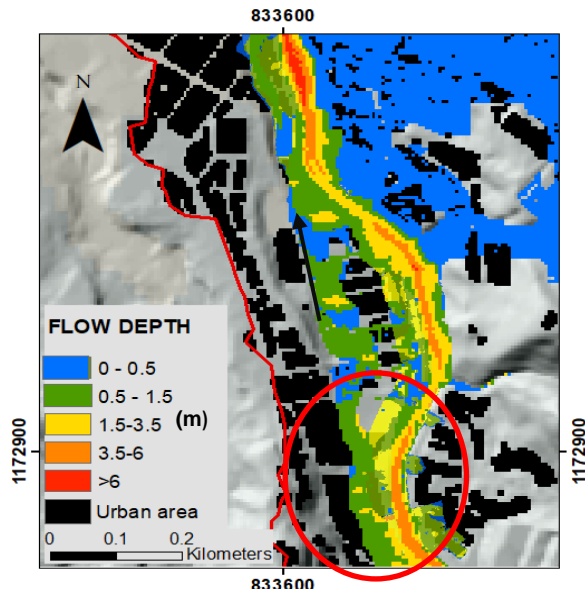


Figure 3-6. Modelled debris flow depth for an event with a Return Period of 25 years in the area of Rosellon.

3.4. Modelling Results

Once the model was set up the configurations were used to model the present and future multi-hazard situation in the AC. As was mentioned earlier in this chapter the hazard was modelled for the return periods of 25, 50, 100 and 200 years. In this section, some of the outcomes for the hazard in the current situation are displayed. The results for future situations are shown in chapter 6.

The modelling outcomes for this research were a map of maximum flood height and a map of maximum debris/hyper-concentrated flow height for each return period. It is relevant to remark that although these maps are separated they are influenced by each other. Similarly, that the maximum values registered, corresponded to different time steps, so not all the processes occur at the same time. In the same manner, the solid/water ratio varies with time and throughout the channel.

3.4.1. Simulated intensity maps for the present situation

In Figure 3-7 the maps for maximum flood height for the return periods of 25 and 200 years are presented.

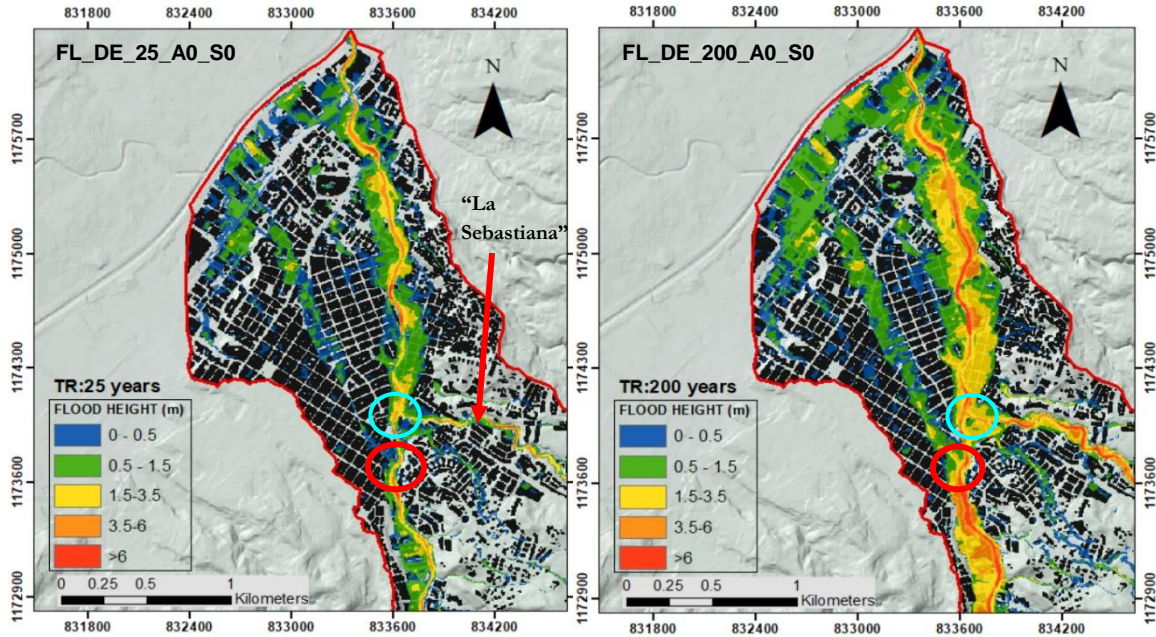


Figure 3-7. Hazard footprint in the urban area of the AC. (Left) water/sediment height for return period of 25 years. (Right) water/sediment height for the return period of 200 years.

As can be seen from Figure 3-7 the highest flood heights are concentrated in the main channel or directly in the vicinity of the Ayura stream. However, similarly, as the model performance by AMVA (2018) with IBER 2D (see section 2.4), the flow simulated with OpenLISEM tends to leave the channel in the area indicated with the red circle for all the return periods. In the area signalled with the cyan circle, the main Hospital of Envigado is located. Notice that this area receives the flooding coming from the Ayura stream and a tributary called La Sebastiana indicated in the map with the red arrow.

A code was associated with each hazard footprint, for example, **FL_DE_25_A0_S0**. These codes differentiate the map phenomena described (FL=flooding, DF=debris flow), their intensity (DE=Depth), the return period modelled, and the alternative (A) and future scenario considered (S). A summary of all hazard maps produced can be found in Annex 5. Chapter 6 explains in detailed what the alternative and scenarios stand for.

While analysing the simulated development of the debris flow in time (using the time series that are part of the OpenLISEM output) it was found that the debris/hyper-concentrated flow occurs in pulses. One first part is generated by tributaries of the Ayura catchment (e.g. La Sebastiana) and later stages are developed for the transport of material from the farthest points of the basin (upper AC). This in agreement with Caballero(1988) and Florez & Parra(1988) for the event of 1988, who reported that locals experienced at least 2 impacts of the flow separated between each other by 5 to 15 minutes.

3.5. Discussion about hazard modelling

From the results and model set-up of OpenLISEM the following points can be highlighted:

- Although it was attempted to calibrate the results of OpenLISEM, based on specific flooded points modelled by AMVA(2018), OpenLISEM results produced larger hazard footprints than the AMVA results (**Figure 3-8**). The differences can be caused by several factors:

- 1) The flooding modelled by AMVA(2018) was one-dimensional using predefined sections, while the OpenLISEM model used 2D modelling;
- 2) In the modelling it was defined that OpenLISEM used the channel described by the DTM, however, this DTM might have errors, such as poorly represented channel depths.

- 3) The OpenLISEM model considered two-phase equations so water and solids interacted, which might be the reason for which water flood was deeper.
- 4) More calibration points should have been taken into account in the model of AMVA.

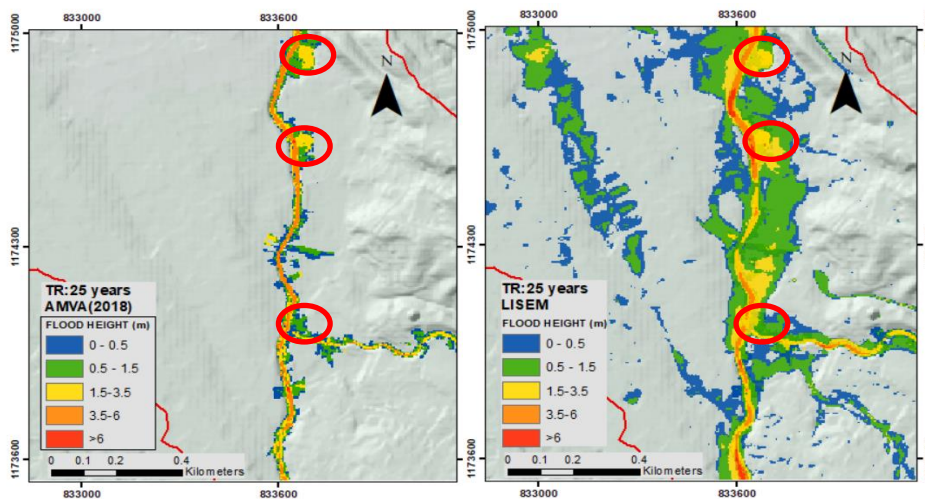


Figure 3-8 Comparison of flooding footprints by AMVA(2018) (Left) and OpenLISEM (right) for the return period of 25 years. In the red circles are some of the points that were used in the attempt to calibrate the OpenLISEM model.

- The calibration based on the probable discharge of OpenLISEM and its correspondence with the hydrological modelling results of AMVA(2018) is only one hypothesis, as it is also not known whether the AMVA model is properly calibrated with discharge data. Further tests need to be undertaken to find the best relation between flood height and discharge. Another alternative is to remove the original channel from the DTM and use only the OpenLISEM channel. However, any method that uses field measured data is required. Such data was lacking, unfortunately.
- Given the problems in model calibration, the depths of flooding and debris flows might have been overestimated. This will have considerable impacts on the risk calculations. Future work needs to concentrate on reducing the epistemic uncertainty of the modelled hazard. As well, different uncertainty analyses are necessary to define maximum and minimum ranges for flood/debris flow and water/solid relations. This analysis can be incorporated in later risk estimation stages.
- The modelling of shallow landslides in the AC with OpenLISEM faced two issues. The first was the resampling method applied to the digital elevation model. The DTM provided by AMVA was resampled to 5m using nearest neighbourhood, this produced some interference pattern propagated to the gradient maps affecting the correct calculation of the slope stability. Although, in this opportunity, the model was calibrated to obtain shallow landslides even with this issue. In future, it is recommended to use bilinear interpolations. The second issue was the lack of historical shallow landslide inventories, for this reason, the antecedent moisture was adjusted to only represent landslides in the upper part of Envigado, according to the estimations of Caballero (1988). For future events, an event-based landslide inventory should be made that can be associated with the associated precipitation to improve the model results and evaluate if the model produces over or underprediction of processes.
- Given the seismic conditions of the AV, the seismic acceleration with a return period of 475 years (suggested by the Colombian normative) was integrated into the OpenLISEM model. As a result, Multiple shallow landslides were generated, the volume carried accumulated in different points that slowed the flow (using a 25 years RP event). However, given the lack of real data no further analysis was possible. It is necessary to evaluate in future the behaviour of OpenLISEM under different seismic intensities and in different catchments affected by an earthquake to evaluate the validity of the results.
- It is necessary to verify in future the soil parameters and soil depths, these are critical parameters for the hydrological and stability model. As it was observed, most of the soil parameters did not correspond to the specific areas but to an extrapolation from other areas that could not represent the AC.
- As hazard modelling was only a first step in the process there was no more time to address the issue indicated above, and the hazard maps were used in the subsequent vulnerability and risk assessment.

4. ELEMENTS AT RISK AND VULNERABILITY ASSESSMENT

This chapter presents the characterisation of the elements-at-risk (EaR) in the study area, as well as the evaluation of their vulnerabilities. The EaR considered in the present research are limited to buildings. First, a data preparation effort to produce a usable EaR database was undertaken. Next, the degree of loss of the buildings and their contents was established using absolute vulnerability curves constructed for selected building categories. These categories are defined based on the available attributes in the EaR database and on the fieldwork observations.

4.1. Elements at risk characterisation

To be able to perform quantification of the risk it is necessary not only to develop representative hazard maps but also a complete database of the EaR. According to van Westen et al., (2011) desirable building attributes required for risk assessment are: building use, construction type, building height/number of floors, floor space and replacement costs. For population characterisation, attributes such as population density, spatial distribution, age group and others are necessary to evaluate population risk.

4.1.1. Generating a building database

The Planning Office of Envigado provided an updated building footprint database elaborated for the Master plan of Envigado (POT, 2011). This database contained a number of shapefiles with detailed and aggregated information for buildings:

- **At detail level:** building footprint features with attributes such as number of floors, footprint area and land use.
- **At aggregated level:** land use by zone, neighbourhood division and future densification planning by zone. Future densifications understood as the replacement of low-rise buildings for high-rise buildings, were provided in terms of maximum number of floors and maximum number of buildings per hectare.



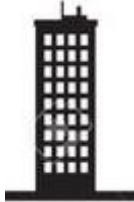
The supplied building footprint database, however, had several issues that required additional treatment:

- 1) The individual building footprints presented numerous topological errors, particularly overlapping polygons. To solve this a GIS tool was used to detect individual errors. However, given a large number of polygons, it was not possible to manually correct all the errors, and only the most visible polygons or features close to the floodplain of the Ayura stream were corrected, as these would have the largest influence on the calculated risk.
- 2) Building features such as elevator spaces, terraces and others, which were in the database as separate polygons, were disaggregated from the main building. These were classified as another construction (in some occasions with different height and use). Given that this would require an exhaustive work for manual editing and reparation, it was decided to filter out polygons with areas inferior to 16m². It was assumed that building footprints with a surface area under this threshold could not be a building but artefacts as the one mentioned above. From the 16874 polygons in the study area, about 1% were catalogued as artefacts and as a consequence, it was not possible to remove the majority of the problematic polygons.
- 3) Building attributes were incomplete. For example, only 47% of the building in the study area, had a proper classification of building use. To solve this the aggregated level shapefile of the neighbourhood which did have land use for all areas was spatially joined to complete the missing land-use attribute in the remaining 53% of buildings. The final building uses considered for this research were: residential (R), commercial (C), educational (E), health care (H) and industrial (I).
- 4) Other building attributes were absent. To solve this the next approaches were taken:
 - Building costs were retrieved from the seismic microzonation of the Abura Valley (AMVA, 2006). This proposed a unit cost per m² for R, C, I uses. The market costs per land use in 2018 were: for residential 630.9 €/m², for commercial 775€/m² and for industrial 725€/m². These values were the result of the

update of the values of 2006 presented by the seismic microzonation. This update was done by using the inflation rate and the consumer price index (IPC) for the last 2 decades in Colombia (an increase of 4.9% per year). On the other hand, the costs for building use as Health and Education were obtained as indicated in section 4.3.2.

- The building categories had to be estimated. Three classes were defined in relation to the number of floors: *1-floor* (or low-rise buildings), *2 to 6 floors* (or medium-rise buildings) and *more than 6 floors* (or high-rise buildings). Unfortunately, there was no information available related to the construction types, so we assumed a relation between the building height and construction type as will be further explained in section 4.3.1. These categories were selected based on the expected losses for flooding and debris flows in terms of structural and non-structural damage and on general building categories as indicated by Bruijn et al., (2014). As shown in section 4.3.1, these categories were used as a key to develop absolute vulnerability curves for the buildings in the study area.

Figure 4-1 Schematic representation of the building types and the reasons for their classification in relation to the risk assessment of floods and debris flows.

Low-rise: Single floor buildings	Medium-rise: Two to six floors	High rise: More than six floors
		
<ul style="list-style-type: none"> • Will sustain structural and non-structural damage during flood & debris flow. • Could be completely destroyed. • Population cannot evacuate to upper floors so are more vulnerable to flood and debris flow. 	<ul style="list-style-type: none"> • Will sustain non-structural damage in lower floors. • May have structural damage in lower floors. • Population can escape to upper floors so population risk is very low. 	<ul style="list-style-type: none"> • Will only sustain non-structural damage in lower floor. • Very limited structural damage. • Population can escape to upper floors so population risk is very low • Parking garage for residential and commercial buildings, which may be subjected to high damage

4.1.2. Data preparation for deriving population attributes

During fieldwork, it was not possible to obtain access to a population database for the study area, at a disaggregated level. The only source of information was an official report of the Health Office of Envigado (Alcaldía de Envigado, 2018a) with an estimation of the population by neighbourhood within the municipality of Envigado based on the projections to 2016 of the in force census in Colombia (2005). Given that population information was vital for this research to produce future scenarios related to the increase in the demand of building floor area (see section 6.1) this report was taken as a basis. In this way, the population in the study area was estimated first, by calculating the population density by neighbourhood. This was done by dividing the number of people per neighbourhood by the total floor space area of residential buildings (footprint area multiplied by the number of floors). Then for each building in the neighbourhood, the number of people was calculated by multiplying the density per neighbourhood with the total floor space for residential buildings. As a result, from the 219.991 inhabitants reported for the whole of Envigado by 2016, 108.737 inhabitants were estimated to be living inside the study area.

Because of the high uncertainty of the population in terms of their static (densities, age composition) and dynamic characteristics (distribution in space or time, also over the other land use types) the population vulnerability and population risk were not calculated in this research. Here only an example of a hypothetical distribution in space/time scenario is presented that might be a good starting point for future works in the study area if better information is not available. This occupation scenario can be related to the damages produced by debris flow and flooding with the loss of people inside a building (van Westen et al., 2011).

To distribute population by neighbourhood at individual building level a tool for micro-spatial dasymmetric redistribution of the population was used: the POPGIS tool produced by Lwin & Murayama (2009). POPGIS has a volumetric approach using equation [9]:

$$BP_i = \left(\frac{CP}{\sum_{k=1}^n (BA_k \cdot BH_k)} \right) BA_i \cdot BH_i$$

Where CP = the census aggregated population information in a polygon, BA_i = area of building i , BH_i = height of building i (Attribute as well found in the building footprint database), k = summation indices and n = number of buildings that fall inside the polygon CP .

To run the tool two shapefiles are necessary: neighbourhoods (or administrative units) with the corresponding population and the building footprint with attributes such as building use and number of floors. Additionally, the tool requires a minimum footprint area, this was assigned as 16 m². A view of the interface of POPGIS is presented in Annex 6.

A night-time occupation scenario was considered. This might be the most critical for the study area if a debris flow-like phenomena occur. During the day a large proportion of the population leaves Envigado to work in Medellin and returns home in the evening. For this scenario, it was assumed that the population that stays in the municipality will leave the non-residential areas (e.g. schools, commercial areas, and industrial areas) in the night. For this reason, the possible areas where the population can be located at the moment of a hazardous event might be the residential areas (R) and health care establishments (H). Although Envigado has also a substantial entertainment sector, we didn't have enough information to include this in the land use classification and in the night-time population scenario.

Once the tool was run, the number of people by the building was calculated. Then the population was distributed per floor, assuming an equal distribution over the floors (which might not be totally realistic, but we did not have enough information to refine this at this point). Considering that the most threatened people are the ones that cannot evacuate to upper floors in case of a flood or debris flow, the people inside of 1-floor buildings were considered to be the most endangered. However, this might not be true if extreme events occur and reach the second floor. This might endanger the population in 2-story buildings.

Table 4-1. Estimation of the number of people per building type (assuming they are in buildings with Residential or Health land use type) for a night-time scenario in the present situation.

Building type	Building use	Number of buildings in the study area	Night-time scenario		
			Number of people on the lower floor	Number of people on the second floor	Potentially Exposed population
1_Floor Low-rise Single floor	Residential	2706	6861	0	6861
	Commercial	730	0	0	0
	Industrial	194	0	0	0
	Educational	77	0	0	0
	Health	15	56	0	56
2-6_Floors Medium rise	Residential	10337	25557	25557	11471
	Commercial	936	0	0	0
	Industrial	130	0	0	0
	Educational	124	0	0	0
	Health	30	299	299	182
More than 6 floors High-rise building	Residential	1407	2394	2394	0
	Commercial	19	0	0	0
	Industrial	2	0	0	0
	Educational	4	0	0	0
	Health	0	0	0	0
Total	Residential	14450	35167	27951	18332
	Commercial	1685	0	0	0
	Industrial	326	0	0	0
	Educational	205	0	0	0
	Health	45	355	299	238

From Table 4-1 it can be said that the potentially exposed population of low-rise buildings in the AC is 6971 inhabitants (6% of the present population). For extreme events where flood height reaches the second floor, of only 2 story buildings, the potentially population exposed in the night scenario would be 11653 inhabitants (11% of the population of the AC). The final exposure will vary according to the return period of the multi-hazard event modelled. However, this was not performed in the present research but could be used for later research to estimate population risk.

It is worthy to mention that the number of buildings presented in the above table can vary with regard to the official records of the municipality. Given to the errors in the building footprints database, for example 1 building could have been divided into 2 or more features that are considered as individual constructions.

4.2. Attributes of Final EaR database

After processing the data to make them usable, a building shapefile of the study area was produced, with attributes on land use, building type, value per floor and number of people per floor.

This shapefile would be overlaid with the various hazard footprints of floods and debris flows for the various return periods described in the previous chapter, to calculate the losses and risk. The final attributes considered for the building footprint database are presented below in Figure 4-2.

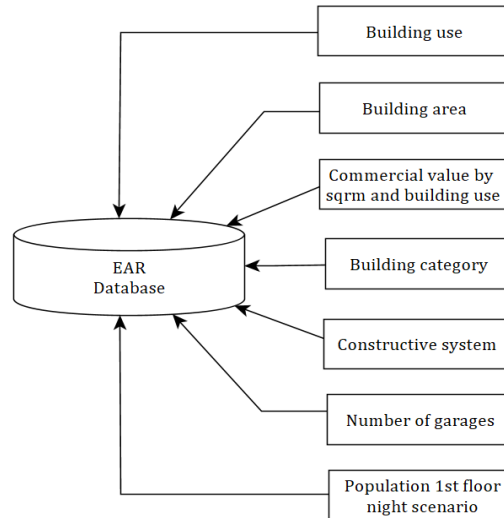


Figure 4-2 Final EaR database configuration.

4.3. Characterisation of physical vulnerability of buildings

For this research, the physical vulnerability assessed was the degree of loss resulting from the interaction between buildings of a certain use and a number of floors with the hazard intensity for floods and debris flows, expressed as material depth (in m). Although it would have been better to express the intensity as impact pressure for assessing the structural damage of flood and debris flows, the resulting velocity data from the OpenLISEM modelling was not considered to be reliable enough. This physical vulnerability was evaluated using absolute vulnerability curves for flooding and debris flow, expressing the absolute damage in Euro/m² as a function of flood or debris flow depth. It was decided to develop absolute curves instead of relative curves (between 0 and 1), due to the presence of many taller buildings, many of which with subterranean garages. The calculation of the loss as the value for the entire building multiplied by the relative physical vulnerability was considered less reliable, than using absolute loss values directly related to depth for the various building types. The exception was for the use of relative physical vulnerability curves for structural damage.

To construct the absolute vulnerability curves four parameters were used: *damage to building contents, structural and non-structural building damage* (only here relative curves were used as will be explained later), *cleaning costs* and *losses of cars in subterranean garages*.

The hazard intensities to be used in the absolute vulnerability curves took into account the multi-hazard (flow-like hazards) character of this research. For this reason, two absolute vulnerability curves were produced: one for water height (flooding) and another for debris flow height, each one defined per building category.

4.3.1. Vulnerability for buildings with residential use (R)

a) Costs of building contents

Building contents, that can be potentially damaged, were calculated by a standard set of possible articles (furniture, equipment etc.) in a surface of reference of 100 m² (which is the estimated adequate space for families of 4-5 people, see section 6.1).

The damage for articles of a single floor and medium-rise buildings was estimated by using the approach shown by van Westen et al., (2011). This approach suggests quantifying the possible damage in function of the water or debris height. For instance, water/debris heights between 0 to 0.5 m will produce complete damage to floor materials (because nowadays, it is common the use of wood or synthetic materials

as decoration of the floor). Similarly, heights between 0.5 to 1 m damage can involve furniture, computers, etc.

For high-rise buildings, the methodology had a slight modification. Since most of the high-rise buildings in Envigado use the first floor as reception (not considered in the damage) and to fit the entrance to the garages, the damage adopted starts from the second floor (above 3.5 m).

The average cost of the articles was obtained from Colombian websites. Subsequently, the total value of articles was calculated by m². Table 4-3 shows the considered articles in the reference surface (100m²); similarly, Table 4-2 displays the differential damage in function of water-sediment or debris flow height.

Table 4-3 Assumed average content for a residence of 100 m²

Article	Number	Price (Euro)
Floor	1	€ 2,857.1
Bed + mattress	3	€ 1,028.6
Tv	2	€ 800.0
Stove	1	€ 285.7
Oven	1	€ 142.9
Fridge	1	€ 571.4
Microwave	1	€ 85.7
Sound system	2	€ 142.9
Washing machine	1	€ 714.3
Sofa	3	€ 857.1
Table	2	€ 228.6
Computer	2	€ 971.4
Curtains	5	€ 428.6
Vacuum cleaner	1	€ 85.7
Kitchen	1	€ 2,857.1
air condition	1	€ 571.4
wardrobe	3	€ 1,285.7
DVD	1	€ 57.1
TOTAL (€)	32	€ 13,971.4

Table 4-2 Possible damage to contents by water-debris heights in residential areas

Flow height(m)	Article	Price(Euro/m2)
0-0.5	Floor	€ 31.4
	1/3(Sofa)	
0.5-1	Bed+mattress	€ 56.6
	Stove	
	Oven	
	Sound system	
	Washing machine	
	2/3Sofa	
	Table	
	Computer	
	1/2 Kitchen	
	Vacuum cleaner	
1-1.50	TV	€ 31.0
	1/2 Kitchen	
	Fridge	
	Microwave	
	1/2 Curtains	
1.50-2	Wardrobe	€ 20.7
	Air conditioning	
	1/2 curtains	
Total		€ 139.7

b) Structural damage to buildings

To obtain the absolute values for structural building damage (excluding the contents) the following approach was taken. 60% of the updated building value per m² (see section 4.1.1) for the residential buildings was multiplied with a damage fraction associated with different relative vulnerability curves for flooding and debris flow. Only 60% of each building value was taken following Bruijn et al., (2014). These authors advice to work with replacement costs rather than the market values (as used by the microzonation of the AV). Because after a disaster the value of reconstruction in principle does not imply profit.

Relative vulnerability curves were researched on literature for flooding and debris flow. However, a large variation was found between the different curves for the same construction types (Bruijn et al., 2014; Godfrey et al., 2015; Huizinga et al., 2017; Nafari & Mendis, 2018). Another issue was that whether vulnerability curves for similar building categories defined in this work are representative for the Latin-American context (e.g. low-rise buildings in developed countries might be not similar to the ones in other regions).

Alternatively, a database of relative vulnerability curves used by CAPRA in the Latin-American context called ERN-Vulnerability (Universidad de los Andes, n.d.) was found. These curves were for buildings with different structural systems and number of floors and relate the damage with flooding depth.

Given the absence of information on the structural systems in the EaR database to relate to the vulnerability curves of CAPRA. A visual comparison between the structure types evaluated by CAPRA (2012), used their relative vulnerability curves, and the constructions observed during field work was

performed (taking into account the building category as a key). As a result, the following typical constructive systems were adopted:

- 1-floor buildings (3.5m) → Construction system: unreinforced, confined or reinforced masonry.
- 2 to 6 floors buildings → Constructive system: reinforced masonry with column-beam systems.
- More than 6 floors buildings → Constructive system: reinforced concrete frames and reinforced concrete walls.

The corresponding vulnerability curves that fulfilled the construction system and building category above from the CAPRA database-ERN-Vulnerability (Universidad de los Andes, n.d.) are presented in Figure 4-3. The curves for medium and high-rise buildings were adapted manually, depending on the number of floors.

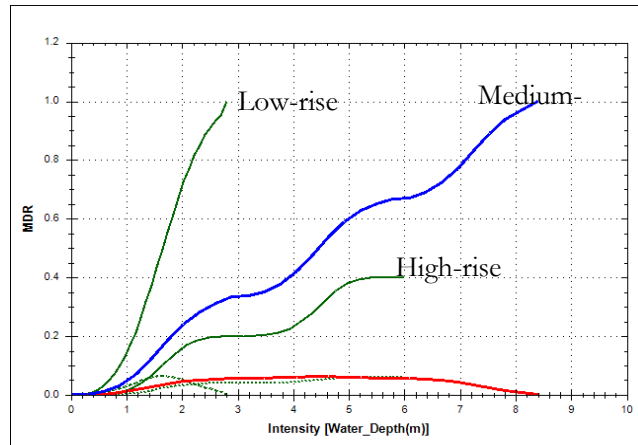


Figure 4-3. Relative vulnerability curves for flooding for residential use and other building uses.

Unfortunately, relations of relative vulnerability for debris flows were not found in the CAPRA database. For this reason, a different approach was taken. Based on the photographic records provided from the municipal authorities (Figure 4-4), buildings of 1 floor (3.5 m) were partially and totally destroyed during the event of 1988 by debris heights around 1-2.4 m (Florez & Parra, 1988). Figure 4-4 shows an area located probably 1 to 2 kilometres upstream of the current urban area of Envigado. From this figure, it can be seen that blocks oscillate between 0.5 to 1.5 m (exceptional sizes were found in the field of 3m).

For the aforementioned a relative vulnerability curve that produces high damage between 1 to 2 m for low-rise buildings was researched in the literature. The selected curve was an empirical curve produced by Ciurean et al., (2017), corresponding to the maximum damage for debris flow height mainly for masonry buildings, see Figure 4-5.



Figure 4-4. Typical material deposited in the Event of 1988 - Source: (AMVA, 2018).

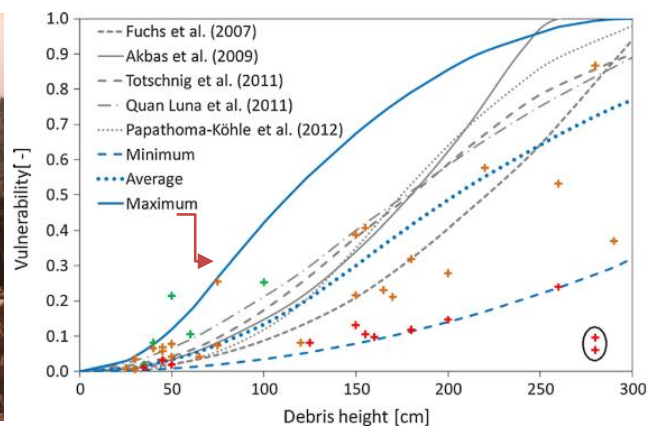


Figure 4-5. Vulnerability curves for buildings between for low-rise buildings (Ciurean et al., 2017).

For medium-rise buildings in the study area, the applicability of relative vulnerability curves was not clear, as it depends very much on the number of floors and construction type. For this reason, it was assumed that buildings under this category will experience structural and non-structural damage only on the first floor, using the same vulnerability curve for low rise buildings. This assumption was taken based on examples of debris flows like the one that occurred in Mocoa in 2017, where buildings of two floors withstood the impact of the debris. This assumption might not apply entirely to the AC since extreme events such as the occurred in Mocoa had immense proportions for the particular setting of the area. However, this cannot be discarded from the catchment in study.

High-rise buildings were considered stronger than medium-rise buildings for the differences in structural systems. As a consequence, the percentage of damage to high-rise buildings was reduced 30% with regard to the medium-rise buildings to represent the resistance provided by reinforcing concrete structures. This value of 30% was considered plausible based on the differences of performance between reinforced masonry and reinforced concrete of different vulnerability curves.

So in summary, for flooding the relative curves were CAPRA used as a basis, but modified for medium and high-rise buildings, and for debris flows the curve of Ciurean et al., (2017) was used as the basis for single floor buildings, but also modified for medium- and high-rise buildings. Eventually, all relative curves were transformed into absolute ones by multiplying with construction costs per floor and land use type. Results will be shown later on in the chapter.

c) Clean-up costs

Two different clean-up costs were used, one for flooding and another for debris flow. Clean-up included water extraction, sediment removal, washing of floors and basic reparations. In this way, 0.57 euros per m² (for water levels between 0 to 1m) were assigned as the rate for the activity. More expensive rates were used, 2.8 euros/m², if flow heights surpass 1m for the added difficulty of cleaning and drying walls. Although these values are assumed based on internet searches of companies that advertised these costs, they were considered reasonable for the salary of construction workers in Colombia. However, if specialised cleaning is required this might increase enormously the price of clean-up costs.

For debris flow, the considered values were substantially higher than for flooding. This is associated with the necessity of removing and transporting heavy solid materials (as rocks, structural elements, wood, mud and water). Thiebes (2016) refers to prices of debris removal in roads of around 1400 € per m³. This, however, was considered excessive for houses, making this task even more costly than the replacement costs of structures. Instead, it was decided to use similar rates as quoted on the internet for debris removal and their respective transport in the building construction sector. This value was estimated as 15 €/m³ (Construdata, 2012; EPM, 2017).

It is important to say that we assumed that all residential and commercial buildings with more than 6 floors had an underground garage with a height of 3.5 m (See assumptions in Figure 4-1). The original garages in the EaR database were not taken into account due to many inconsistencies found (e.g. buildings with one floor presenting more than 1 underground garage). This made it difficult to judge if the reported underground garages were real (e.g. commercial parking) or were due to errors in the EaR database.

The consequence of including underground garages for high-rise buildings was that if they were flooded it would result in additional cleaning costs, and also the removal of cars will need to be considered inside cleaning costs. For this reason, it was assumed that once the flood or debris flow reached 1 m depth on the surface, it would flow in the garage entrance and the garage would be completely filled with material. Under that level, only a basic clean-up for flooding or debris was used. To obtain the clean-up costs of debris in m³ per m² a surface of 1m² is multiplied by the flood or debris height.

d) Loss of cars in underground garages

As mentioned above, flood and debris flow levels of more than 1m were expected to fill completely the underground garages of buildings with more than 6 floors. This would probably create complete losses of all vehicles in these garages. To estimate the value of cars per m² in a garage (supposing full occupation) the following assumptions were taken:

- The floor space of the garage is the same as the floor space of the residential or commercial building with more than 6 floors.
- 30% of the floor space of the garage of high-rise buildings will be occupied by columns, access lanes and other structural components reducing the net space.
- A standard car has an approximate area of 7 m² (4 x 1.7m), and unit value of 14.200 Euro.

Based on the above, an average of 10 cars could be fitted in each garage. As a consequence, considering that a standard car in Colombia is approximately 14200 euros, the potential damage value per m² for flooded garages would be 1420 euros. We have to be aware that this calculation was only because we did not calculate exactly how many cars would be needed to store per building, as very tall buildings might have more households with cars and therefore multi-level underground parking garages. Also, social class and its relation with car values were not considered.

4.3.2. Vulnerability for non-residential buildings

Due to constraints of time and available data, it was not possible to make a similar exercise for non-residential buildings like the one presented for residential ones. To retrieve the value of the contents of commercial (C), educational (E), Industrial (I) and health (H) related buildings, it was necessary to use conversion factors presented by Huizinga et al., (2017), to transform structure values (replacement costs) into content values. These factors are summarized as follows:

- **Damage for contents in commercial areas:** 100% of the commercial building value taking as a reference occupancy types as retail trade, baking, wholesale trade and others.
- **Damage for content in industrial areas:** 150% of the industrial building value considering occupancies as heavy and light industry, food industry and others.
- **Damage for content in educational areas:** 100% of the commercial building taking as a reference occupancy types as professional and technical services, recreation and theatres.
- **Damage for content in health care areas:** 150% of the commercial building.

For the structural damages, the same building categories and structural system of residential areas were adopted. An exception was the building use H (Health) which was assumed with a structure similar to high-rise buildings. This was based on the Colombian regulation that classifies hospitals as special structures.

In terms of clean-up costs, the values proposed for residential structures were used as well. Again an exception was done for the hospitals which will require further cleaning for hygienic reasons. Because value for this task was not found the cleaning costs for hospitals was multiplied by 5, assuming that specialized labour will be required.

In terms of damage to underground parking garages for I,H,E, unfortunately, this aspect was not considered because it was very difficult to estimate the number of cars present, as this depends on time of the day and year and land use. Data for this was lacking. Conversely, commercial areas (that also include governmental buildings) were assigned a garage for high rise buildings, using the same values as in residential areas.

4.4. Vulnerability results: absolute vulnerability curves

Once the costs for building contents, structural and non-structural elements, clean-up and garages contents were estimated per m² they were added. The added value varied in function of the hazard intensity (water and debris flow height). In total 30 absolute vulnerability curves were generated in the form of tables presented in Annex 7. One example of these tables and their graphical representation for medium-rise residential buildings and debris flow is presented in Table 4-4 and Figure 4-6 respectively.

Debris Flow in commercial buildings 2-6 floors					Code:	CF2-6
DF Height(m)	Content	Damage ratio	Structure Replacement	Clean_up	Garage	Absolute value (euro/m ²)
0-0.5	104.6	0.1	46.5	8.1	0.0	€ 159.15
0.5-1	292.9	0.40	186.0	15.6	0.0	€ 494.48
1-1.5	396.1	0.60	279.0	25.4	0.0	€ 700.46
1.5-2	465.0	0.85	395.3	32.9	0.0	€ 893.11
2-2.5	465.0	0.90	418.5	40.4	0.0	€ 923.86
2.5-3	465.0	1.00	465.0	47.9	0.0	€ 977.86
3-3.5	465.0	1.00	465.0	55.4	0.0	€ 985.36
3.5-4	569.6	1.00	465.0	63.4	0.0	€ 1,098.01
4-4.5	757.9	1.00	465.0	70.9	0.0	€ 1,293.84
4.5-5	861.1	1.00	465.0	81.3	0.0	€ 1,407.38
5-5.5	930.0	1.00	465.0	88.8	0.0	€ 1,483.79
5.5-6	930.0	1.00	465.0	96.3	0.0	€ 1,491.29
6-6.5	930.0	1.00	465.0	103.8	0.0	€ 1,498.79
6.5-7	930.0	1.00	465.0	111.3	0.0	€ 1,506.29
7-7.5	1034.6	1.00	465.0	119.4	0.0	€ 1,618.94
7.5-8	1222.9	1.00	465.0	127.4	0.0	€ 1,815.34
8-8.5	1326.1	1.00	465.0	137.8	0.0	€ 1,928.88
8.5-9	1395.0	1.00	465.0	145.3	0.0	€ 2,005.29
9-9.5	1395.0	1.00	465.0	152.8	0.0	€ 2,012.79
9.5-10	1395.0	1.00	465.0	160.3	0.0	€ 2,020.29
>10	1395.0	1.00	465.0	160.3	0.0	€ 2,020.29

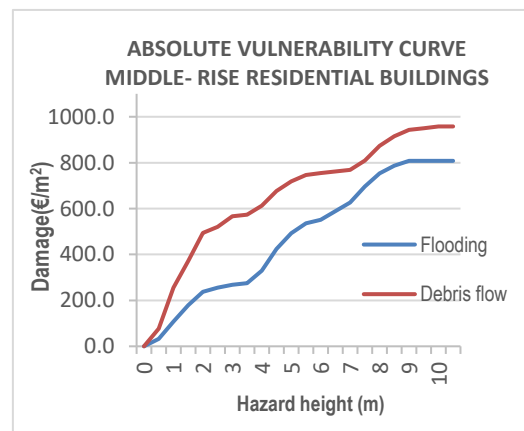


Figure 4-6. Graphical representation of the absolute vulnerability curve for medium-rise commercial buildings

Table 4-4. Example of absolute vulnerability curve for medium-rise commercial buildings and its parameters

In Table 4-4 the field “Content”, for buildings with more than 1 floor (3.5m) the values increase again accumulatively because it was considered that the second floor (3.5-7m) was also residential, and flood or debris flow higher than 3.5 m would affect

that floor. The same consideration was taken for clean-up costs. In Table 4-4 the field “*damage ratio*” corresponds to the damage fractions extracted from the relative vulnerability curve corresponding to the building category. These values were used to obtain replacement costs (or “*Structure replacement*”).

Notice in the same table that commercial buildings have a value of 0 “*Garages*”. In high-rise buildings, this value is replaced by 1420 euros per m² which would entail a high increase in the absolute vulnerability values related to the presence of cars.

4.5. Discussion on the generation of elements at risk and vulnerability data

As it was noticed in former sections, the quantitative analysis of EaR and their vulnerabilities involved a considerable number of assumptions which were related to the lack of data. This implied that the epistemic uncertainty in this evaluation was high. However, the advantage of the approach taken in this research was that it could contribute to the identification of the missing points in the data collection or its availability. Also in cases where it is difficult to acquire the information, similar approaches can be taken to overcome the issues. In this section, some of the main issues related to the methods and assumptions will be discussed.

4.5.1. Discussion for elements at risk

As it was observed in the earlier sections the generation of a workable EaR database for further analyses at local scale requires an extensive number of parameters and assumptions. In the research, building footprints were the basic mapping unit to which the different attributes were related. It is important to work at the building level, as the hazard intensities (flood and debris flow) vary locally and exposure at building level is the only way to assess this. Generalisations and inferences for attributes as building use, structure type and value were necessary. These can impact enormously the results in the later stages of risk calculations, as would also the variations in hazard intensity.

With respect to the classification of building use the hospitals and schools (H and E) were identified manually using satellite imagery, Google Earth and Google StreetView. We had other spatially inaccurate shapefiles with institutional buildings, which could not be properly linked with the building footprints and had to be discarded. The commercial category (C) included the institutional buildings and other not classified categories. The category residential included common buildings with mixed use of residential and commercial. This is common in Colombia and it is necessary for further research to either make a new category or identify the prevalent use of the building. In future research, the building uses might be separated into 8 categories as shown in comprehensive Colombian risk assessments as Yamin et al., 2013). This will allow to improve risk estimations and to homogenize EaR databases at the municipal and national level.

The structural characterisation used was only a generalisation of the typical buildings that can be found in the study area. In future research, a basic characterisation at individual building level or neighbourhood level could be undertaken to get a better vision of the type of structures present in the AC.

A database of values for the buildings was provided by the planning office of Envigado, however, it could not be utilised because the building footprints were merged with units of a greater level of aggregation(parcel). The value of EaR is essential for the calculation of economic risk. Further improvements to the values adopted in this research can be used to calibrate them with a real estate database or data from insurance companies. However, it is preferable to generate a database with the estimated building costs and content costs or if not possible at this detailed level for each land use type. In our study, only residential was estimated in detail.

Another important assumption that was a source of uncertainty is the assumed presence of garages, impacting enormously the value of buildings. Future works need to undertake a real identification of underground parking areas in the areas at risk.

The distribution analysis of population in space and time was complicated as data may not be available for security or privacy reasons. Tools as POPGIS are useful for distribution of population at the aggregated level, using a dasymetric approach. However, unavoidable topological problems of the building footprints in the EaR database produced certain problems. Some buildings (820) were not considered in the distribution of population for the night-time scenario, due to these problems. The integration of the results of POPGIS with the EaR database produced double counting in some buildings which might be related to the topological errors. For future works, the results of POP GIS need to be verified with real building occupation samples taken in the field before making use of them.

4.5.2. The vulnerability of the Elements at risk

The constructed absolute physical vulnerability curves are highly dependent on the amount and quality of the information available. This is especially important for parameters as cleaning costs, which were evaluated with considerable less certainty in comparison with structure and contents. Further work needs to be done in the estimation of the real value of these activities because they might have a significant effect on the risk calculations.

Concerning the application of relative vulnerability curves used to estimate the replacement costs in function of the hazard intensity, some limitations are important to be mentioned:

- 1) First, for both cases, flooding and debris flow, only one descriptor of the hazard intensity (water/debris height) was used: the depth. Given the nature of the impact by debris flow and flash flood (flood caused by excessive rain in short time), it would be better to use impact pressure, but the velocity results from the hazard modelling were too uncertain for that. For example, in some areas water ranging between 1-2m depth for return periods of 25 years seemed to develop flow velocities above 4 m/s. This, according to Clausen & Clark (1990), would produce damage and even complete destruction that might not be considered in relative vulnerability curves based only material height.

For the aforementioned, although impact pressures might not make a difference in the functions used for low-rise buildings they might increase the vulnerability of medium-rise buildings and even of high-rise buildings. Therefore, future works need to explore the influence of impact pressure on the relative vulnerability curves of the structures of the AC. Also, the velocity results from OpenLISEM need to be examined to evaluate their representativity in real conditions.

- 2) The relative curves used in the research were not specifically calibrated for the study area. Specific work with insurance claims could improve this in future.
- 3) By analysing the relative vulnerability curves, the mean Damage Ratio for medium and high rise buildings is very large and depend on the number of floors. For example, in the case of medium-rise buildings, although these curves might be representative 2-floor constructions, this might not be completely true for buildings with more stories.
- 4) The vulnerability curves tried to represent the damage level of events like the one that occurred in 1988. However, up to date, it is known that many of the constructions have changed so variations in the vulnerability might occur. Future research can be done to validate, calibrate or change the relative curves used in this research. For this, historical and post-disaster information of recent events in other catchments and for different building categories and typologies in the AV can be used.

5. ESTIMATION OF PRESENT RISK

This chapter presents the approach used for quantitative risk assessment (QRA) in the present situation (year 2018) for the study area. The risk corresponds to the economic risk of buildings, exposed to hydrometeorological hazards such as flooding and debris flow. The risk results are presented as the average annual loss in Euros using the approach of the risk curve. Some examples of the losses for certain elements at risk (in particular the hospital of the municipality) are presented in the form of maps for the urban area of the AC.

5.1. Methodological approach

In this study, to calculate the potential losses or risk associated with the multi-hazards, the equation presented by van Westen & Greiving (2018) was adapted to represent the multi-hazard risk in the study area:

$$Risk = \sum_{\text{all hazards}} \left(\int_{P_T=0}^{P_T=1} P_{(T|HS)} \times \left(\sum_{\text{all EaR}} \left(P_{(S|HS)} \times \max(A_{(ER|HS)} \times V_{(ER|HS)}) \right) \right) \right) \quad [10]$$

Where:

$P_{(T|HS)}$ = The temporal probability of a hazard scenario or event (HS).

$P_{(S|HS)}$ = The spatial probability that a particular area is affected by the hazard event

$A_{(ER|HS)}$ = The quantification of the exposed EaR for each hazard event (number of buildings)

$V_{(ER|HS)}$ = The vulnerability of EaR given the hazard intensity (for this research in absolute values €/m²)

As flooding or debris flow can occur simultaneously or sequentially during the same event, the damage to buildings cannot be double counted. The original equation of van Westen & Greiving (2018) was modified adding the operator max in part of the equation that defines the losses (resulting from the quantification of the exposed EaR to the hazard footprint multiplied by their vulnerabilities).

With respect to the spatial probability $P_{(S|HS)}$ the value considered was 1. This value indicates the probability that a certain element is actually affected by the hazard. We assumed that when it was modelled as having a certain depth, the spatial probability was 1. In fact, when running many different models the spatial probability could vary depending on the parameter uncertainty used in the model. Due to the long time required for running the OpenLISEM model, and a large number of model runs required, this was not considered feasible. This highlights the deterministic approach used in this research.

With regard to the temporal probability, $P_{(T|HS)}$, this was considered equal to the inverse of the return periods of the triggering event (precipitation) that were used to model the different multi-hazard scenarios in the AC. In short, the temporal probabilities used were 1/25, 1/50, 1/100, and 1/200 years.

The presented risk equation can be implemented in GIS software. Given that the calculation of loss needed to be performed for each hazard scenario the operation was automatized. For this, a script adapted from van Westen (2014) was used in the GIS tool ILWIS 3.4. This script was presented in Annex 8. A loss calculation was needed for every combination of hazard type (flood or debris flow) and return period. For the present situation, this resulted in the calculation of 8 loss scenarios.

To calculate the risk the approach of the loss curves was used. Loss curves plot the temporal probability against the loss for the different scenarios with different frequencies. A curve is fitted through the points. In this curve events of higher magnitude occur with lower frequency and events with low magnitude produce more frequent losses over time. The area under this curve is known as the average annual economic risk. For the AC this economic risk was associated with building losses.

Similar as it was done for the calculation of losses, a second script was run in ILWIS to calculate the area under the loss curve to calculate the risk. This script was presented in Annex 9.

As a summary, Figure 5-1 presents an overview of the steps followed to calculate the risk with ILWIS.

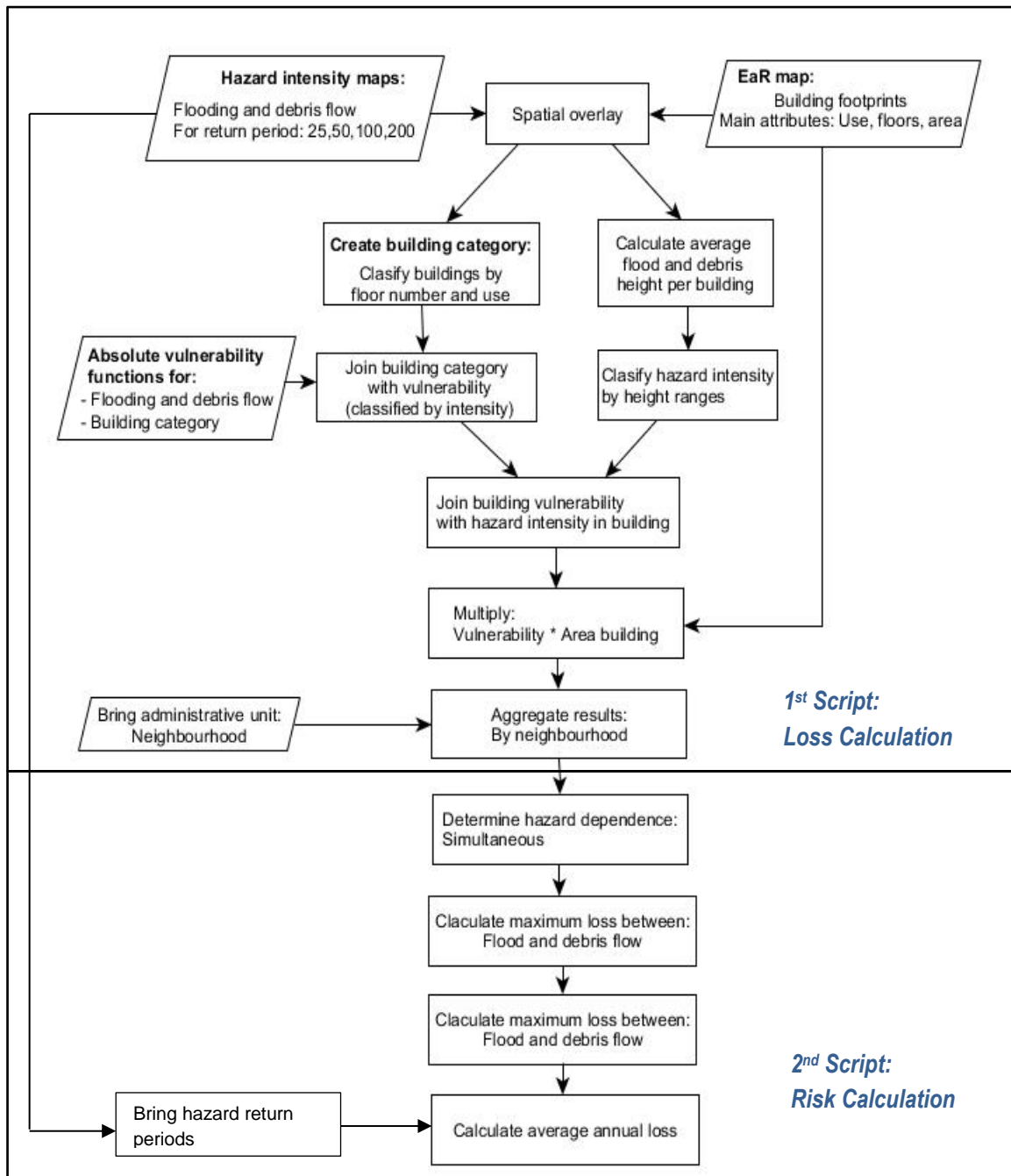


Figure 5-1 Flowchart process implemented to calculate losses and risk for multi-hazards

Two important considerations in the flowchart presented above need to be highlighted:

- 1) Since the spatial overlay between building and hazard footprints was done with raster maps having a pixel size of 1 m resolution, different water/debris heights can be found in each building. Therefore, the average hazard intensity was taken to avoid over/underestimations that were produced when using maximum or predominant values.
- 2) Given that flooding and debris flow developed simultaneously or sequentially, in the risk component, the maximum loss produced between these two hazards was taken. In this way, it was avoided that the damage in one building was counted twice. However, one could argue that when a building is hit by flooding and then by debris flows, the vulnerability would change, and different damage would occur.

5.2. Loss assessment and Risk analysis results

The risk for the current scenario was calculated based on the flood and debris flow height maps for events with return periods of 25, 50, 100 and 200 years, the building map representing the situation for the year 2018, and the obtained absolute vulnerability curves (see chapter 4). As a result, the losses at the level of footprint were obtained and the results were aggregated to the neighbourhood level. The total area under the curve was calculated to define the risk (average annual loss). Figure 5-2 presents the losses in the area of the main hospital of Envigado.

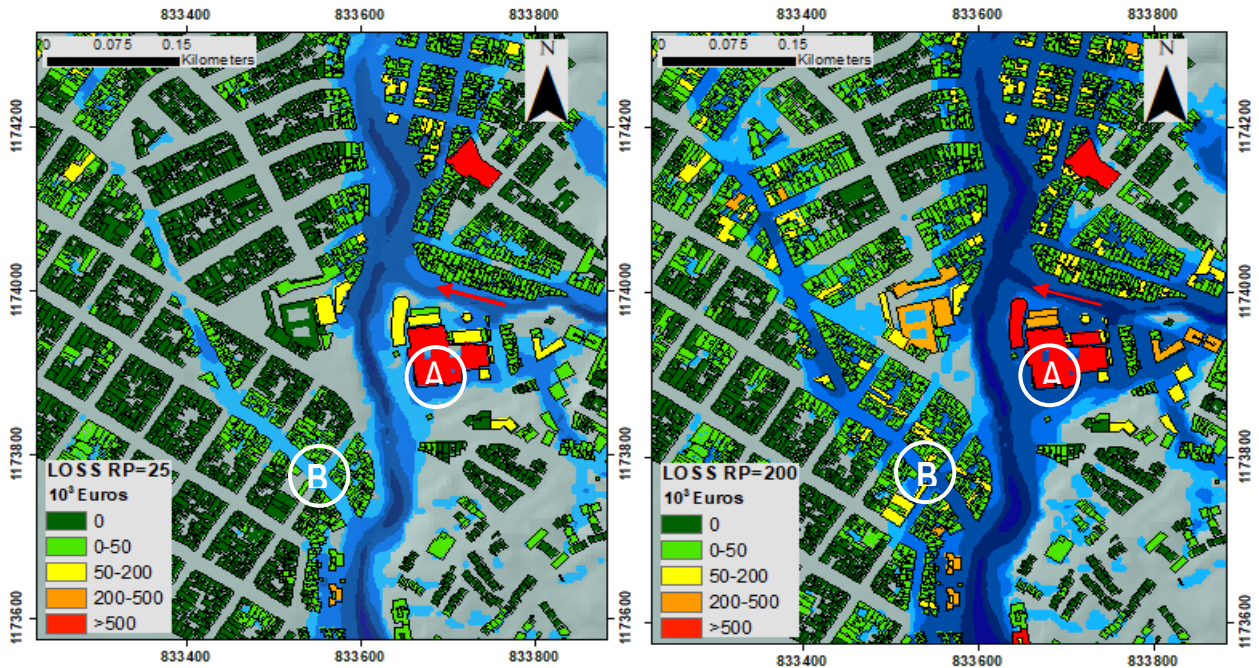


Figure 5-2. Losses in the area of the hospital of Envigado for flow-like phenomena in the return periods of 25 and 200 years. The letter A indicates the location of this hospital.

In the maps shown above, it is possible to see the influence of the rise of water depth in the generation of losses. In this manner, as the return period increased more areas report losses. Although the main building of the hospital of Envigado remained in the same range of loss, it is possible to observe that the increased flow depth from the Ayura stream and the tributary La Sebastiana (indicated with a red arrow) produced a transformation of losses.

It is relevant to highlight that although in the hospital and other buildings the loss maintained in the same range this did not indicate that both scenarios (25 and 200 years) produced the same damage. This was just the effect of the ranges selected as a graphical representation in Figure 5-2. For example, for the hospital the associated loss in the 25 years return period event was 2.5 million euros, while for the return period of 200 years the loss is 4.4 million euros. For this reason, it is necessary for the future to analyse the individual local variation in the loss.

As a summary for the study area, in the Table 5-1 are presented the corresponding values that were obtained for each component of the hazard modelled and their combination understood as the maximum damage between flood and debris flow (see conceptual equation [10]). This maximum value of the losses was calculated by the administrative unit (as indicated in Figure 5-1) or neighbourhoods.

Table 5-1. Potential losses in the present situation in the Ayura Catchment for flow-like phenomena

Hazard Return Period	Flooding	Debris flow	combined average any
25	€ 102,968,649	€ 56,250,681	€ 118,021,830
50	€ 135,502,359	€ 100,305,622	€ 163,339,003
100	€ 168,600,013	€ 127,090,499	€ 202,450,318
200	€ 219,204,378	€ 184,098,003	€ 268,244,953

As it is shown in Table 5-1, the losses for most of the events might surpass 100 million euros. Subsequently, by plotting the values of losses for flooding, debris flow and combined effects, the risks curves for the present situation in the Ayura catchment were obtained (See Figure 5-3).

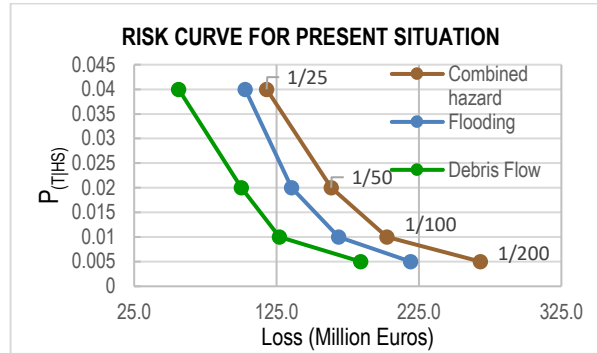


Figure 5-3. Risk curves for flow-like phenomena in the present situation.

As can be seen in Figure 5-3 the combined hazard events produced a risk curve displaced to the right with regard to the individual components. This allowed concluding that effectively multi-hazards produce an increased risk results in the study area. As it can be seen in the figure, for the study area the debris flow produce fewer losses (curve to the left of flooding), however, in other settings or particular extreme events (e.g influence of earthquake), the debris risk curve can displace to the right of flooding. This at the same time might have a substantial effect on the combined losses.

By expressing graphically the losses at the neighbourhood level for multi-hazard events (called before as combined) for the events of 25 and 200 years return period, the maps in Figure 5-4.

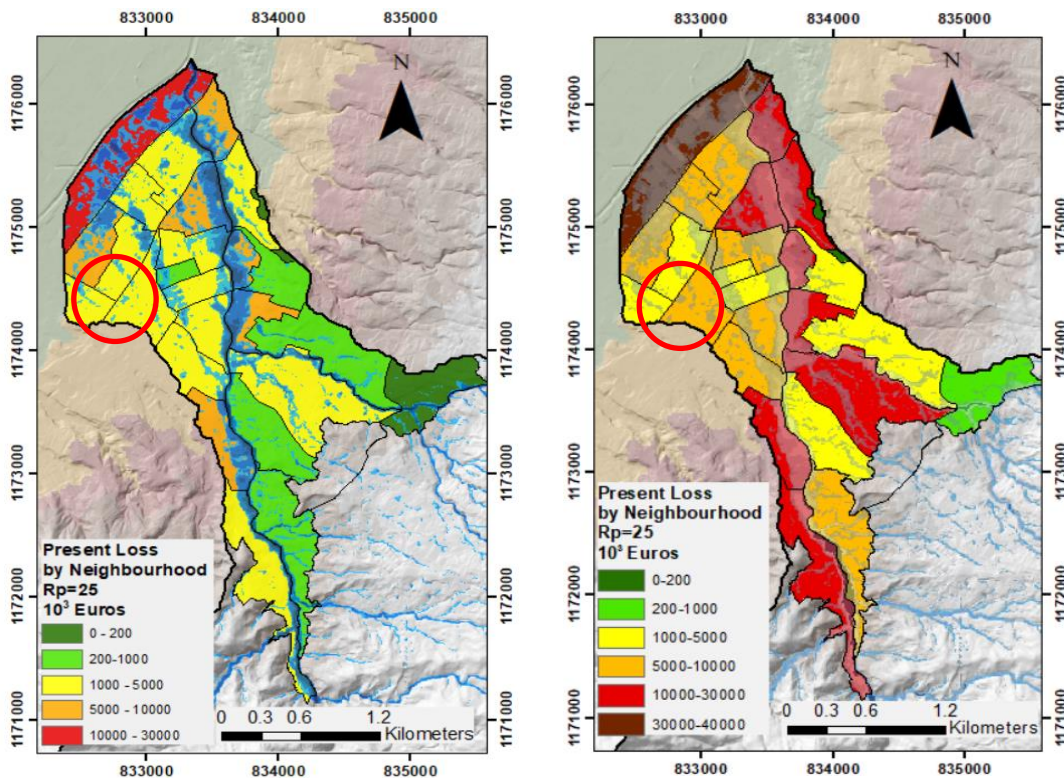


Figure 5-4. Losses for flood and debris flood occurring simultaneously for the present situation in the return period 25 and 200 years.

By aggregating the losses by administrative units as in Figure 5-4, it was possible to better visualise the change between the potential consequences for different multi-hazard events for the whole Urban area

of the Ayura catchment. Interestingly, inside the red circle in the figure, it can be noticed that although the hazard footprint does not significantly overlay the surrounding neighbourhoods, still the losses are above the million Euros.

In terms of the risk for the entire study area, by calculating the area under of the combined curve (see Figure 5-3), the equivalent average annual risk was **6.4 million Euros/year** (for the present situation). This result was further studied and compared with the risk for several future scenarios and with the changing risk due to the implementation of possible planning alternatives (See chapter 6).

5.3. Discussion

The results indicated that the occurrence of flow-like phenomena in the AC will produced losses that could surpass 100 million Euros even for precipitation with a return periods of 25 years. This raises the question if the results are realistic.

When comparing the results with the damage reported in the International Disaster Database EMDAT of the Centre for Research on the Epidemiology of Disasters (CRED, 2019), the disaster of Mocoa in 2017 left losses of approximately 92 million euros. Although this event was a debris flow of enormous proportions carrying blocks of significant sizes (10m diameter), disasters in the study area might be equal or more expensive. This is because, even under lower intensity events as the one in Mocoa, the exposure of EaR in the study area is much higher. The population of the urban area in the study area is three times higher than the population of Mocoa. Also, Envigado has been a centre of investment in the last decades and is known as one of the cities with the best quality of life in the Aburra Valley.

However, this still does not mean that the high level of the calculated loss results is realistic. They depend on three components: the hazard modelling, the characterisation of the EaR and their vulnerabilities. Each of had important uncertainties which were difficult to quantify and were incorporated in the risk modelling. Possible means of improvement for this work are:

- 1) Improved parametrization of the hazard models. This is one of the most important improvements. It is necessary to make sure that the model is using realistic input parameters that represent also the spatial variability.
- 2) Further calibration of the hazard modelling. As mentioned in previous chapters difficulties in the calibration were found. It is not discarded that water and debris height can be lower.
- 3) Consideration of other hazards such as earthquake. As indicated in chapter 2, despite the absence of recent earthquakes in the Aburra Valley, the region is an area with intermediate earthquake hazard. Earthquakes might trigger landslides that under rainfalls of lower return periods will trigger shallow landslides and possibly debris flow as was demonstrated in other environments (e.g. Sichuan, China).
- 4) A more exhaustive characterisation of the buildings is needed. This is true for all attributes, but specifically for the attribute concerning the presence and capacity of underground garages. Similarly, it is necessary to improve the characterisation of the spatial distribution of garages. This research, in the absence of more detailed information, assumed their distribution on the basis of the number of floors which does not reflect the reality. For example, in the city of Envigado, it was observed that medium-rise buildings had parking places.
- 5) In this research the detailed losses were not analysed because the aim was to get a general overview. Nevertheless, the analysis of more detailed losses can be done in loss ranges such as 0-50000 euros (see Figure 5-2). This is important if it is required to know specific buildings or block of buildings might be affected the most. This especially relevant for low and medium rise buildings because 50000 Euros in losses are considerable costs at the level of a single house. However this need to be done with care and supported with detailed risk analysis because the uncertainties related to the model developed in this research.
- 6) Risk cannot be considered as an exact value but a range of confidence. It is important to evaluate the maximum and minimum expected damages using scenarios. As well, it is relevant to evaluate the influence of the uncertainty of the three main input components of the risk. For example, Ke (2014) found that for Shanghai damage functions have the greatest impact on damage for flooding hazard.
- 7) The registered losses in places where the overlay hazard-EaR was not representative might be due to local accumulation pluvial water in DTM pits. This might be a factor of overestimation in the risk in the study area. These problems need to be addressed in future by modifying the DTM or coupling Lisem results with urban flood models because the water can be drained by the city sewers.

6. FUTURE SCENARIOS AND PLANNING ALTERNATIVES

Global and economic changes lead to the modification of the temporal patterns of natural hazards and exposure of the elements at risk (CHANGES, 2014). As a consequence, the risk is expected to change considerably which will make it necessary to consider planning alternatives to respond and reduce the risk. A better knowledge of how the risk will vary can help decision-makers to undertake actions not only for the present situation but as well for future conditions with the maximum benefit for society.

To visualise the possible effects of the economic, population and climate changes the use of scenarios is a solution, which are defined by Malek & Boerboom (2015) as “plausible pictures of the future”. Scenarios are possible future developments, where current decision makers have limited possibilities in influencing which scenario might develop in reality. They can make decisions on possible risk reduction measures that could be implemented now. In this research, four scenarios for the study area for the future year of 2050 were defined (See Figure 6.1). Equally four possible planning alternatives for risk reduction were proposed as seen in Figure 6.1.

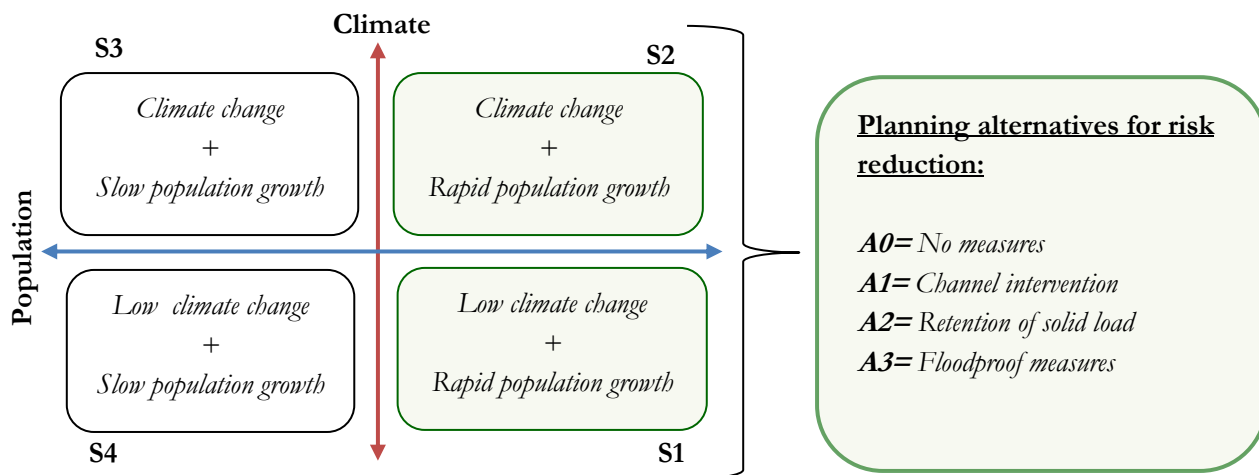


Figure 6-1. Scenarios and planning alternatives for risk reduction. The notation S indicates a scenario, and A means alternative.

For this work, scenarios S3 and S4 were not studied because they were considered as less probable. This is based on the fact that Envigado registers sustained population growth during the last decades, according to the National Planning Department of Colombia (DANE, 2019). For this reason, the scenarios S0 (present situation), S1 and S2 and their combination with the different planning alternatives (A0, A1, A2, and A3) were taken as a reference for the present study.

For the selection of alternatives, the characteristics and state of the catchment were taken into account. It was noticed during fieldwork that the Ayura stream has been already intervened in different ways to reduce the risk. For example, by widening the channel of the Ayura stream, managing the erosion in the mountainous areas and the regulation to restrict the location of new buildings in the areas considered at risk. For this reason, possible ways to strengthen or complement the mentioned measures were to continue improving the hydraulic capacity of the existing channel, the capture of sediments and rocks to avoid the formation of phenomena as debris flow and as well to reduce the vulnerability of EaR already placed in areas at risk that for the demand of floor space require the placement of new infrastructure in threatened areas.

Before introducing how the different scenarios and alternatives were constructed, it is important to highlight the different relations and effects they develop in the modification of the hazard, the elements at risk and their vulnerabilities. This is presented in Figure 6-2.

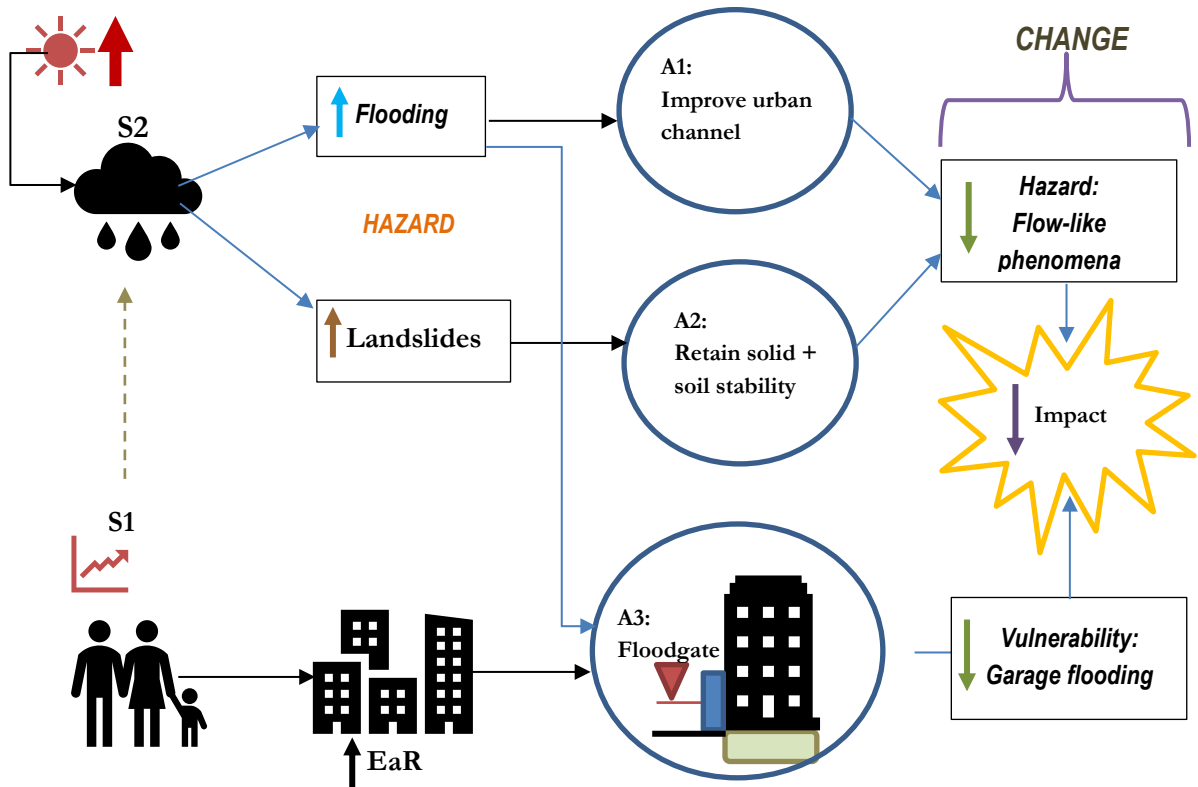


Figure 6-2 Interaction between global scenarios and alternatives in the change of future impacts

6.1. Scenario 1 (S1): Rapid population growth and low climate change

This scenario describes the pressure that rapid population growth will exert on the available residential areas resulting in the transformation of certain parts of the city into more dense residential areas with higher buildings. In terms of climate change, it was assumed that the precipitation does not present such major changes. Therefore, the hazard maps were the same as in the present situation (2018).

6.1.1. Population growth

According to DANE(2019) and Horbath (2016), Envigado has an average population growth rate of 2.06% per year based on the number of inhabitants from 1985 to 2016. If this rate of growth is sustained in time by applying a prediction formula (University of Oregon, 2002) the population by 2050 in the whole municipality of Envigado might be:

$$Pop_{2050} = 219991(1 + 2.06\%)^{2050-2019} = 440.0042 \text{ inhabitants}$$

However, currently, around 10 per cent of an approximate million immigrants from Venezuela have arrived in the region where the AV is located (Portafolio, 2019). For this reason, under the lack of accurate data, it was assumed, that most of the incoming population will locate in four of the most important municipalities of the Aburra Valley (Medellin, Envigado, Itagui and Bello). This might produce a major shift in the population and will result in an additional demand of floor space. Therefore, by projecting to 2050 the population in Envigado might reach 500.000 inhabitants.

To estimate the floors space in m² that the new population will require by 2050, it was necessary to define the minimum required area per person. In Colombia, the legal minimum area for inhabitant is 35 m² for 4 people or 8.75 m² per person (Ministerio de Ambiente Vivienda y Desarrollo Territorial, 2004). This norm applies mainly to the so-called housing of social interest constructed in low socio-economical levels.

Although the general economic conditions of the population of Envigado are higher, in this research we considered using a minimum area per inhabitant of 20 m², which is comparable to the average

floor area per capita of countries as Serbia and Romania (European Union, 2008). Based on the above the required floor space for 2050 is calculated as follows:

Additional population by 2050 for Envigado \approx 280.000 inhabitants

Additional population by 2050 for the study area \approx 140.000 inhabitants

$$\text{Additional floorspace m}^2 \text{ AC}_{2050} \approx 140000 \text{ inhabitants} * \frac{20 \text{ m}^2}{\text{person}} = 2.8 \text{ million m}^2$$

In principle, the increase in floor space will require an expansion of the total building footprint area in the study area. If not controlled, this will produce vast urbanisation towards the rural part of the catchment.

6.1.2. Densifications and new building expansions

In view of the expected growth in Envigado, the Master plan of the municipality (POT, 2011) proposed a number of spatial planning guidelines for future land use. These guidelines were interpreted, for the present study, as urban densifications in height and expansions in specific areas.

Since the POT (2011) only gave general directions at aggregated level rather than identify the specific areas for expansions or densifications by sector, it was still uncertain which specific areas or buildings would be transformed. Therefore, the following assumptions were taken:

a) 70% of the required footprint area (2 million m²) would be located in current residential areas that would be densified, by new taller buildings. Candidate buildings inside those areas were selected based on two thresholds:

- buildings with a height of 3 or fewer floors would be converted to tall buildings,
- buildings should have a minimum surface area of 100 m².

The criteria to assign these thresholds were based on different assumptions such as:

- Most of the residential buildings of 1-3 floors are already older and should be replaced, as long as they do not have important cultural heritage value.
- Surfaces area above the 100 m² are economically profitable and are adequate for the size of average Colombian family (4 to 5 people).

An evaluation of the buildings that met these criteria was made resulting in a total area of more than 2 million m² of floor space. Therefore a random selection was made.

b) 30% of the required floor space in 2050 (0.8 million m²) should come from new expansion areas (nearby to the already urbanised areas). The type of construction to fulfil this was 30% with multifamily apartment buildings with more than 6 floors. The maximum height possible was taken from the POT (2011) and this ranges between 8 to 16 floors depending on the area (POT, 2011).

In this way, 899 existing residential buildings were selected to be densified in height. On the other hand, 337 multi-familiar units were created in expansion areas (0.8 million m²). The population displaced from existing buildings (for densification in height) were located in the expansion areas. For this reason, additional buildings were supplied. In summary, the additional floor space provided was 3'016.132 m², which has the potential to serve a population of 151.000 inhabitants approximately.

Given that Envigado has a clear normative that determines the occupation of the territory it is not expected that the new population can occupy the rural area. For this reason, major alterations in the land cover and in the hydrological processes in the Ayura catchment were not considered, and therefore the urban changes do not directly affect the hazard processes. Changes in the hazard were only produced by climate change.

Densifications would lead to changes in the construction types, number of floors and structural systems, which require a new building map for 2050. Also, the vulnerability of the buildings would change. For example, in the densification areas, most of the buildings are intended to surpass the 6 floors. This will require the introduction of underground garages, which will alter the vulnerability substantially.

In Annex 10 the possible buildings to be densified and the new buildings for expansion are represented spatially.

6.2. Scenario 2 (S2): Rapid population growth and climate change

For this scenario, the same population grown and its consequences described in section 6.1 was used. However, it was considered that climate change will modify the frequency and intensity of the precipitation which is the driving force of intensification of the hazard situation in the catchment. To represent the change in precipitation the IDF curves of the present situation (2018) were modified.

6.2.1. Climate change and its effect on hydro-meteorological hazards

The special report on extremes (SREX), published by the IPCC (2012), highlights that the frequency of heavy precipitation will likely increase in the current century. Changes in the frequency of precipitation periods can lead to positive feedbacks in terms of detonated events. More frequent intense rainfall will affect directly the production of shallow landslides and flow-like phenomena with solid phase, while increases in total rainfall will influence the detonation of deep-seated landslides (Gariano & Guzzetti, 2016).

IPCC (2012) mentioned that climate change can produce that annual maximum precipitations with a return period of 20 years occur more frequently, for example with return periods of 5 -15 years. In this way, to represent modifications in precipitation the rainfall was increased for each of the return periods used to model the hazard of the present situation or 2018 (see section 3.1.8). To do that, the IDF curves for 2018 (see section 3.1.8) were modified, projecting them to 2050.

AMVA (2018) projected the present IDF for a 100 years period, by multiplying the rainfall intensity of the 99 percentile with a growth rate. This rate was found using an analysis of the historical precipitation from 1996 to 2016 in the different catchments of the AV (see Figure 6-3). These projections according to the authors are valid for rains of short duration (less than 3 hours), so they affect mainly the rainfall intensity.

The equation of the IDF curves produced by AMVA (2018) for climate change is shown below; as well their graphic representation in Figure 6-4. Same as in section 3.1.8 the alternate block method was used to produce synthetic rainfall events from the IDF.

$$I = \frac{1167.8 * t^{0.23}}{(d + 7.3)^{0.89}} \tag{11}$$

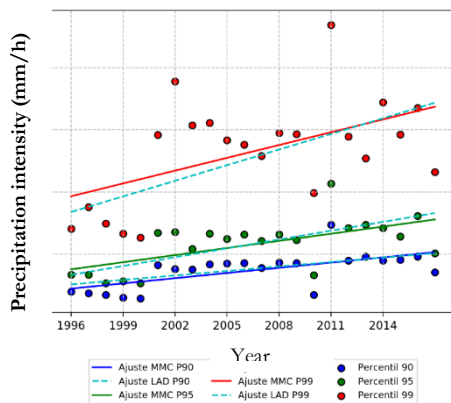


Figure 6-3 Precipitation trend graph produced by climate change by AMVA(2018).

Although the values are not visible the most important is to see the growing precipitation intensity.

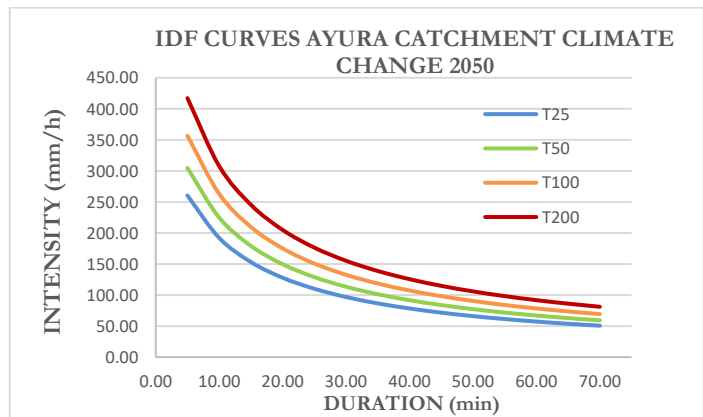


Figure 6-4 IDF curve produced for climate change in the AC

The new hazard situation with climate change was modelled with OpenLISEM for the return periods of 25, 50, 100 and 200 years. A series of eight new maps were produced for debris flow and flooding for the year 2050. Figure 6-5 shows the percentage of change between the flooding map in 2018 and 2050 with the influence of climate change for a return period of 25 years. As can be seen in this map, a large part of the area flooded by the same frequency event in 2018 might experience an increase in water height between 20-50 per cent by 2050. This, in combination with the increased value of the exposed elements-at-risk, will result in an increase in risk by 2050 (following this scenario).

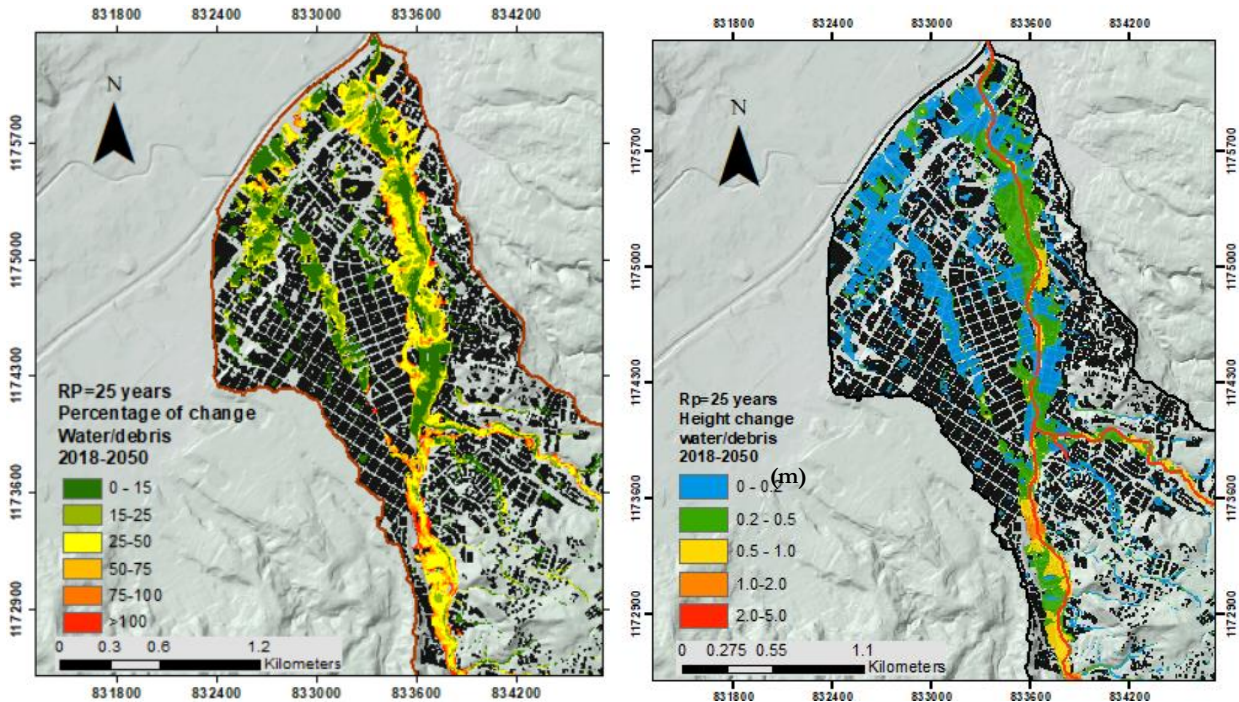


Figure 6-5 (left) Percentage of change in flow height between 2018 and 2050 for the action of climate change. Notice that this change was only for pixels that were flooded in 2018 and 2050. However, by 2050 additional flooded pixels might appear. These were not taken into account in the calculations. (Right) The corresponding absolute map (in m) indicates the increase of water level for climate change action.

6.3. Alternative 0 (A0): No alternative

This alternative assumes that the municipality does not implement any new risk reduction alternative in response to the increase in risk. Therefore the current hazard, EaR and vulnerability were used to calculate the risk for the present situation. In Scenario 1 and 2, the modified building map for 2050 was used either in combination with new hazard maps (for scenario S2) or the existing hazard maps (for Scenario 1).

6.4. Alternative 1 (A1) : Channel intervention

One of the obvious risk reduction alternatives was to improve the hydraulic capacity of the Ayura stream to reduce the impact of hazards in the urban area. For this, some actions needed to be undertaken. First the removal of obstacles and the cleaning of the channelized section of the Ayura stream. Low bridges were considered as obstacles because they reduced the section of the current channel. Cleaning consisted in the removal of debris and other materials to allow a faster flow on the concrete surface of the channel bottom. Second, the expansion and the deepening of the channel in specific areas.

Given that removal of individual obstructions would require a detailed modification of the DTM, an alternative procedure was followed. The original channel of the Ayura stream was removed by interpolating the elevations of the pixels nearby to the margins. Subsequently, a new rectangular channel with dimensions of 15m wide and 5m deep was subtracted from the filled DTM. Finally, the original margins of the river/channel were re-established to avoid the generation of false low points contributing to flooding. It is important to remark that also a fraction of the tributary stream “La Sabastiana” mentioned in section 5.2 was modified as well to obtain a channel with a cross section of 10 x 5 m (see Figure 6-6). The goal of this was to improve the water flow in proximity to the main Hospital of Envigado and reduce flooding.

The average dimensions for the channel with full hydraulic capacity (section 15 x 5 m) were selected in accordance with 24 sections measured in the field by AMVA (2018). The removal of obstructions, in general, improved the general hydraulic capacity (see Figure 6-6) but certain issues appeared. In some areas, the original channel was more than 5m deep, but the implementation of the new section in the DTM overlooked these features (reducing the original hydraulic capacity). As a solution, in the points where the problem occurred the original depth prevailed.

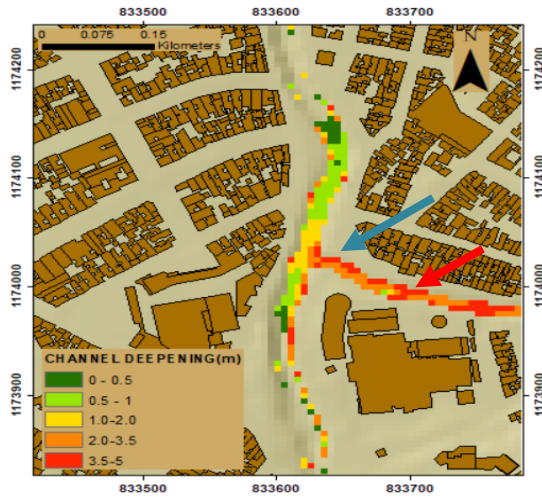


Figure 6-6 Channel improvement in the area of the Hospital of Envigado. The map was produced by subtracting the DTM with the improved channel from the original DTM. The blue arrow indicates the discharge of the tributary "La Sebastiana" in the Ayura stream. The red arrow shows some of the inconsistencies found. It was unexpected to find highly deepened pixels in the middle of the channel, this could have occurred for defects on the DTM.

To simulate the cleaning of the channel the rugosity of the channel was altered by reducing the Manning's n value. In this way, the original Manning value (0.053) was reduced to values of clean concrete (0.015), according to Chow (1959). Manning reductions were expected to increase the flow speed and reduce the loss of energy caused by obstructions (Phillips & Tadayan, 2007), which will derive in a faster evacuation of water and less flooding. For this alternative, the existent concrete channel was expanded in the DTM 1.2 km upstream. This expansion was performed to confine more the flow. This measure might reduce the impact of potential debris flows (Mavroulli et al., 2014).

Once the DTM was modified to place the improved channel, OpenLISEM modelling was carried out with the new set-up. This was done for the combinations between the Alternative (A1) and the Scenarios S0, S1 and S2. The corresponding hazard maps for debris flow/hyper-concentrated flow and flooding were produced and used as input for chapter 7. Figure 6-7 shows the reduction of hazard intensity (expressed in percentage) for the implementation of this alternative. In Figure 6-7, only the effect of the channel intervention is shown for the return period of 25 years under climate change.

As it can be seen in Figure 6-7, the intervention of the channel might produce a general reduction of the flow depth (water/solids) mainly along the main channel of the Ayura stream. However, it is important to notice that in some areas of the map the implementation of the channel might lead to an increase of the hazard intensity. This might have occurred because probably in those areas some hydraulic insufficiencies were present. Therefore, higher transported volumes of material in the channel will produce increased flooding in those areas.

In Annex 11 it is presented a view of the modifications undertaken in the entire channel of the Ayura stream.

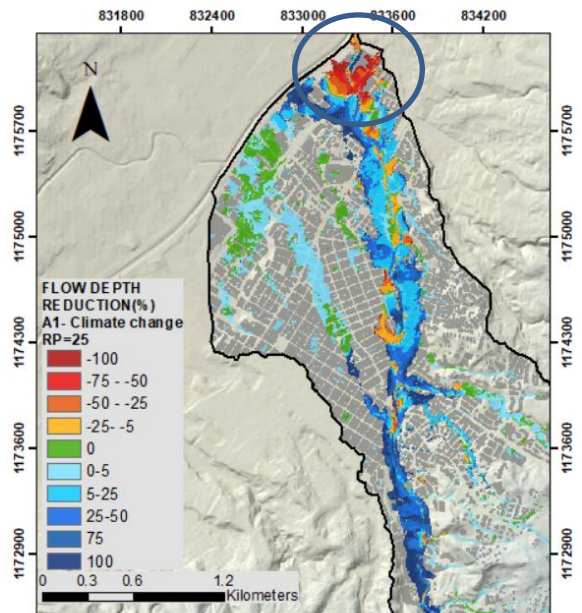


Figure 6-7 Flow depth reduction rate for the implementation for channel improvement. Return period of hazard: 25 years under climate change

6.5. Alternative 2 (A2): Solid load retention measures and slope stability measures

As mentioned by Mavroulli et al., (2014), flow-like phenomena such as debris flow can be difficult to handle because the generation points can cover immense areas in very different locations. While slope stability works can help locally, the management of the mountain system can be approached with ecologic measures aimed to increase the resistance to erosion and cohesion produced by root systems. The existence of added cohesion for root action might prevent the occurrence of shallow landslides under high-intensity rainfall (Kuriakose et al., 2006).

Additional measures can be taken to reduce the hazard intensity:

- Barriers for shallow landslides in prone areas (Wendeler et al., 2014).
- Catchment-scale solutions that intervene in the soil-water path. These solutions contribute to the reduction of the flow energy by adding jumps (using check dams) or by reducing the number of sediments and rocks, for example, retention basins, high resistance nets, by-passes etc (see Figure 6-8).



Figure 6-8 Example of retention structures. Retention net of high resistance for the capture of solid load. Source: Wendeler (2016)

Given that the historical occurrence of destructive debris flow in the AC is not very high (taking into account the common life span of civil engineering works) the above solutions can be implemented without incurring in highly recurrent maintenance that could make these projects less feasible.

For the present work, retention basins were modelled with OpenLISEM but the results were not used in the final analysis (see discussions section 6.8). Instead, a package of solutions intended to reduce shallow landslides occurrence and to capture sediments and rocks was proposed as Alternative 2. It was assumed that this package of solutions would perform correctly avoiding the formation of debris flows. As consequence, no debris flows were expected for this alternative, and therefore, intensity maps of 0 values were used. In other words, in the calculation of risk, only the flood hazard maps were considered for Alternative 2.

6.6. Alternative 3 (A3): Risk reduction measures – Hydraulic protection for parking places

For this alternative, no modifications of the hazard were made, but interventions with flood gates to protect the underground garages in high-rise buildings were proposed. The configuration of these solutions was such that they can seal the underground parking completely, avoiding the entrance of water and debris.

This countermeasure was aimed to reduce the vulnerability itself of residential and commercial buildings. For this reason, the hazard is not modified and accordingly OpenLISEM is not used to model a new situation. Therefore, to reflect the effect of this counter measures the absolute vulnerability curves are modified removing the damages of vehicles and the cleaning of the underground garages.



Figure 6-9. Example of protection system to seal off underground garage entrance to avoid flooding

6.7. Integration of possible future scenarios and planning alternatives

Table 6-1 summarises in a matrix the possible combination between scenarios and alternatives used for the research:

Table 6-1 Combination of scenarios and alternatives for the AC

Scenario	Alternative	Year		What changed in modelling? With respect to 2018 S0 A0		
		2018	2050	Hazard	EaR	Vulnerability
S0 Current situation	A0 no alternative	A0_S0	No future trends taken into account Hazard, EaR and vulnerabilities are constant	No	No	No
	A1 Channel intervention	A1_S0		Yes	No	No
	A2 Retention of solids	A2_S0		Yes	No	No
	A3 Floodproof garages	A3_S0		No	No	Yes
S1 Only population change	A0	Does not exist	A0_S1	No	Yes	No
	A1		A1_S1	Yes	No	No
	A2		A2_S1	Yes	No	No
	A3		A3_S1	No	No	Yes
S2 Climate and population change	A0	Does not exist	A0_S2	Yes	Yes	No
	A1		A1_S2	Yes	No	No
	A2		A2_S2	Yes	No	No
	A3		A3_S2	No	No	Yes

From the above table, it is worthy to mention that although for the present study the alternatives did not modify the EaR, measures as A1 and A2 might require the relocation of certain buildings. This will produce an impact in the EaR, however, relocation effects were not considered, but need to be considered in future studies.

Annex 5 presents the different hazard maps produced for each combination of scenarios and alternatives. These maps were used in chapter 7 for the quantitative estimation of risk changes.

6.8. Discussion

6.8.1. Rapid population growth and its effects

Some limitations in the estimation of future population and its effects in the demand of new floor space were:

- 1) The population by 2050 was estimated using a future growth formula and a hypothetical incoming migrating population. Although the population projection was done with a procedure widely used, it is possible to apply more robust methodologies as the cohort method that considers different components in the urban growth such as survived population, number of births and migration (Smith et al., 2013). This would imply that more information is available especially data about migration because it has a major impact on the projections. For example, the number of people assumed by 2050 from the Venezuelan migration. If this population would not have been considered, the amount of additional floor space would be reduced by 1.2 million m², which is equivalent to 750 multi-familiar apartment buildings of 100 m² with 16 floors. Therefore, it is necessary that in future works accurate information about migration, age groups are collected to make a better projections. However, as there is no certainty about changes in political and economic development, they remain possible, but not certain, scenarios.
- 2) The Master Plan of Envigado has validity up to 2023, so the expansion regulations used might change in future years and might change completely as compared to the one used in this study. Also, the expansion scenario was one interpretation of the POT (2011), for this reason, it is necessary that future works focus on joint work with the planning office of Envigado to improve this interpretation and represent with the higher quality the planning strategies of the municipality. Close collaboration with urban planners is needed.
- 3) As mentioned a distribution of 70/30 % was respectively used to model the future densifications and expansions. However, other distributions such as 50/50 were tested. As a result, given that the allowed densities in some expansion areas were only of 2 floors, the city would require to expand in the rural areas. This would lead to a drastic transformation of the catchment landcover, as it has occurred in other

catchments in the AV where steep slopes were occupied. This led to the conclusion that it is necessary for future works to evaluate more scenarios, for instance, unplanned growth options.

6.8.2. The validity of the climate change scenario

A concern with the IDF curves for the scenario development of climate change was their representativity for 2050. The IDF curves were projected for a climate change scenario for the subsequent 100 years. For this reason, a validation process was undertaken using a climate change report of the Meteorological office of Colombia (Armenta et al., 2014). According to this study, for the scenario RCP 8.5 in the region of the Aburra Valley, the precipitation might vary between 10-20% for the years 2011-2040. This percentual range is in agreement with the precipitation increase (14.3%) showed by the IDF of the present and future situation by AMVA (2018). Therefore, under the lack of more detailed information, the IDF curves for climate change were adopted. This assumption was a source of important uncertainty, making it necessary to further study climate change trends for different years and ranges in the AV.

6.8.3. Modelling the hazard of alternative A2

To model the planning Alternative A2 in OpenLISEM the model was adjusted to not simulate neither the solid fraction in flow (that creates the interaction between landslides and flowing water) nor the slope stability (shallow landslides). Surprisingly, contrary to what was expected, it was found that the flood map produced higher water levels in different parts of the area creating even more risk than with the inclusion of solids. As a consequence, it was preferred to use only the flooding maps.

A clear explanation, for the mentioned unexpected behaviour, was not found. However, by looking at the modelled flood time series (using PCRaster) with and without sediments, it was noticed that in certain areas if sediments are considered, water overflows earlier (upstream), generating a dissipation effect downstream. Therefore the maximum water level is reduced in the area. Conversely, without sediments although water is more confined to the channel (avoiding early flooding upstream), in specific locations where the channel (downstream) has hydraulic insufficiency, the entire water mass cannot be managed. As consequence, a localised but bigger water volume flood certain areas.

The above is one hypothesis that needs to be tested in future works along with a careful application of the risk for these kind conditions. It is expected that debris flow produces more risk, therefore an approach to reflect this in the results is including impact pressure in the setting of the model.

Other tests to model sediment retention structures in OpenLISEM were performed by creating holes in the DTM, in early deposition areas of the Ayura stream and its tributaries. These holes simulated retention basins with a total capacity of 25.000 m³. The results showed that apparently in some areas (e.g. area de Rosellon, see Figure 6-10) the debris flow was reduced. It is important to test further the implementation of this type of solutions using OpenLISEM in order to evaluate if their behaviour can be well represented.

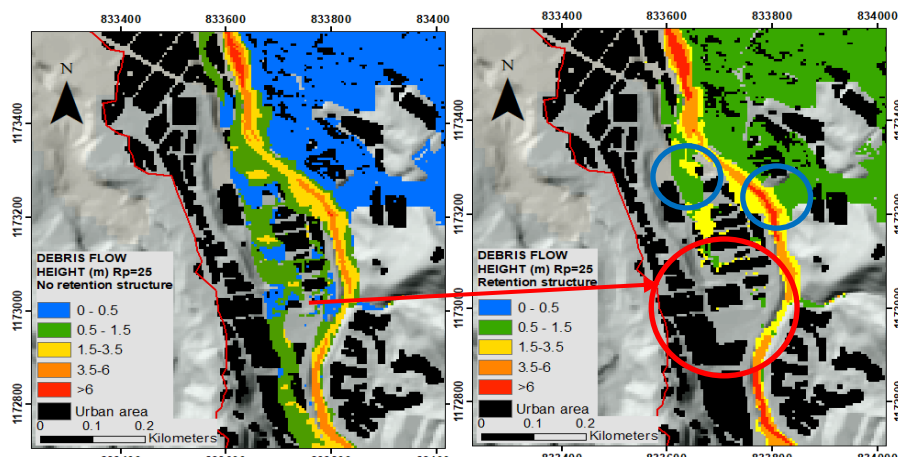


Figure 6-10. Debris flow height before and after the implementation the sediment retention structure. Although there is an apparent reduction of the debris flow (red circle), in some areas the debris height increased.

7. ANALYSING CHANGING RISK

As it was presented in previous chapters, the action and interaction of different components on the natural and social system can produce that the hazard, the elements at risk and their vulnerabilities vary over time. This explains the dynamic nature of the risk. Not considering this fact can lead to unexpected outcomes if a hazard hits a community.

The study of changes in risk is vital in planning for disaster risk reduction. First, it creates the awareness that actions need to be tailored not only for today’s problems but for future challenges. Second, and most importantly, it increases the levels of decision support. This is because the quantification of the future change is the key to visualise which planning alternative for risk reduction perform the best under different circumstances.

The aforementioned is a clear necessity of decision makers. Commonly, as mentioned by Newman et al., (2017), the studies intended to support the decision making identify hazard areas, the consequences and in some cases they test different risk reduction options. However, the evaluation of the performance of these options is less explored leaving the decision makers without a sense of the trade-offs of each alternative. Therefore, the final choices either do not integrate the risk information or implement actions that easily become obsolete.

In light of the previously mentioned, this chapter illustrates how the risk changed in the AC for the influence of the scenarios and the alternatives exposed in previous chapters. So first, the modification of losses were calculated using the same methodology of chapter 5, second the modifications of risk were estimated taking into account the risk reduction of each alternative, and third an overview of the variation in the performance of the different alternatives is presented. In addition, a preliminary economic evaluation for the alternatives with the highest risk reduction was undertaken to evaluate their feasibility using Cost-benefit-analysis(CBA). This evaluation is presented in the Annexes.

7.1. Changes in losses for the influence of the scenarios of population growth and climate change

By using the scripts exposed in chapter 5, the losses for the scenarios S1 and S2 were estimated and expressed using the loss curve.

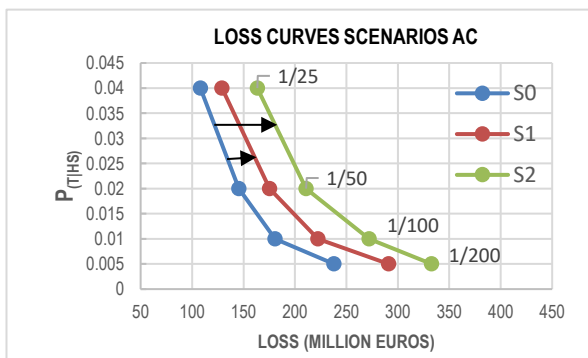


Figure 7-1. Loss curve for the present situation (S0) and for future scenarios: population growth and low climate change(S1) and for population growth and climate change (S2).

As can be noticed in the Figure 7-1, the effect of the scenarios is an increase of the losses with regard to the present situation(S0). This is visualised as a lateral displacement to the right of the loss curve of the scenarios S1 and S2 with regard to S0.

By calculating the area under each loss curve the average annual risk of each scenario was:

Table 7-1. Average of Annual risk of present and future scenarios in the AC

Scenario	Average annual risk	Risk Increase
S0	€ 6,400,111.84	-
S1	€ 7,769,521.55	21%
S2	€ 9,333,129.13	46%

In Annex 12 the losses for the occurrence of a multi-hazard event with a return period of 25 years under the scenarios S0, S1 and S2 scenarios is presented. This representation was useful to observe the influence of the different scenarios in the generation of potential losses for the entire urban area.

7.2. Changes in risk for the implementation of alternatives

To reduce the risk in the different scenarios, the alternatives (A1, A2, A3) proposed in chapter 6 were implemented. 3 combinations of the alternatives were explored: risk reduction (in euros) for the implementation of individual alternatives, risk reduction for the combination of alternatives for hazard reduction (A1+A2,) and the risk reduction for the combination of the 3 alternatives (A1+A2+A3). The results are shown as follows:

7.2.1. Changes in risk for the implementation of alternatives in the present situation(S0)

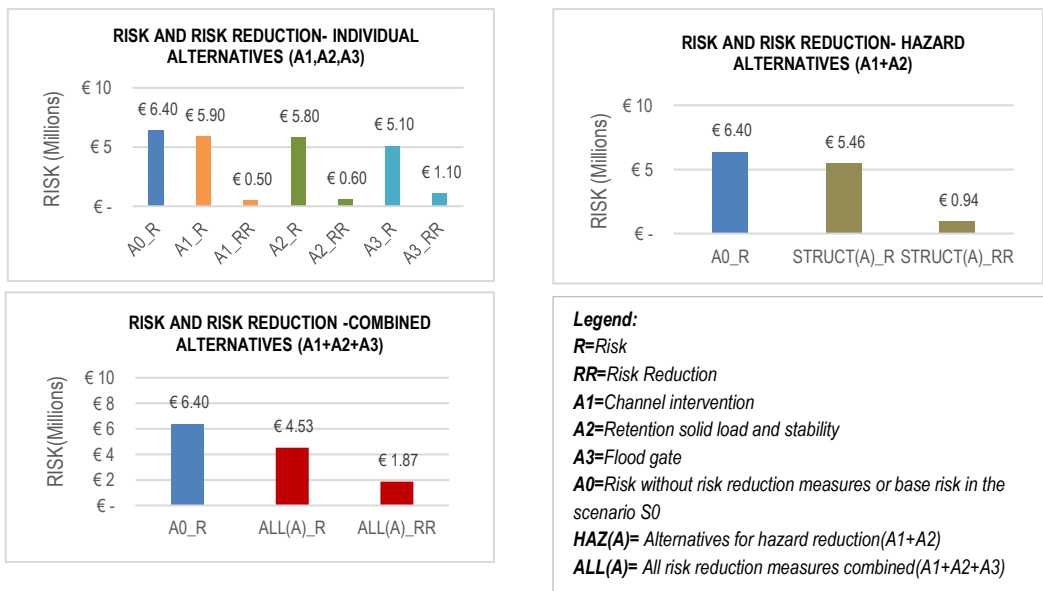


Figure 7-2. Risk reduction of risk reduction measures in present scenario(2018)

7.2.2. Changes in risk for the implementation of alternatives in the future situation(S1)

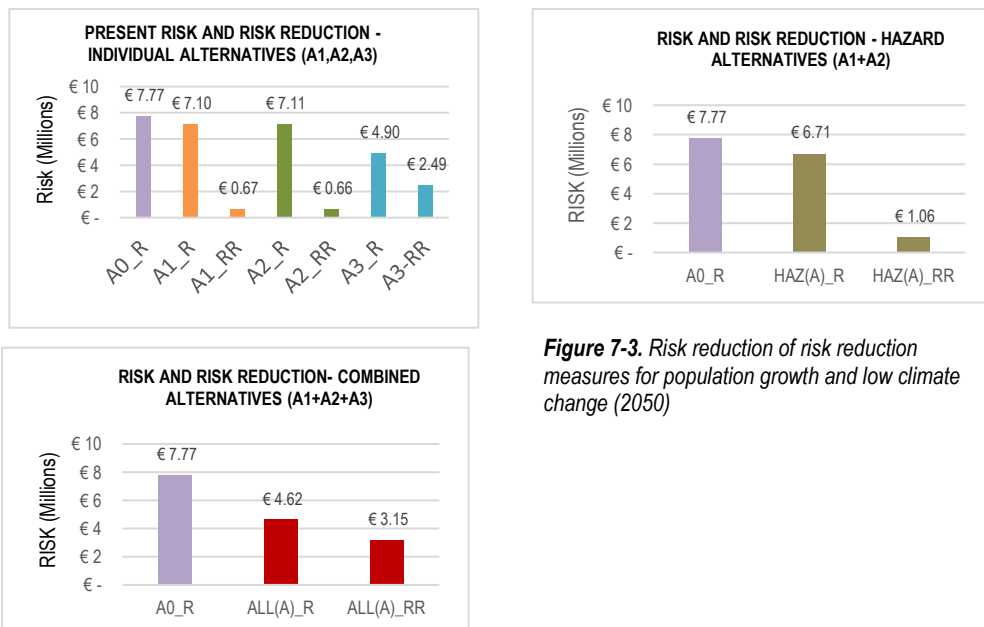


Figure 7-3. Risk reduction of risk reduction measures for population growth and low climate change (2050)

7.2.3. Changes in risk for the implementation of alternatives in the future situation(S2)

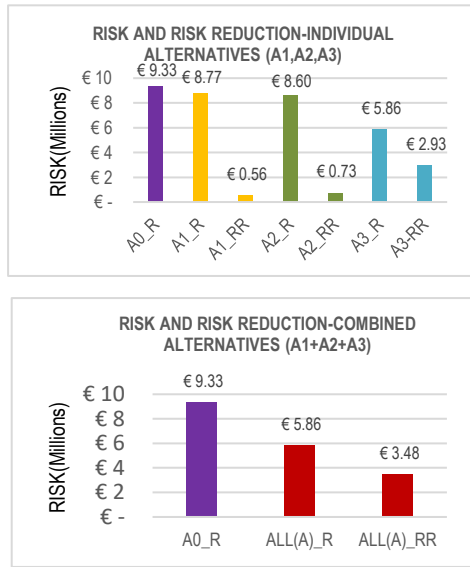


Figure 7-4 Risk reduction of risk reduction measures for population growth and climate change (2050)

By looking the Figure 7-2, Figure 7-3, and Figure 7-4 it can be concluded:

- In Figure 7-2 it was noticeable that the risk reduction for the present situation (A0_R) of the alternatives A1 and A2 (A1_RR, A2_RR) was very low. On the other hand, the alternative A3(A3_RR) presented a better performance in risk reduction compared to A1 and A2. By combining the alternatives A1 and A2, the risk reduction did not present a substantial improvement. But if all the alternatives were combined(ALL(A)_RR). the risk would be reduced approximately 30%
- In Figure 7-3 the risk for the future scenario S1 increased 20% with regard to the present situation (S0). The alternatives A1, A2 in the scenario S1 reduced almost the same risk than they do in the present situation. However, the risk reduction of A3 was 32% taking the scenarioS1(A0_R) as a reference. On the other hand, by combining all the alternatives the risk change was approximately 40%.
- In Figure 7-4 the risk for the scenario S2 increased approximately 46% compared to the present situation, and 20% with regard to the scenario S1. Same as it happened in S0 and S1 the alternatives A1 and A2 did not show a representative risk reduction neither individually nor coupled. Conversely, the alternative A3 (A3_RR) produced a 31% of risk reduction taking the base risk in S2 (A0_R) as a reference. All the alternatives combined produced a risk reduction (ALL(A)_R) of 37%.

7.3. Loss changes for the influence of the scenarios of population growth and climate change

The risk reduction previously calculated is the result of the variation in losses for the implementation of the alternatives. One example of this shown below:

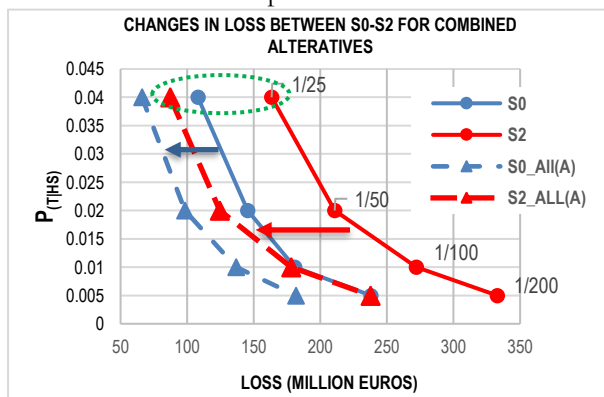


Figure 7-5. Reduction of the losses in the scenarios(S0) and the future scenario with climate change (S2) for the implementation of planning alternatives.

As it can be seen in Figure 7-5 the introduction of the alternatives produced a displacement of the loss curve towards the left as signalled by the blue and red arrows.

In Figure 7-6, it is presented the spatial representation of the losses associated to an event with a return period of 25 years (dotted area in Figure 7-5) in the area of the Hospital of Envigado.

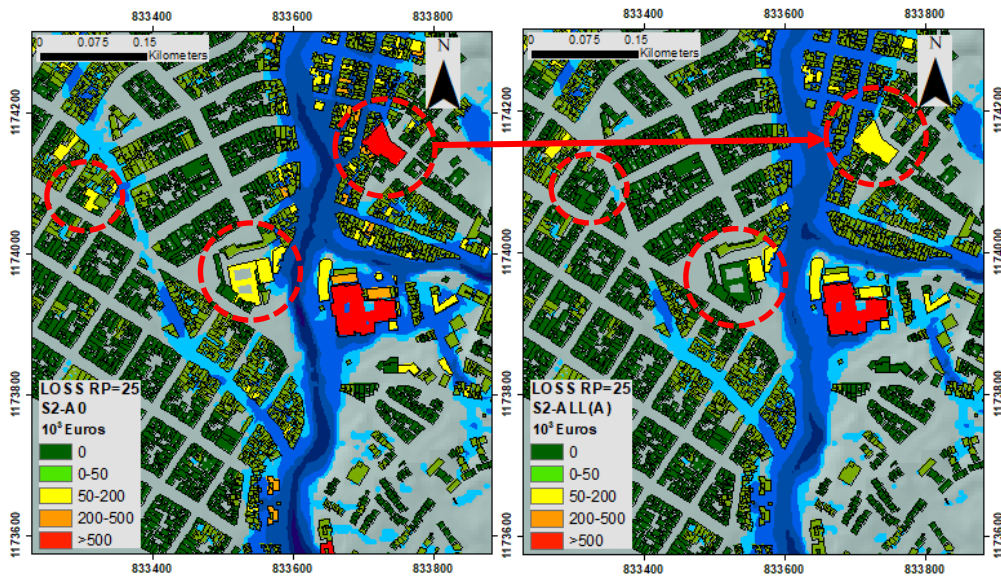
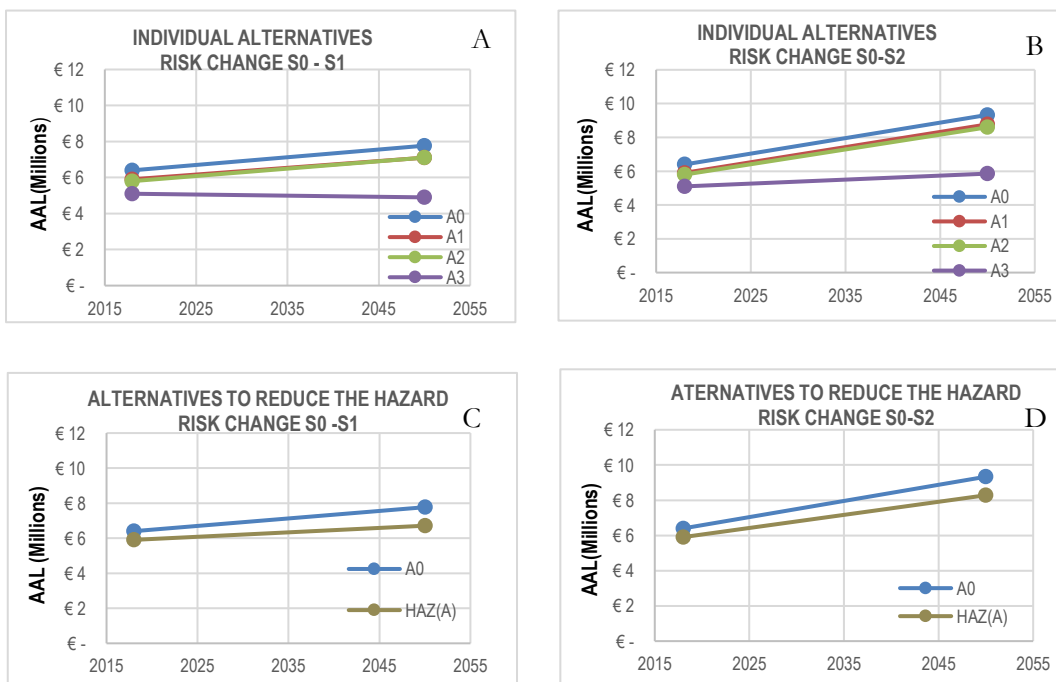


Figure 7-6 Loss reduction (change) for the introduction of the combination of alternatives in the scenario of climate change and return period of 25 years.

In Figure 7-6, it is presented, inside the red circles, the loss in some building footprints for the implementation of the combined alternatives (A1+A2 +A3). For the hospital, the loss without planning alternatives under climate change (or S2) was 2.5 million Euro. When the combined alternatives were implemented the loss in the hospital reduced to 1.9 million Euro, which was equivalent to a reduction of the 24%.

7.4. The behaviour of alternatives – Risk changes between scenarios

The risk reduction values of the previous section indicate that the most efficient alternative for all scenarios was the combination of A1, A2 and A3. Nonetheless, the behaviour of each alternative was explored to visualise how the risk change from one scenario to other. This is shown in the following charts:



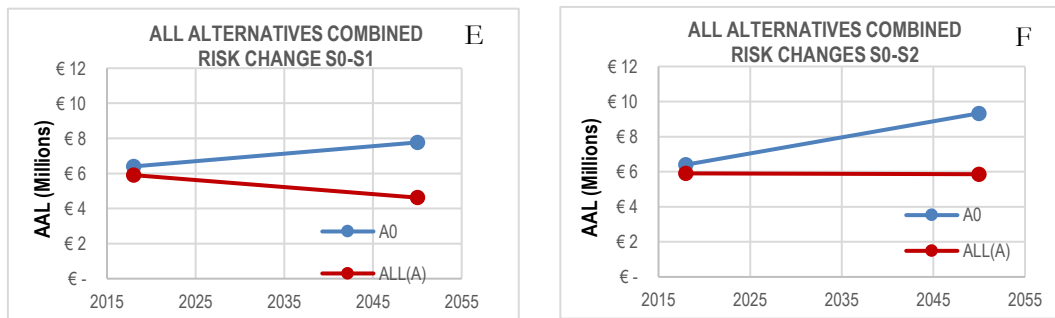


Figure 7-7 Changing in the behaviour of the alternatives by scenario

- In charts A and B, it is noticeable that A1 and A2 offered almost the same proportion of risk reduction in the time and for both scenarios (S1 and S2). Charts C and D allow visualising that when both hazard measures (A1 and A2) are combined the proportion of risk reduction lightly increases in the future situation (2050).
- In charts A and B, as the time pass the alternative A3 tended to maintain the risk levels. When the alternative A3 is combined with A1 and A2, an interesting effect was noticed: the alternative (ALL(A)) either was capable to maintain constant the levels of risk in time considering the scenario of climate change (see chart F) or managed to reduce the risk into a lower levels than in the present situation (see chart E).

7.5. Best performing alternative for risk reduction in the Ayura catchment (AC)

In the light of the calculation of risk reduction and the analysis of the behaviour of the alternatives in time, the alternative with the best performance to reduce the risk in the AC associated to flow-like phenomena is the combination of the alternatives A1, A2 and A3. Nonetheless, A3 seemed to be the alternative that produces the highest proportion in the risk reduction.

However, the highest risk reduction is not a sufficient criterion to select an alternative since different constraints can play a role. One of them can be the economic feasibility. In this manner, if the alternative performs correctly but the costs of undertaking it exceed the benefits received in time, the alternative will need to be re-evaluated or rejected. A tool to perform this evaluation is known as cost-benefit analysis (CBA). For this reason, in Annex 13 a preliminary CBA was performed to evaluate the economic feasibility of the two alternatives with highest risk reduction obtained in this research: the combined alternatives (A1+A2+A3) and the alternative to reduce vulnerability (A3). These results were only one indicative but require further development in a full and comprehensive economic evaluation that was not possible in this study.

7.6. Discussions

The estimation of the risk changes developed in this research left some interesting points to be highlighted:

- 1) Contrary to what was expected the planning alternatives for hazard reduction did not produce a significant risk reduction for any of the scenarios considered in this research. This does not indicate that structural solutions for the channel solutions are directly discarded. Before it is necessary to explore other configurations with the contribution of stakeholders as engineers and the planning office. Subsequently, a new risk analysis needs to be run again to evaluate if improved measures provide a considerable increase in risk reduction and economic feasibility.
- 2) During the elaboration of planning alternatives in chapter 6, it was possible to foresee that the implementation of floodgates would represent the highest reduction of the risk. This was because the alternative avoided the damage of expensive assets such as vehicles inside the garages. As a consequence, it can be said that planning alternatives for vulnerability reduction have an important role in the study area. Thus further exploration about the impact of these measures is required. Some options that can be assessed are flood-proof measures for low and medium rise buildings.

- 3) By analysing the situation of the Hospital of Envigado it could be noticed that the implementation of all alternatives in a climate change scenario reduced only the 25% of losses in this place (of a total of 2.6 million euros). This allowed visualising some of the limitations of CBA to define which alternative is the best. Since CBA cannot consider where is the loss, even if high reductions are achieved, when vital places as the hospital of Envigado get damaged, the risk might not be tolerable and new measures would require to be analysed.
- 4) Newman et al., (2014) remarked that the costs of risk reduction need to be contrasted with the wealth of the party that will address the investments. For this reason, in the economic evaluation of measures for the municipality, the investment always needs to be contrasted with the availability of economic resources. Otherwise, the development of a well-performing measure could not have the economic support, making the alternative unfeasible from the perspective of the municipality and external funding would be required. As well stakeholders need to be consulted before implementation, floodgates can be polemic among the community and can be rejected. Therefore, new measures would be required to be evaluated .
- 5) The preliminary economic analysis developed in this study only considered direct damage. The implementation of the alternatives might avoid the disruption of activities that were not considered in the analysis. Similarly, structural measures for risk reduction were considered in the analysis. Similarly, the benefits of non-structural measures such as early warning systems, spatial planning and ecological measures are difficult to be implemented in a CBA s. However, measures such as the restriction of the construction of buildings with more than 6 floors outside of hazard footprints can represent also an enormous reduction in future losses (because garages would not be flooded). On the other hand, combining structural and ecological measures, for example in natural areas, can serve as points for the capture of water and solids and as well as touristic points. This condition can be found upstream of the area of the Rosellon close to the beginning of the urban area. This is called the park of El Salado, which is a zone for tourism and nature enjoyment. This might be adapted as for water and solid load retention.
- 6) Concerning to the methodology used to analyse risk changes, this needs to be strengthened in the sense of supplying the simultaneous visualisation of:
 - The risk reduction amount (how much).
 - The location of risk reduction (where).

This could help decision makers to ask or propose adjustments tailored to the needs of specific areas.

8. FINAL DISCUSSION AND CONCLUSIONS

8.1. General discussion on the estimation of risk changes

Each of the chapters of this thesis contained a discussion section that highlighted the findings and limitations of the individual components in the process of studying the risk changes. Based on these discussions a common denominator found was the role the uncertainty, and a large number of assumptions that had to be made.

According to van Westen & Greiving (2017), the uncertainty is ingrained in all the components of risk assessment. However, although uncertainties will always be part of the study of the risk, it is necessary to understand what are their sources and to quantify them. This allows visualising to what extent uncertainty can be reduced with further studies. The benefit of an improved understanding of the uncertainty not only allows to represent better the reality but also to make more accurate predictions as well to reduce the number of unexpected outcomes when hazards occur.

A clear source of uncertainty of this work were the assumptions used to perform the quantitative risk assessment. For this reason, in Table 8-1 a list of the most important assumptions with a qualitative evaluation of their impact in the risk estimations is presented.

As can be seen in Table 8-1, there were many assumptions mainly related to the lack of data or data quality. Conversely, fewer sources of aleatory uncertainty (non-reducible with the methods currently known) were found. Starting with the latter, one example of aleatory uncertainty is the soil depth. Soil depth can vary spatially from site to site; therefore the prediction of soil depth is only applicable at small scales. This entails that different initiation points of shallow landslides were not modelled or were overpredicted according to the local conditions.

With regards to epistemic uncertainty, assumptions that can be further discussed are: soil data, inclusion of buildings in the DTM, the model calibration, the applicability of vulnerability curves, location of new high of new high rise buildings for densifications, climate change scenarios and validity of flood gates and linked assumptions for the solution of flooding for underground garages (see Table 8-1).

In terms of soil parameters of the Ayura catchment, the soil type classification was a major source of uncertainty. Which was, in this case, epistemic uncertainty as there was not enough knowledge and data available to map soil types in the forested and the urbanized areas in the watershed. However, while is true that for the catchment a more detailed characterisation of soil parameters can be done to improve the model, during fieldwork a considerable heterogeneity of the materials was noticed, due to the complex geology and heterogenous colluvial soil masses. This makes a detailed characterisation of the materials by soil units a challenging task that might be difficult to be carried out by the municipality. The colluvial soil materials are highly heterogeneous and their characterisation needs to be done in detail which is difficult at catchment level. The generalisation of soil parameters leads to an overall generalisation in the modelling that is rather problematic, especially for landslide related modelling. It is recommended that all geotechnical investigations are recorded in a central database linked to soil types so that over the years the characterization of soils improves.

The overall impression after carrying out the hazard and risk modelling is that the hazard scenarios tend to overpredict the flood and debris flow hazards, especially for the short return periods, given the fact that apart from the poorly documented 1988 event, there had not been devastating debris flows or floods in the study area. Also, the effect of the mitigation measures on reducing the hazard intensities is considered too low. This should be further addressed in future research.

Model calibration was a very particular issue. Given the lack of data about the specific landslide locations in the upper part of the AC and discharge data in the outlet or water height produced by precipitation events, it was not possible to calibrate the model with measured features. The only option was a comparison with other models outputs by AMVA(2018). These outputs were produced with 1D flood models constrained to the stream section and nearby areas. However, the modelled footprints with OpenLISEM were more widely distributed in the area. Although in control points of calibration, water heights corresponded between models, the spread areas cannot be judged. More detailed data for calibration is essential to define if the OpenLISEM results were overestimated. In terms of landslides, it is essential to map past landslides as polygons, differentiating the areas of initiation and runoff. In future they should be

Table 8-1 Summary of main assumptions in the research and their probable effects on risk.

COMPONENT	Assumption	Estimated level of uncertainty	Effect level on the research risk analysis
Hazard Modelling	Soil type distribution and properties	Medium-High	High
	No Inclusion of buildings in the DTM is a good representation of reality for modelling	Unknown	Unknown
	Model Calibration assumptions	Medium-high	Very high
	DTM represents the area correctly	Unknown	Very high
	No inclusion of root cohesion	Medium	Medium
	Land cover was developed with updated imagery and with good accuracy	Medium	Medium-high
	Non-inclusion of seismic results	Medium	High
	Modelled antecedent rainfall is accurate	High	High
Elements at Risk	Building footprints are accurate	Medium-High	High
	Building use assumptions	Medium	High
	Building valuation results	Medium	Medium
	Buildings >6 floors with garage	Low	Very high
	Construction type-construction system	Low-medium	High
	Building class or category	Medium	High
	Population distribution over buildings	High	Low
	House occupation in night scenario	High	Low
Vulnerability	Distribution of population by floor	Medium	Unknown
	Composition of the vulnerability curves	Medium-high	Very high
	Resistance of medium-rise buildings to debris-flow on the first floor	High	High
	Health care structural system stronger for medium and high rise buildings	Medium	Low-medium
	Content cost estimation per package	Medium	Very high
	Clean-up costs estimation	High	High
	Flow height on surface that fills entire garage	Low-Medium	Medium
	Effective surface area for cars in garages	High	High
QRA	Occupation level of garages	High	Very high
	Temporal probability equals to the return period of triggering hazard event	Medium-High	High
Future scenario development	Spatial probability is modelled area and is 1	Medium	Medium
	Climate change scenario- Precipitation increase	Medium	Very high
	Rapid population growth	Low	Very high
	Migratory population from Venezuela	High	Very high
	Land occupation normative is used	Low-medium	Very high
	Building type of new buildings	High	High
	Minimum area of new apartment buildings	Medium-High	Medium
	Location of building densification and expansions	Medium-high	Very high
Risk reduction alternative development	Possibility to acquire old buildings to build new ones	High	Very high
	Change in the sediment production by deepening channels is managed	Medium-high	Medium
	Solid load retention measures fully work	High	High
	Flood gates can be implemented everywhere	High	Very high
Risk change analysis	Flood gates withstand debris flow	High	High
	IRR value	Low	High
	Investment required in countermeasures	High	High

they should be mapped regularly, together with the occurrence date and the associated precipitation (including antecedent precipitation).

In terms of vulnerability, the absolute curves that were considered valid for the study area. However, these assumptions might differ from reality and should be based on a calibration with the damage recorded in an actual disaster event in the study area, based on insurance records and other damage data. Additionally, the variation of vulnerability and the level of uncertainty should be quantified. Vulnerability curves can produce different outcomes with the same water height depending on building age, the variability of contents due to differences in income levels of the population, duration of flooding and warning time.

With regards to new high-rise buildings for the densification scenario, a random location in the study area was assumed. This was unrealistic because the normative of Envigado in the POT (2011) restricts the construction of new buildings near to the river. In future to solve this problem, with the collaboration of the urban planning office, a buffer along the stream can be created to restrict building construction inside of this buffer zone. However, one should be aware that new areas need to be found which might also be problematic from other points of view (e.g. earthquakes, technological hazards).

Concerning the changes in frequency related to climate change, although the estimations of precipitation by AMVA(2018) reflects an increasing trend, it is difficult in the light of the period evaluated (1996-2018) to say that this tendency can be extrapolated to 2050 and even 2100 (as performed originally in the study of AMVA). More studies need to be developed in the area including downscaling of regional precipitation ensemble forecasts.

Finally, the limitations about the selection of floodgates as the best performing alternative need to be raised. The risk associated with this measure was calculated using several assumptions. First, that only buildings with more than 6 floors would have an underground garage. For this reason, it is necessary to make a correct characterisation of the parking places. Second, a questionable assumption was that all parking places were fully occupied at the moment of the flood and debris flow simulations. In order to improve this, it is necessary to include the probability that certain number of parking places are used at the moment of an event occurrence. A third assumption was that the flood gates are strong enough to also withstand debris flow impact. It is necessary to evaluate the changes in vulnerability of future floodproof measures using a multi-hazard view. This requires to consider the behaviour of the alternative under impact pressures that can be developed at high speed and high solid load. A fourth assumption was that the implementation of floodgates was adjusted to the investment proposed. This is questionable, because, even if part of the costs can be absorbed by constructors, it is not sure who will bear the elevated costs (e.g. insurance companies, an organisation of apartment owners, or local governments). High cost for producing higher impact-protecting systems could make that the alternative turns unfeasible.

8.2. Conclusions and future work

Global and economic changes lead to the modification of the temporal patterns of natural hazards and exposure of the elements at risk (CHANGES, 2014). When these modifications have the potential of producing negative outcomes, society tries to respond either by eliminating or reducing the impacts. After this, a new state in the system is generated which can be influenced by further changes in a dynamic cyclic process.

Aligned with the aforementioned, the aim of this research was to use a quantitative risk assessment to estimate the changes in multi-hazard risk in a mountainous area of Colombia prone to flow-like phenomena. The drivers of the risk changes were scenarios of population growth and climate change and the use of planning alternatives for risk reduction. To undertake this study different assumptions were necessary to overcome the lack of data and to visualise possible future situations. With these assumptions, the different components of the risk were addressed. First the hazard, second the assessment of the EaR, third the estimation of the present risk, fourth the visualisation and construction of future scenarios and the proposal of planning alternatives, and finally the assessment of risk changes.

In terms of hazard, the multi-hazard model OpenLISEM was used to characterise flow-like phenomena such as flooding, hyper-concentrated flow and debris flow. To parametrise this model different secondary data was collected and adapted to be used as input layers for the modelling. The calibration was done trying to reproduce the water height of other models developed in the same region and the discharge modelled by hydrological studies. Given the lack of information about shallow landslide occurrence in the official inventories, validation was undertaken by reproducing some of the footprints left by a flow-like

event (debris-low) in the year 1988. As result, two different hazard maps were produced. These were Flooding and debris flow depth maps. These were modelled for different return periods, based on the analysis of historical rainfall condensed in IDF curves. Although it cannot be proven with other data, the impression was that the hazard maps overpredicted the debris flow and flood depths, especially for the lower return periods. Also, the modelled hazard reduction effects of the proposed risk reduction alternatives (e.g. channel widening, and sediment retention structures) had relatively limited effect on reducing the modelled flood and debris flow depths. Future works need to address issues as improved parameterization, development of calibration schemes, integrating the influence of seismic forces, the treatment of DTM with high-resolution data to make it compatible with the requirements of OpenLISEM especially with regard to the artificial channel that the model used to calculate discharge and flooding.

The characterisation of the Elements-at-risk was done by collecting from the municipal planning office of Envigado the information about building footprints and creating a final database with attributes such as building use, building category, value, constructive system and presence of garages. All these attributes presented different issues that were solved with different methodologies. In particular, the information on building use was not complete for the building footprints, so aggregated information was used to fill the missing information. Information on structural systems was not available, for this reason the buildings were classified in categories based on number floors. These categories and observation in the field were then used to extrapolate the structure of all urban buildings in the study area. One important attribute that could not be retrieved for inconsistencies in the original database was the presence of garages. Therefore it was assumed that only high-rise buildings had this. Many topological errors and inconsistencies in building features were found, and many of these errors could not be solved. Future works in the area need to aim to produce databases with complete attributes and free of errors. LiDAR point cloud processing would be one of the best options to obtain new building footprints and associated elevations. The absence of attribute characterisation can be overcome partially with the census developed in Colombia every five years. The next census was executed in 2018 but the results will be available after 2019.

The characterisation of the vulnerability was done by constructing absolute vulnerability curves that considered contents, clean up, garages and structural and not structural damages associated to flow height (main hazard intensity parameter considered). It was questionable whether depth is the best intensity indicator for debris flows, and future work should also focus on modelling this with physically based models. It is important also to improve the absolute structural/non-structural vulnerability curves, obtained from CAPRA and studies of debris flow events elsewhere. Future work needs to be directed to obtain relative vulnerability curves for structural damages tailored to the structural types in the study area. Recent events in the region can be used as a reference either to construct new curves or make calibrations.

The estimation of the present risk was performed using ILWIS scripts to automatize the calculations. The results indicate that for extreme rainfall events, that include antecedent rainfall, with return periods of more than 25 years the losses can surpass 100 million Euros and the Average Annual loss for the study area is estimated to be around 6 million Euro per year. Similarly based on the loss results, given that the values for combined events were very close for the events of 25 and 50 years, mitigation for the 25 years return period event might have a high impact in the risk reduction. However, this needs to be re-evaluated with a well-calibrated model. along with the adjustment of the elements-at-risk and their absolute vulnerability values in Euro.

Visualised future scenarios corresponded to the combination of rapid population growth and the variation in the effects of climate change by 2050. This future year was selected because the policies of future development in the municipality reach up to 2030, and at that time the effects of climate change might become evident. To define population growth the projections of the census of 2016 were used as a basis to estimate population by 2050. An additional increase was done for the immigration of Venezuelan migrants. Of course, the latter is depending on the political and economic developments in Venezuela and Colombia, and these may be entirely different from now in 2050. The impacts of this population growth on the risk changes were modelled by generating a series of densifications and expansions of multi-storey apartment buildings. This is applicable only if the general urban planning lineaments of Envigado are followed. On the other hand, climate change projections were based on IDF curves developed for the municipality in which the precipitation for each return period was increased. By comparing the present precipitation for the different return periods it was estimated that climate change in average will produce an increase of the 14% in precipitation amounts by 2050. The climate change IDF curves were used to generate new precipitation events which were modelled again in OpenLISEM to produce new hazard maps. As results, higher floods

and debris flows were modelled as expected. As concluding remark, future works require to address the following points: 1) Static vulnerability. In this study, the vulnerability of the EaR did not vary with time. The future vulnerability curves need to include factors as the ageing of structures and other aspects. 2) Validation of IDF curves for climate change. Given the limited data used to elaborate climate change IDF curves, it is not possible to confirm their validity. Therefore more studies about climate change in the region of the Aburra Valley are recommended or included in the estimations.

The definition of planning alternatives was done taking into account the current state of the intervention of the studied catchment. In terms of the hazard, given that the main stream of the municipality has already been intervened with a concrete channel, additional works were recommended to confine the flood and debris flow inside the channel. In addition, structures to retain solid load carried for the streams were proposed. In terms of vulnerability, given the high value of vehicles in underground garages, the effect of floodgates to seal the entrance of material was considered the most important risk mitigation measure. With regard to elements-at-risk, no alternatives were recommended (e.g. relocation), but future densifications and expansions were taken as a reference and located in a way that the catchment did not suffer more transformations.

To model the modification of the hazard for the implementation of the alternatives OpenLISEM was used. However, not sufficient successfully results were obtained. First, the removal of sediments from the modelling simulation produced higher flood depths. Given this unexpected and unexplainable result, only the flooding map was considered in risk calculations. Second, the improvement and expansion of the channel did not reduce the water levels considerably to produce an important decrease in the risk. Further work needs to address comprehensively the introduction of structural measures in the multi-hazard model OpenLISEM and study their impact on the multi-hazard results.

Finally, with regard to the analysis of the risk changes, ILWIS was used again to calculate the future Average Annual loss and the risk reduction for the various alternatives. First modelling each alternative individually, then coupling the alternatives to reduce the hazard, and finally all alternatives together. As it was expected, the combination of alternatives produced the maximum risk reduction. However, most of the risk reduction was done by the alternative for vulnerability reduction. The contribution of hazard alternatives was considered as too low. Further research is required in the implementation of structural measures in the multi-hazard model other configurations can increase substantially the risk reduction. An option might be further widening of the channel or even the increase in height of channel walls.

In addition, the first attempt at a cost-benefit analysis(CBA) was performed. This indicated that the alternative for vulnerability reduction was the one with the best risk reduction and highest performance. The hazard measures without the inclusion of the vulnerability alternative were not economically feasible. However, this CBA requires a more in-depth economic study. For this reason, its results are only one indicative rather than the final product.

It is important to highlight that alternatives to reduce the vulnerability cannot be implemented directly, others need to be taken into account. For example, economical constraints, social acceptance etc. Future research needs to integrate the results of the risk analysis within Spatial decision Support systems that apply Multi-Criteria Evaluations about possible risk reduction planning alternatives to give better support to decision makers. Figure 8-1 shows a conceptual framework in which the results of the risk analysis can be integrated into Spatial Decision Support Systems.

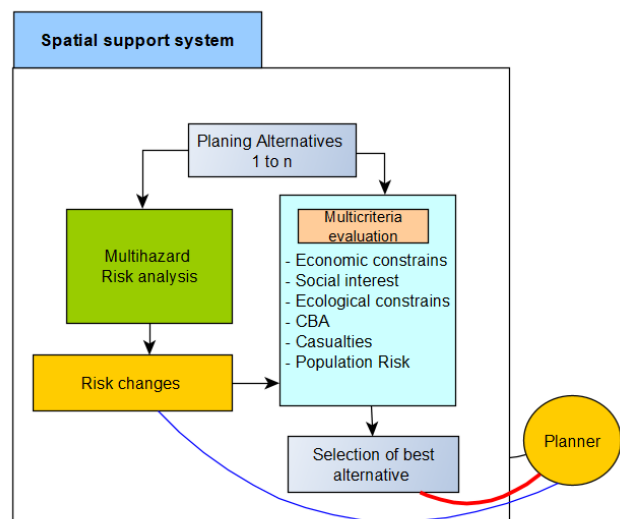


Figure 8-1. Conceptualisation of the integration of the risk results inside Spatial Decision Support systems

LIST OF REFERENCES

- 100 Resilient cities. (2016). Resilient Medellin - A strategy for our future. Alcaldía de Medellín, The Rockefeller foundation. Retrieved from <https://www.100resilientcities.org/cities/medellin/>
- ADB (Asian Development Bank). (2018). Understanding disaster risk for advancing resilient development, (September).
- Alcaldía de Envigado. (2018a). Situación de salud 2017 del municipio de Envigado, 21–40.
- Alcaldía de Envigado. (2018b). Ubicación Geográfica | Nuestro Municipio | Alcaldía de Envigado. Retrieved January 16, 2019, from <https://www.envigado.gov.co/nuestro-municipio/paginas/contenido/ubicacion/ubicacion-geografica>
- AMVA. (2006). Microzonificación Sísmica Detallada De Los Municipios De Barbosa, Girardota, Copacabana, Sabaneta, La Estrella, Caldas y Envigado, Informe Final. *Área Metropolitana Del Valle de Aburrá*, 745. <https://doi.org/10.4454/JPP.V96I2.031>
- AMVA. (2018). Estudios básicos de amenaza por movimientos en masa, inundaciones y avenidas torrenciales en los municipios de Caldas, la Estrella, Envigado, Itagüí, Bello, Copacabana y Barbosa, para la incorporación de la gestión del riesgo en la planificación territorial, 257.
- Arcement, G., & Schneider, V. (1989). Guide for Selecting Manning's Roughness Coefficients for Natural Channels and Flood Plains. *Water-Supply Paper 2339*, (2339), 44. <https://doi.org/Report No. FHWA-TS-84-204>
- Aristizábal, E., & Gómez, J. (2007). Inventario de emergencias y desastres en el Valle de Aburrá. *Gestión y Ambiente*, (2), 17–30. <https://doi.org/http://dx.doi.org/10.1155/2012/894869>
- Aristizábal, E., Gonzalez, T., Montoya, J. D., Velez, J. I., Martinez, H., & Guerra, A. (2011). Analisis de umbrales empiricos de lluvia para el pronostico de moviimientos en masa en el Valle de Aburrá, Colombia. *Revista de La EIA*, 15(c), 95–111.
- Aristizábal, E., Vélez, J. I., Martínez, H. E., & Jaboyedoff, M. (2016). SHIA_Landslide: a distributed conceptual and physically based model to forecast the temporal and spatial occurrence of shallow landslides triggered by rainfall in tropical and mountainous basins. *Landslides*, 13(3), 497–517. <https://doi.org/10.1007/s10346-015-0580-7>
- Aristizábal, E., Velez, J., & Martinez, H. (2016). Influences of antecedent rainfall and hydraulic conductivity on landslides triggered by rainfall occurrence using the model SHIA _ landslide, (65), 31–46.
- Armenta, G., Dorado, J., Rodriguez, A., & Ruiz, J. (2014). Escenarios de Cambio Climático para precipitación y temperaturas en Colombia. *Instituto de Hidrología, Meteorología y Estudios Ambientales de Colombia IDEAM*.
- Australian Geomechanics Society. (2000). Landslide Risk Management Concepts and Guidelines. *Australian Geomechanics*, (March), 49–92. Retrieved from <http://scholar.google.com/scholar?hl=en&btnG=Search&q=intitle:LANDSLIDE+RISK+MANAGEMENT+CONCEPTS+AND+GUIDELINES+AUSTRALIAN+GEOMECHANICS+SOCIETY+SUB-COMMITTEE+ON+LANDSLIDE+RISK+MANAGEMENT#2>
- Barnes, H. (1967). Roughness characteristics of natural channels. *U.S Geological Survey Water-Supply Paper*, (1849), 219.
- Bell, R., & Glade, T. (2004). Quantitative risk analysis for landslides – Examples from Bıldudalur, NW-Iceland. *Natural Hazards and Earth System Science*, 4(1), 117–131. <https://doi.org/10.5194/nhess-4-117-2004>
- Bonzanigo, L., & Kalra, N. (2014). Making Informed Investment Decisions in an Uncertain World: A Short Demonstration, (February), 20.
- Bout, B., Jetten, V., De Roo, A., Wesseling, C., & Ritsema, C. (2018). OpenLISEM- Multi-Hazard Land Surface Process Model. Enschede, Netherlands: University of Twente- Faculty of Geo-Information and Earth Observation (ITC).
- Bout, B., Lombardo, L., van Westen, C. J., & Jetten, V. G. (2018). Integration of two-phase solid fluid equations in a catchment model for flashfloods, debris flows and shallow slope failures. *Environmental Modelling and Software*, 105, 1–16. <https://doi.org/10.1016/j.envsoft.2018.03.017>
- Bruijn, K. de, Wagenaar, D., Slager, K., Bel, M. de, & Burzel, A. (2014). Updated and improved method for flood damage assessment, 2015(version 2).

- Caballero Acosta, J. H. (2011). Las avenidas torrenciales. *Gestión y Ambiente*, 45(3), 45–50. Retrieved from http://www.bdigital.unal.edu.co/6118/1/Gest._y_Amb._Vol.14%2C_no._3.pdf
- Caballero, H. (1988). Algunos comentarios acerca del evento torrencial de la Quebrada Ayura (Envigado) y sus implicaciones en la amenaza del municipio. Ingeominas-Regional Medellín.
- Cannon, S. H., & De. (2009). The Increasing Wildfire and Post-Fire Debris-Flow Threat in Western USA, and Implications for Consequences of Climate Change. In *Landslides-Disaster Risk Reduction* (p. 638). <https://doi.org/10.1007/978-3-540-69970-5>
- CAPRA. (2012). Vulnerability modeling from a probabilistic risk assessment perspective. Port of Spain.
- Catani, F., Segoni, S., & Falorni, G. (2010). An empirical geomorphology-based approach to the spatial prediction of soil thickness at catchment scale. *Water Resources Research*, 46(5). <https://doi.org/10.1029/2008WR007450>
- CHANGES. (2014). Changing Hydro-meteorological Risks – as Analyzed by a New Generation of European Scientists. Marie Curie Initial Training Network.
- CHARIM. (2014). 6.3 Cost-benefit analysis for disaster reduction measures | CHARIM. Retrieved February 21, 2019, from <http://charim.net/methodology/64>
- Chen, L., van Westen, C. J., Hussin, H., Ciurean, R. L., Turkington, T., Chavarro-Rincon, D., & Shrestha, D. P. (2016). Integrating expert opinion with modelling for quantitative multi-hazard risk assessment in the Eastern Italian Alps. *Geomorphology*, 273, 150–167. <https://doi.org/10.1016/j.geomorph.2016.07.041>
- Chow, V.T., 1959, Open-channel hydraulics: New York, McGraw-Hill, 680 p.
- Ciurean, R., Hussin, H., van Westen, C. J., Jaboyedoff, M., Nicolet, P., Chen, L., ... Glade, T. (2017). Multi-scale debris flow vulnerability assessment and direct loss estimation of buildings in the Eastern Italian Alps. *Natural Hazards*, 85(2), 929–957. <https://doi.org/10.1007/s11069-016-2612-6>
- Clausen, L. & Clark, P.B. 1990. The development of criteria for predicting dambreak flood damages using modelling of historical dam failures. In: International Conference on River Flood Hydraulics, edited by W. R. White. 17. - 20. September, 1990. John Wiley & Sons Ltd. Hydraulics Research Limited, 1990. pp. 369-380.
- Construdata. (2012). Analisis de precios unitarios en Bogota. Retrieved February 3, 2019, from <http://www.construdata.com/BuscarNew.asp?Filtro=3,1%7CBogot&Bloque=2&Pagina=16&Palabra=volqueta>
- Corominas, J., van Westen, C., Frattini, P., Cascini, L., Malet, J. P., Fotopoulou, S., ... Smith, J. T. (2014). Recommendations for the quantitative analysis of landslide risk. *Bulletin of Engineering Geology and the Environment*, 73(2), 209–263. <https://doi.org/10.1007/s10064-013-0538-8>
- Costa J.E. (1988). Rheologic, geomorphic, and sedimentologic differentiation of water floods, hyperconcentrated flows, and debris flows. In: Baker VR, Kochel RC, Patton PC (eds), Flood Geomorphology. John Wiley and Sons, Inc., New York, pp. 113-122
- Coussot, P., & Meunier, M. (1996). Recognition, classification and mechanical description of debris flows. *Earth-Science Reviews*, 40(3–4), 209–227. [https://doi.org/10.1016/0012-8252\(95\)00065-8](https://doi.org/10.1016/0012-8252(95)00065-8)
- CRED. (2019). The International Disaster Database. Retrieved February 12, 2019, from https://www.emdat.be/emdat_db/
- Cruden, D. M., & Varnes, D. J. (1996). Landslides: investigation and mitigation. Chapter 3-Landslide types and processes. *Special Report - National Research Council, Transportation Research Board*, 247(JANUARY 1996), 36–75. <https://doi.org/10.1007/s10346-009-0175-2>
- DANE. (2019). Estimación y proyección de población nacional, departamental y municipal total por área 1985-2020. Retrieved August 27, 2018, from http://www.dane.gov.co/files/investigaciones/poblacion/proyepobla06_20/Municipal_area_1985-2020.xls
- De Chiara, G. (2013). Quantifying the risk to life posed by hyperconcentrated flows.
- Dilley, M., Chen, R. S., Deichmann, U., Lerner-Lam, A. L., Arnold, M., Agwe, J., ... Gregory, Y. (2005). *Natural Disaster Hotspots A Global Risk. Disaster Risk Management Series*. <https://doi.org/10.1080/01944360902967228>
- EPM. (2017). Costos de recolección de materiales- Medellín. Retrieved February 3, 2019, from <https://www.emvarias.com.co/clientes-usuarios/home/servicios-y-tarifas>
- European Union. (2008). Average floor area per capita. Retrieved January 10, 2019, from <http://www.entranze.enerdata.eu/>

- Fell, R., Corominas, J., Bonnard, C., Cascini, L., Leroi, E., & Savage, W. Z. (2008). Guidelines for landslide susceptibility, hazard and risk zoning for land use planning. *Engineering Geology*, 102(3–4), 85–98. <https://doi.org/10.1016/j.enggeo.2008.03.022>
- Fell, R., Ho, K. K. S., Lacasse, S., & Leroi, E. (2005). A framework for landslide risk assessment and management. *International Conference on Landslide Risk Management*, 23.
- Ferlisi, S., De Chiara, G., & Cascini, L. (2016). Quantitative risk analysis for hyperconcentrated flows in Nocera Inferiore (southern Italy). *Natural Hazards*, 81(1), 89–115. <https://doi.org/10.1007/s11069-015-1784-9>
- Florez, M. J., & Parra, L. (1988). Avalancha de la Querada Ayura del 14 de abril de 1988, 22.
- Gallina, V., Torresan, S., Critto, A., Sperotto, A., Glade, T., & Marcomini, A. (2016). A review of multi-risk methodologies for natural hazards: Consequences and challenges for a climate change impact assessment. *Journal of Environmental Management*, 168, 123–132. <https://doi.org/10.1016/j.jenvman.2015.11.011>
- García-Gaines, R. A., & Frankenstein, S. (2015). ERDC/CRREL TR-15-4 “USCS and the USDA Soil Classification System: Development of a Mapping Scheme,” (March). Retrieved from www.erdcc.usace.army.mil.
- García, C. (2006). Estado del conocimiento de los depósitos de vertiente del Valle de Aburrá. *Boletín de Ciencias de La Tierra*, 19, 101–112.
- Gill, J. C., & Malamud, B. D. (2017). Anthropogenic processes, natural hazards, and interactions in a multi-hazard framework. *Earth-Science Reviews*, 166, 246–269. <https://doi.org/10.1016/j.earscirev.2017.01.002>
- Gill, J., & Malamud, B. D. (2014). Reviewing and visualizing the interactions of natural hazards, 680–722. <https://doi.org/10.1002/2013RG000445>. Received
- Gill, J., & Malamud, B. D. (2016). Hazard interactions and interaction networks (cascades) within multi-hazard methodologies, 659–679. <https://doi.org/10.5194/esd-7-659-2016>
- Godfrey, A., Ciurean, R. L., van Westen, C. J., Kingma, N. C., & Glade, T. (2015). Assessing vulnerability of buildings to hydro-meteorological hazards using an expert based approach - An application in Nehoiu Valley, Romania. *International Journal of Disaster Risk Reduction*, 13, 229–241. <https://doi.org/10.1016/j.ijdrr.2015.06.001>
- Greiving, S., & Fleischhauer, M. (2006). Spatial Planning Response Towards Natural and Technological Hazards. *Geological Survey of Finland, Special Paper*, 42, 109–123.
- Griffiths, D. V., Huang, J., & Fenton, G. A. (2011). Probabilistic infinite slope analysis. *Computers and Geotechnics*, 38(4), 577–584. <https://doi.org/10.1016/j.compgeo.2011.03.006>
- Henao, J. D., & Monsalve, G. (2018). Geological inferences about the upper crustal configuration of the Medellín – Aburra Valley (Colombia) using strong motion seismic records. *Geodesy and Geodynamics*, 9(1), 67–76. <https://doi.org/10.1016/j.geog.2017.06.005>
- Hermelin, M. (2007). Valle de Aburrá. *Gobernación de Antioquia*, (2), 7–16. Retrieved from <http://www.bdigital.unal.edu.co/13787/1/1408-6745-1-PB.pdf>
- Hermelin, M.; Toro, G. y Velásquez, A., 1984. Génesis de los depósitos de vertiente en el sur del Valle de Aburrá. Resúmenes I Conferencia sobre Riesgos Geológicos en el Valle de Aburrá.
- Hewitt, K., and I. Burton (1971), *The Hazardousness of a Place: A Regional Ecology of Damaging Events*, Univ. of Toronto Press, Toronto, Canada. Hincks, T., B. D. Malamud, R. S. J. Sparks, M. J. Wooster, and T. J. Lynham (2013), Risk assessment and management of wildfires, in *Risk and Uncertainty Assessment for Natural Hazards*, edited by J. C. Rougier, R. S. J. Sparks, and L. J. Hill, pp. 398–444, Cambridge Univ. Press, Cambridge, U. K.
- Horbath, J. E. (2016). *Tendencias y proyecciones de la población del área metropolitana del Valle de Aburrá en Colombia, 2010-2030. Notas de Población* (Vol. 43). <https://doi.org/10.18356/9d3ffa22-es>
- Huizinga, H. J., de Moel, H., & Szewczyk, W. (2017). *Global flood depth-damage functions - Methodology and the database with guidelines*. <https://doi.org/10.2760/16510>
- Hungr, O., Evans, S. G., Bovis, M. J., & Hutchinson, J. N. (2001). A review of the classification of landslides of the flow type. *Environmental and Engineering Geoscience*, 7(3), 221–238. <https://doi.org/10.2113/gseegeosci.7.3.221>
- Hungr, O., Leroueil, S., & Picarelli, L. (2015). The Varnes classification of landslide types, an update. *Journal of Animal and Plant Sciences*, 25(3), 28–32. <https://doi.org/10.1007/s10346-013-0436-y>

- Hutchinson JN (1988) General report: morphological and geotechnical parameters of landslides in relation to geology and hydrogeology. In: Proceedings of the 5th International Symposium on Landslides, Lausanne, 1:3–35
- IPCC. (2012). *Managing the risks of extreme events and disasters*. <https://doi.org/10.1017/CBO9781139177245>
- Jayawardena, A. W. (2015). Hydro-meteorological disasters: Causes, effects and mitigation measures with special reference to early warning with data driven approaches of forecasting. *Procedia IUTAM*, 17(2013), 3–12. <https://doi.org/10.1016/j.piutam.2015.06.003>
- Jong, S. M. De, & Jetten, V. G. (2007). Estimating spatial patterns of rainfall interception from remotely sensed vegetation indices and spectral mixture analysis Article, (May 2014). <https://doi.org/10.1080/13658810601064884>
- Kappes, M., Keiler, M., & Glade, T. (2010). From Single- to Multi-Hazard Risk Analyses: a concept addressing emerging challenges. *Geomorphological Systems and Risk Research*, (November), 351–356.
- Kappes, M., Keiler, M., von Elverfeldt, K., & Glade, T. (2012). Challenges of analyzing multi-hazard risk: A review. *Natural Hazards*, 64(2), 1925–1958. <https://doi.org/10.1007/s11069-012-0294-2>
- Ke, Q. (2014). *Flood risk analysis for metropolitan areas – a case study for Shanghai*. <https://doi.org/10.4233/uuid:61986b2d-72de-45e7-8f2a-bd61c725325d>
- Koliji, A. (2008). Geotechdata.info. Retrieved January 28, 2019, from <http://www.geotechdata.info/About-us.html>
- Krol, B., Boerboom, L., Looijen, J., & Westen, C. Van. (2016). Ecosystem-Based Disaster Risk Reduction and Adaptation in Practice, 42, 161–179. <https://doi.org/10.1007/978-3-319-43633-3>
- Kuriakose, S. L., Devkota, S., Rossiter, D. G., & Jetten, V. G. (2009). Prediction of soil depth using environmental variables in an anthropogenic landscape, a case study in the Western Ghats of Kerala, India. *Catena*, 79(1), 27–38. <https://doi.org/10.1016/j.catena.2009.05.005>
- Kuriakose, S., van Westen, C. J., Lakhera, R., van Beek, L., Sankar, G., Alkema, D., ... Jayadev, S. (2006). Effect of vegetation on debris flow initiation: Conceptualization and parameterization of a dynamic model for debris flow initiation in Tikovil river basin, Kerala, India, using PCraster. *International Symposium on Geo-Information for Disaster Management(Gi4DM)- Remote Sensing and GIS Techniques for Monitoring and Prediction of Disasters*, 2–7.
- Linnerooth-Bayer, J. A., Scolobig, A., Ferlisi, S., Cascini, L., & Thompson, M. (2016). Expert engagement in participatory processes: translating stakeholder discourses into policy options. *Natural Hazards*, 81(1), 69–88. <https://doi.org/10.1007/s11069-015-1805-8>
- Liu, B., Ling, Y., & Gordon, S. (2017). A quantitative model for estimating risk from multiple interacting natural hazards : an application to northeast Zhejiang , China. *Stochastic Environmental Research and Risk Assessment*, 31(6), 1319–1340. <https://doi.org/10.1007/s00477-016-1250-6>
- Lu, Ning; Godt, J. W. (2013). *HILLSLOPE HYDROLOGY AND STABILITY.pdf*.
- Lwin, K. K., & Murayama, Y. (2009). A GIS approach to estimation of building population for micro-spatial analysis. *Transactions in GIS*, 13(4), 401–414. <https://doi.org/10.1111/j.1467-9671.2009.01171.x>
- Ma, C. (2018). Comparing and Evaluating Two Physically-Based Models : Openlisem and Scoops3D , for Landslide Volume Prediction, (February).
- Mavroulli, O. C., Alessandro, C., & Corominas, J. (2014). Disaster Mitigation by corrective and Protection measures. In T. Van Asch, J. Corominas, S. Greiving, J.-P. Malet, & S. Sterlacchini (Eds.), *Mountain Risks: From Prediction to Management and Governance* (pp. 201–231). Dordrecht: Springer Netherlands. https://doi.org/10.1007/978-94-007-6769-0_7
- Ministerio de Ambiente Vivienda y Desarrollo Territorial. (2004). Decreto 2060 de 2004, (2060), 1–2.
- Nafari, R. H., & Mendis, P. (2018). Flood Damage Assessment in Urban Areas By Roozbeh Hasanzadeh Nafari, (May), 0–2.
- Narasimhan, H., Ferlisi, S., Cascini, L., De Chiara, G., & Faber, M. H. (2016). A cost–benefit analysis of mitigation options for optimal management of risks posed by flow-like phenomena. *Natural Hazards*, 81, 117–144. <https://doi.org/10.1007/s11069-015-1755-1>
- Newman, J., Maier, H., Van Delden, H., Aaron, C., Dandy, G. C., Riddell, G., & Newland, C. (2014). Literature Review on Decision Support Systems for Optimising Long-Term Natural Hazard Mitigation Policy and Project Portfolios.
- Newman, J. P., Maier, H. R., Riddell, G. A., Zecchin, A. C., Daniell, J. E., Schaefer, A. M., ... Newland, C. P. (2017). Review of literature on decision support systems for natural hazard risk reduction: Current status and future research directions. *Environmental Modelling and Software*, 96, 378–409.

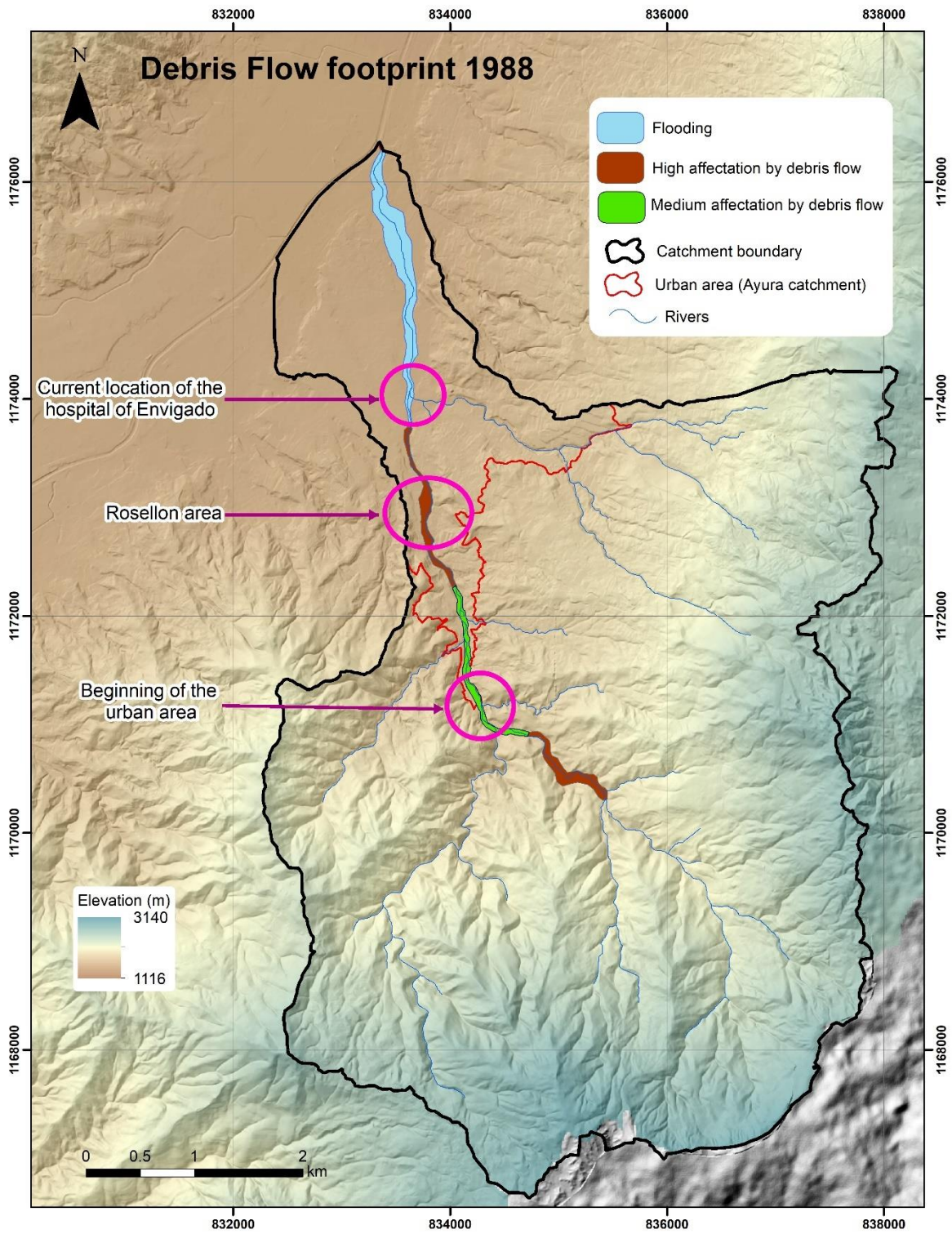
- <https://doi.org/10.1016/j.envsoft.2017.06.042>
- Parra, M., & Hidalgo, C. A. (2015). Evaluation of the Variability of Mechanical Parameters of Some Formations from East of Medellín. *XV Panamerican Conference on Soil Mechanics and Geotechnical Engineering*, (November 2015).
- Phillips, J., & Tadayon, S. (2007). Selection of Manning's Roughness Coefficient for Natural and Constructed Vegetated and Non-Vegetated Channels, and Vegetation Maintenance Plan Guidelines for Vegetated Channels in Central Arizona. *Scientific Investigations Report 2006-5108*. USGS, 49.
- Portafolio. (2019). ¿En qué ciudad de Colombia está radicado el mayor número de venezolanos? | Economía | Portafolio. Retrieved February 13, 2019, from <https://www.portafolio.co/economia/en-que-ciudad-de-colombia-esta-radicado-el-mayor-numero-de-venezolanos-519202>
- POT. (2011). Plan de Ordenamiento Territorial Envigado 2011-2023. Retrieved from <http://www.suenosytieras.com/biblioteca/Envigado-P.O.T-ACUERDO-010-2011.pdf>
- Pudasaini, S. (1952). A general two-phase debris flow model. *The Journal of Biological Chemistry*, 198(2), 491–494. <https://doi.org/10.1029/2011JF002186>
- Quan Luna, B., Blahut, J., Camera, C., van Westen, C., Apuani, T., Jetten, V., & Sterlacchini, S. (2014). Physically based dynamic run-out modelling for quantitative debris flow risk assessment: A case study in Tresenda, northern Italy. *Environmental Earth Sciences*, 72(3), 645–661. <https://doi.org/10.1007/s12665-013-2986-7>
- Quan Luna, B. R. (2012). *Dynamic numerical run out modeling for quantitative landslide risk assessment*. Thesis of University of Twente, ITC. Retrieved from <http://www.academia.edu/download/31071636/luan.pdf>
- Rawls, W.J., L.R. Ahuja, and D.L. Brakensiek. 1989. Estimating soil hydraulic properties from soils data. p. 329–340. In M.Th. Van Genuchten et al., (ed.) *Indirect methods for estimating the hydraulic properties of unsaturated soils*. Univ. of California, Riverside, CA.
- Restrepo, J. (1981). *Medellín: su origen, progreso y desarrollo*. Servigraficas. Retrieved from https://en.wikipedia.org/wiki/Aburrá_Valley
- Risk Office of Envigado. (2010). Estudio Geotecnico para el manejo de una inestabilidad en el sector de Astilleros. Retrieved from <http://search.proquest.com/docview/467590403?accountid=48947>
- Shlemon, R., 1979. Zonas de deslizamientos en los alrededores de Medellín, Antioquia (Colombia). Boletín Geológico INGEOMINAS, Publicación Especial 5, 45 P.111
- Schmidt-Thomé, P. (2006). Integration of natural hazards, risk and climate change into spatial planning practices by Philipp Schmidt-Thomé. *Academic Dissertation*.
- Shi, P., Yang, X., Xu, W., & Wang, J. (2016). Mapping Global Mortality and Affected Population Risks for Multiple Natural Hazards. *International Journal of Disaster Risk Science*, 7(1), 54–62. <https://doi.org/10.1007/s13753-016-0079-4>
- Smith, S. K., Tayman, J., & Swanson, D. A. (2013). *A practitioner's guide to State and Local population projections*. Springer Dordrecht Heidelberg New York London: Springer Science+Business Media. <https://doi.org/DOI.10.1007/978-94-007-7551-0>
- Starkloff, T., & Stolte, J. (2014). Applied comparison of the erosion risk models EROSION 3D and LISEM for a small catchment in Norway. *Catena*, 118, 154–167. <https://doi.org/10.1016/j.catena.2014.02.004>
- Thiebes, B. (2016). Landslide cost modelling for transportation infrastructures: a methodological approach, (JANUARY), 2015–2016. <https://doi.org/10.1007/s10346>
- UNAL. (2014). Actualización del mapa de coberturas vegetales, análisis multitemporal y métrica del paisaje del municipio de Envigado.
- UNISDR. (2015). *Sendai Framework for Disaster Risk Reduction 2015 - 2030*. Third World Conference on Disaster Risk Reduction. Sendai. Retrieved from http://drmkc.jrc.ec.europa.eu/portals/0/Knowledge/ScienceforDRM/ch02/ch02_subch0201.pdf
- Universidad de los Andes. (n.d.). Vulnerability | CAPRA | Probabilistic Risk Assessment Platform. Retrieved February 10, 2019, from <https://ecapra.org/topics/vulnerability>
- Universidad de los Andes. (2018). CAPRA | Probabilistic Risk Assessment Platform |. Retrieved June 24, 2018, from <http://www.ecapra.org/>
- University of da Coruna. (2019). Iberaula. Retrieved February 25, 2019, from <http://www.iberaula.es/>
- University of Oregon. (2002). Calculating Growth Rates. Retrieved February 19, 2019, from <https://pages.uoregon.edu/rgp/PPPM613/class8a.htm>
- Valencia, Y. (2005). *Las Propiedades Y Comportamiento De Dos Perfiles De Alteración Originados De Rocas*

Metamórficas.

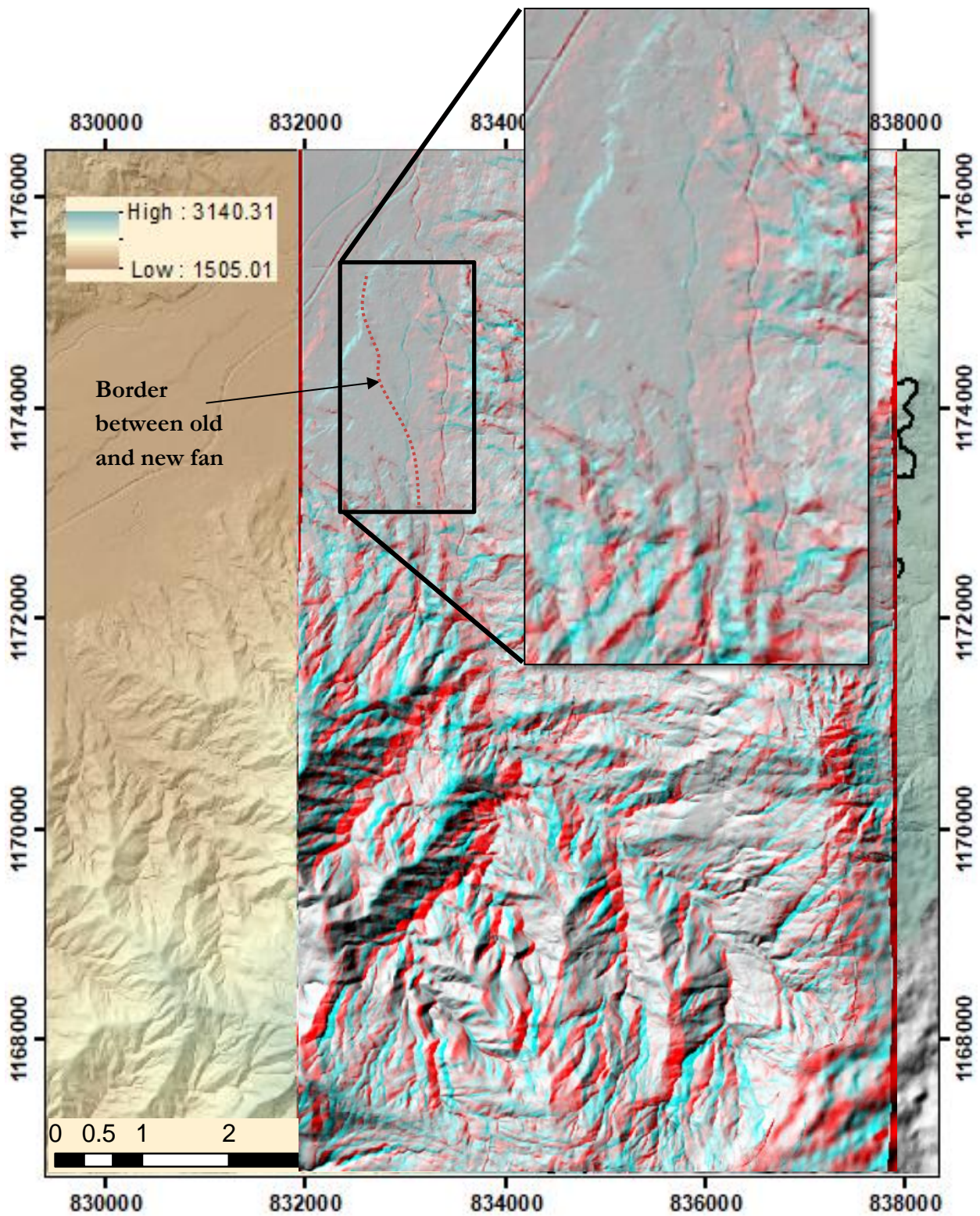
- van Westen, C. (2014). Analyzing Changing Risk and Planning Alternatives : a Case Study of a Small Island Country . Enschede, Netherlands: University of Twente- Faculty of Geo-Information and Earth Observation (ITC). <https://doi.org/10.13140/RG.2.2.18620.03204>
- van Westen, C. (2016). Cooperative Earth Observation through Complex Space Information Networks (INCREO). European Union-7th Framework programme.
- van Westen, C., Alkema, D., Damen, M., Kerle, N., & Kingma, N. (2011). *Multi-hazard risk assessment- Guide book*. United Nations University – ITC School on Disaster Geoinformation Management (UNU-ITC DGIM).
- van Westen, C. J., & Greiving, S. (2017). Environmental Hazards Methodologies for Risk Assessment and Management. In: Environmental hazards Methodologies for Risk Assessment and Management. In *Environmental hazards Methodologies for Risk Assessment and Management* (Dalezios, pp. 31–94). London: IWA Publishing. <https://doi.org/10.4135/9781446247648.n15>
- van Westen, C., Kappes, M. S., Quan Luna, B., Frigerio, S., Glade, T., & Malet, J.-P. (2014). Medium-Scale Multi-hazard Risk Assessment of Gravitational Processes. In *Mountain Risks: From Prediction to Management and Governance* (Vol. 34, p. 414). <https://doi.org/10.1007/978-94-007-6769-0>
- Varnes, D. J. 1978. Slope movement types and processes. In: Special Report 176: Landslides: Analysis and Control (Eds: Schuster, R. L. & Krizek, R. J.). Transportation and Road Research Board, National Academy of Science, Washington D. C., 11-33.
- Vega, J. A. (2013). Estimación do Risco por Deslizamentos de Encostas Gerados por Eventos Sísmicos na Cidade de Medellín Usando Ferramentas da Geomática: Caso Aplicado a Edificações Urbanas (em espanhol)., 31. <https://doi.org/10.2516/ogst:2003002>
- Von Ruetze, J., Lehmann, P., & Or, D. (2013). Rainfall-triggered shallow landslides at catchment scale: Threshold mechanics-based modeling for abruptness and localization. *Water Resources Research*, 49(10), 6266–6285. <https://doi.org/10.1002/wrcr.20418>
- Von Hoyningen-Huene, J. (1981). Die Interzeption des Niederschlags in landwirtschaftlichen Pflanzenbeständen. Arbeitsbericht Deutscher Verband für Wasserwirtschaft und Kulturbau, DVWK.
- Wendeler, C., Engineering, C., & Budimir, V. (2014). Multiple load case on flexible shallow landslide barriers – mudslide and rockfall. *International Conference on Road and Rail Infrastructure*.
- Yamin, L., Ghesquiere, F., Cardona, O., & Ordaz, M. (2013). *Modelación probabilista para la gestión del riesgo de desastre, El caso de Bogotá, Colombia*.

ANNEXES

Annex 1. Map indicating the possible footprint for the event of 1988 in The Ayura catchment



Annex 2. Anaglyph map of the Ayura catchment with detail in of new and old fan



Annex 3. Monthly multi-year precipitation of the Ayura Catchment

Empresas Publicas de Medellin

HYMONTH V109 Output 30/05/2014

Site 2701093 AYURA

Site 2701093.B

Variable 10.04 Total rain in milimetres, digital sensor

Figures are for period ending 24:00

	Jan	Feb	Mar	Apr	May	Jun	Jul	Aug	Sep	Oct	Nov	Dec	Month	ly To	tal Days
1972	[]	[]0.00	[]58.10	[]218.1	[]301.1	[]172.0	[]83.50	[]142.6	[]89.30	[]200.7	[]167.6	[]85.50	[]138.0	[]1518	[] 58
1973	38.6	*14.00	*78.60	*99.90	*197.5	*227.8	*131.9	*224.1	*358.8	*168.6	*160.1	*264.3	*163.7	*1964	* 0
1974	142.2	*153.5	*213.4	*215.1	*138.3	*144.9	*135.5	*184.9	*274.9	*300.3	*210.1	*30.70	*178.6	*2144	* 0
1975	13.6	*150.7	*127.3	*130.3	*230.7	*243.8	*240.6	*241.7	*194.0	*232.9	*241.8	*209.6	*188.1	*2257	* 0
1976	53.8	*53.90	*101.9	*214.0	*163.8	*147.3	*3.400	*67.80	*79.20	*209.7	*127.6	*38.40	*105.0	*1260	* 0
1977	12.2	*41.40	*82.40	*164.4	*216.5	*253.5	*118.7	*149.2	*200.0	*165.9	*108.0	*65.70	*131.5	*1578	* 0
1978	50.2	*39.30	*191.3	*309.8	*245.8	*166.9	*101.2	*55.30	*172.4	*238.0	*180.6	*58.00	*150.7	*1809	* 0
1979	55.49	*29.80	*156.3	*129.3	*272.5	*97.50	*125.6	*192.8	*115.1	*237.8	*177.0	*166.4	*146.3	*1755	* 0
1980	73.4	*57.60	*23.80	*179.0	*104.5	*115.7	*78.50	*72.40	*130.3	*196.9	*156.3	*141.5	*110.8	*1330	* 0
1981	23.7	*16.90	*169.7	*257.0	*405.9	*204.6	*184.2	*211.6	*168.9	*331.8	*225.8	*85.20	*190.4	*2285	* 0
1982	151.1	*159.3	*167.6	*321.5	*270.0	*103.6	*90.40	*59.60	*172.2	*351.0	*191.4	*94.80	*177.7	*2132	* 0
1983	34.5	*66.60	*122.4	*179.2	*148.0	*89.10	*113.1	*129.9	*133.9	*155.0	*173.5	*184.9	*127.5	*1530	* 0
1984	81.4	*94.20	*81.20	*159.2	*229.0	*213.5	*202.9	*208.7	*219.7	*395.7	*137.1	*48.60	*172.6	*2071	* 0
1985	26.6	*65.20	*141.6	*201.7	*188.7	*103.5	*105.3	*227.0	*319.6	*179.2	*137.5	*70.60	*147.2	*1766	* 0
1986	52.1	*110.6	*87.30	*208.1	*156.1	*196.5	*32.00	*137.6	*173.6	*305.0	*121.6	*65.70	*137.1	*1646	* 0
1987	16.5	*34.10	*42.50	*170.2	*261.2	*43.50	*173.1	*78.70	*215.3	*233.6	*126.0	*156.9	*129.3	*1551	* 0
1988	70.7	*63.20	*63.7	*246.7	*210.4	*230.3	*177.5	*325.1	*249.6	*231.3	*302.8	*229.4	*200.0	*2400	* 0
1989	105.5	*66.50	*347.8	*106.3	*245.7	*141.2	*95.19	*164.3	*314.7	*269.5	*114.0	*59.79	*169.2	*2030	* 0
1990	65.1	*96.40	*110.0	*182.2	*236.8	*121.4	*113.8	*99.70	*200.0	*366.3	*253.1	*58.60	*158.6	*1903	* 0
1991	107.4	*48.30	*229.4	*136.2	*199.4	*140.4	*114.2	*68.00	*156.8	*275.9	*163.4	*129.2	*147.3	*1768	* 0
1992	83.2	*24.40	*50.10	*103.6	*219.7	*96.60	*60.10	*140.4	*302.7	*99.70	*170.4	*186.4	*128.1	*1537	* 0
1993	107.6	*38.60	*159.6	*182.2	*260.8	*84.70	*114.7	*109.3	*252.5	*190.0	*267.7	*159.6	*160.6	*1927	* 14
1994	81.4	*115.8	*199.70	*177.3	*154.0	*109.7	*68.30	*102.1	[] []	M200.3	*221.2	*38.80	*124.4	*1368	* 48
1995	28.12	*51.98	[87.05]	169.2	[206.5	[155.24	[179.6	[283.8	*104.7	*172.5	*86.89	*147.0	[131.0	[1573	[] 33
1996	153.9	*109.8	*282.8	[208.3	*300.2	[213.3	*163.1	*177.7	[90.09]	[98.72	[138.13	[141.19	[156.4	[1877	[] 46
1997	260	*85.49	*149.8	*144.3	*156.51	[191.3	[24.68	[116.73	[117.9	[118.3	[121.5	[1184.4	[107.3	[1288	[] 63
1998	54.95	[39.13	[18.193	[68.30	[241.7	*104.8	*169.8	*141.2	[224.6	[215.0	[198.5	*175.6	[136.8	[1642	[] 51
1999	129.8	[235.7	*105.8	[134.6	[182.1	[66.92]	[53.04	[53.86	[324.5	[230.2	[207.4	*300.2	[168.7	[2024	[] 51
2000	84.4	*139.5	*122.0	*175.9	*336.5	*247.7	*160.8	*154.1	*248.2	*182.7	*130.8	*93.48	*173.0	*2076	* 0
2001	66.08	*56.11	*99.05	73.15	164.5	97.02	135.3	18.54	166.6	239.6	146.8	174.4	119.8	*1437	* 0
2002	41.65	69.34	102.6	278.1	222.5	121.4	120.3	63.49	132	196.3	145.5	173.7	138.9	1667	0
2003	3.81	0 73.40	145.2	188.9	175.2	200.9	55.11	145	180	294.8	193.2	164.5	151.7	1820	0
2004	150.3	97.53	122.6	314.8	256.6	60.7	172.4	107.4	213.6	227.5	237.4	122.6	173.6	2084	0
2005	125.7	41.65	101	156.2	364.4	175	200.6	117.7	174.8	270.2	163.3	133.3	168.6	2024	0

Annex 4. OpenLISEM Script used to model antecedent rainfall in the Ayura catchment

```
#####
# Model: simple slope based groundwater flow #
# Author: Bastian van den Bout #
#####
binding

DT = 6; ## timestep in hours

SD = soildepth.map; ## input soil depth, soildepth.map in mm
ThetaS = thetas1.map; ## porosity of the soil (-)
Thetal = thetai1.map; ## initial soil moisture content of the soil (-)
ThetaR = thetasr.map; ## porosity of the soil (-)
KSat = ksats1.map; ## saturated hydraulic conductivity of the soil (mm/h)
DEM = dem.map; ## elevation model (m)

Thetareport = thetair.map; ## bind output map
Hreport = SoilH.map; ## bind output map
Hinitial = SoilHi.map; ## bind initial output map
areamap
mask_n.map; ## mask indicates the area for calculation

timer
1 60 1; ## start timestep, final timestep, increment time step → Final time step Equivalent to 15 days
rep = 1, 1 + 1..endtime; ## report every timestep
initial

SD = SD/1000.0; ## soil depth to meters
KSat = KSat/1000.0; ## saturated conductivity to meters per hour
H = Thetal * SD; ## effective water height
report SoilHi.map = H;
Q = scalar(0.0); ## total discharge
Qx = scalar(0.0); ## x direction discharge
Qy = scalar(0.0); ## y direction discharge
Sx = scalar(0.0); ## x direction slope
Sy = scalar(0.0); ## y direction slope

dynamic

Sx = -(cover(shift(DEM + H,0,1),DEM) - cover(shift(DEM + H,0,-1),DEM)); ## calculate slope
Sy = -(cover(shift(DEM + H,1,0),DEM) - cover(shift(DEM + H,-1,0),DEM)); ## calculate slope
Qx = DT * KSat * Sx * H; ## calculate groundwater discharge
Qy = DT * KSat * Sy * H; ## calculate groundwater discharge

Qx = if(Qx gt 0.0,1.0,-1.0) * min(0.3 * H,abs(Qx)); ## limit by available water
Qy = if(Qy gt 0.0,1.0,-1.0) * min(0.3 * H,abs(Qy)); ## limit by available water
H = H + min(0.0, -abs(Qx) -abs(Qy)); ## subtract outflow

H = H + abs(min(0.0,cover(shift(Qx,0,1),0.0))); ## add inflow x direction
H = H + abs(max(0.0,cover(shift(Qx,0,-1),0.0))); ## add inflow x direction
H = H + abs(min(0.0,cover(shift(Qy,1,0),0.0))); ## add inflow y direction
H = H + abs(max(0.0,cover(shift(Qy,-1,0),0.0))); ## add inflow y direction
H = max(ThetaR * SD,min(ThetaS * SD,H)); ## if oversaturation, remove
H = windowaverage(H,celllength() * 2.0); ## take spatial average of 2 cells width to smoothen dem errors

report (rep) Hreport = H; ## reports map in SoilH.map
report (rep) Thetareport = max(ThetaR,min(ThetaS,H/SD)); ## reports map in SoilH.map
```

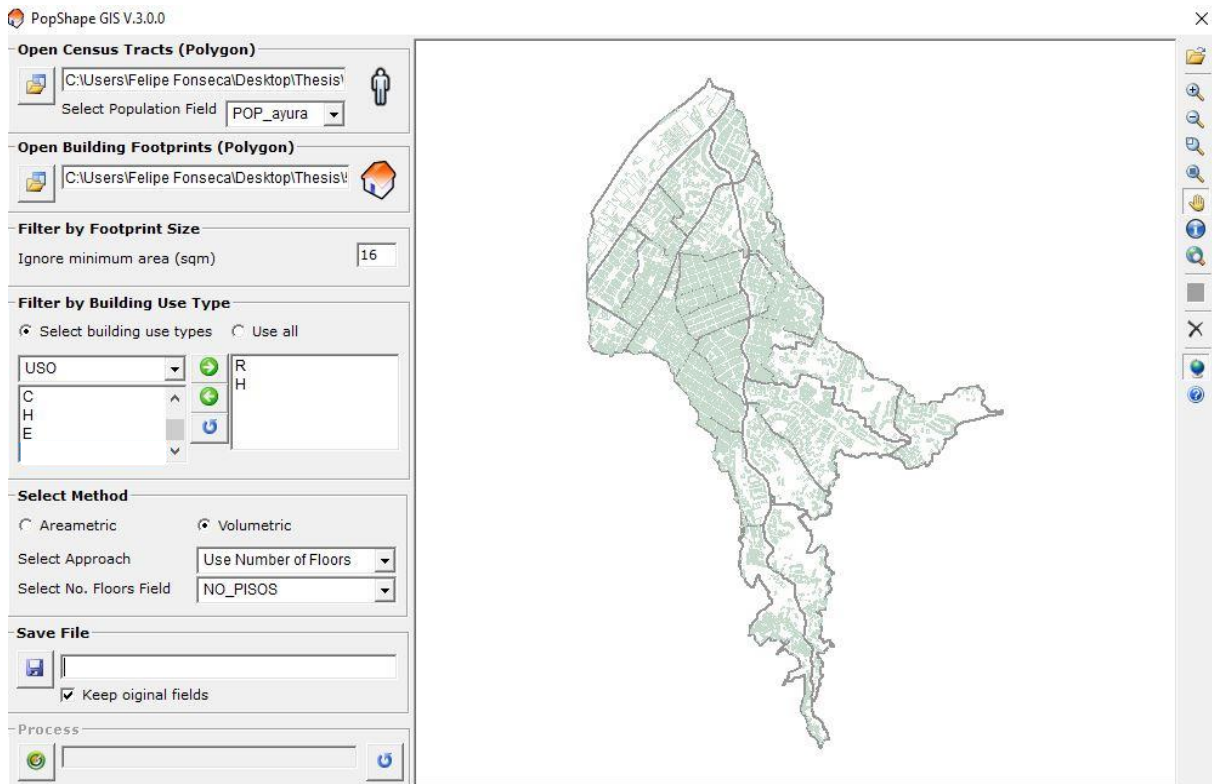
Annex 5 Overview of Hazard maps obtained for different scenarios and alternatives.

Scenario	Hazard fraction	Return period	Hazard maps for combined scenarios and individual alternatives			
			A0	A1	A2	A3
S0 2018	Flood (FL)	25	FL_DE_25_A0_S0	FL_DE_25_A1_S0	FL_DE_25_A2_S0	FL_DE_25_A3_S0
		50	FL_DE_50_A0_S0	FL_DE_50_A1_S0	FL_DE_50_A2_S0	FL_DE_50_A3_S0
		100	FL_DE_100_A0_S0	FL_DE_100_A1_S0	FL_DE_100_A2_S0	FL_DE_100_A3_S0
		200	FL_DE_200_A0_S0	FL_DE_200_A1_S0	FL_DE_200_A2_S0	FL_DE_200_A3_S0
	Debris Flow (DF)	25	DF_DE_25_A0_S0	DF_DE_25_A1_S0	DF_DE_25_A2_S0	DF_DE_25_A3_S0
		50	DF_DE_50_A0_S0	DF_DE_50_A1_S0	DF_DE_50_A2_S0	DF_DE_50_A3_S0
		100	DF_DE_100_A0_S0	DF_DE_100_A1_S0	DF_DE_100_A2_S0	DF_DE_100_A3_S0
		200	DF_DE_200_A0_S0	DF_DE_200_A1_S0	DF_DE_200_A2_S0	DF_DE_200_A3_S0
S1 2050	Flood (FL)	25	FL_DE_25_A0_S1	FL_DE_25_A1_S1	FL_DE_25_A2_S1	FL_DE_25_A3_S1
		50	FL_DE_50_A0_S1	FL_DE_50_A1_S1	FL_DE_50_A2_S1	FL_DE_50_A3_S1
		100	FL_DE_100_A0_S1	FL_DE_100_A1_S1	FL_DE_100_A2_S1	FL_DE_100_A3_S1
		200	FL_DE_200_A0_S1	FL_DE_200_A1_S1	FL_DE_200_A2_S1	FL_DE_200_A3_S1
	Debris Flow (DF)	25	DF_DE_25_A0_S1	DF_DE_25_A1_S1	DF_DE_25_A2_S1	DF_DE_25_A3_S1
		50	DF_DE_50_A0_S1	DF_DE_50_A1_S1	DF_DE_50_A2_S1	DF_DE_50_A3_S1
		100	DF_DE_100_A0_S1	DF_DE_100_A1_S1	DF_DE_100_A2_S1	DF_DE_100_A3_S1
		200	DF_DE_200_A0_S1	DF_DE_200_A1_S1	DF_DE_200_A2_S1	DF_DE_200_A3_S1
S2 2050	Flood (FL)	25	FL_DE_25_A0_S2	FL_DE_25_A1_S2	FL_DE_25_A2_S2	FL_DE_25_A3_S2
		50	FL_DE_50_A0_S2	FL_DE_50_A1_S2	FL_DE_50_A2_S2	FL_DE_50_A3_S2
		100	FL_DE_100_A0_S2	FL_DE_100_A1_S2	FL_DE_100_A2_S2	FL_DE_100_A3_S2
		200	FL_DE_200_A0_S2	FL_DE_200_A1_S2	FL_DE_200_A2_S2	FL_DE_200_A3_S2
	Debris Flow (DF)	25	DF_DE_25_A0_S2	DF_DE_25_A1_S2	DF_DE_25_A2_S2	DF_DE_25_A3_S2
		50	DF_DE_50_A0_S2	DF_DE_50_A1_S2	DF_DE_50_A2_S2	DF_DE_50_A3_S2
		100	DF_DE_100_A0_S2	DF_DE_100_A1_S2	DF_DE_100_A2_S2	DF_DE_100_A3_S2
		200	DF_DE_200_A0_S2	DF_DE_200_A1_S2	DF_DE_200_A2_S2	DF_DE_200_A3_S2

Notes:

In the table notation DE indicates the hazard intensity parameter used for the research. That is to say, DE=DEPTH of flood or debris flow.
 In the Column A0 besides to represent the “No measures” alternative as well represent the situation either for 2018 or 2050.
 In the column A2 and row S0,S1 and S2. The hazard map is changed for a map “Cero” to represent the Debris flow mitigation.
 In the column A3 all hazard maps used are equals to the ones used in A0. This is because the alternative only modify the vulnerability.

Annex 6. Interface of POP GIS- Micro-spatial tool to distribute population in municipality units to building footprints



POPGIS is a tool that can be acquired without charge directly with the authors Lwin & Murayama(2009).

Annex 7. Absolute vulnerability tables - Residential

Use:	Flood					Flood					Flood				
Residential	1 Floor	Code=			RF1	2_6 Floors	Code=			RF2_6	FM6	Code=			RFm6
Flow depth	Content	Structure	Clean_up	Garage	Total	Content	Structure	Clean_up	Garage	Total	Content	Structure	Clean_up	Garage	Total
0.0	0.0	0.0	0.0	0.0	0.0	0.0	0.0	0.0	0.0	0.0	0.0	0.0	0.0	0.0	0.0
0-0.5	31.4	7.6	0.6	0.0	39.6	31.4	0.0	0.6	0.0	32.0	0.0	0.0	0.6	0.0	0.6
0.5-1	88.0	56.8	0.6	0.0	145.4	88.0	18.9	0.6	0.0	107.5	0.0	7.6	3.4	1420.0	1431.0
1-1.5	119.0	151.4	2.9	0.0	273.3	119.0	56.8	2.9	0.0	178.6	0.0	26.5	5.7	1420.0	1452.2
1.5-2	139.7	265.0	2.9	0.0	407.5	139.7	94.6	2.9	0.0	237.2	0.0	60.6	5.7	1420.0	1486.3
2-2.5	139.7	340.7	2.9	0.0	483.2	139.7	113.6	2.9	0.0	256.1	0.0	71.9	5.7	1420.0	1497.6
2.5-3	139.7	359.6	2.9	0.0	502.2	139.7	124.9	2.9	0.0	267.5	0.0	75.7	5.7	1420.0	1501.4
3-3.5	139.7	378.5	2.9	0.0	521.1	139.7	132.5	2.9	0.0	275.0	0.0	79.5	5.7	1420.0	1505.2
3.5-4	139.7	378.5	2.9	0.0	521.1	171.1	155.2	3.4	0.0	329.7	31.4	87.1	6.3	1420.0	1544.7
4-4.5	139.7	378.5	2.9	0.0	521.1	227.7	193.1	3.4	0.0	424.2	88.0	113.6	6.3	1420.0	1627.8
4.5-5	139.7	378.5	2.9	0.0	521.1	258.7	227.1	6.3	0.0	492.1	119.0	143.8	9.1	1420.0	1692.0
5-5.5	139.7	378.5	2.9	0.0	521.1	279.4	249.8	6.3	0.0	535.5	139.7	151.4	9.1	1420.0	1720.3
5.5-6	139.7	378.5	2.9	0.0	521.1	279.4	265.0	6.3	0.0	550.7	139.7	151.4	9.1	1420.0	1720.3
6-6.5	139.7	378.5	2.9	0.0	521.1	279.4	302.8	6.3	0.0	588.5	139.7	151.4	9.1	1420.0	1720.3
6.5-7	139.7	378.5	2.9	0.0	521.1	279.4	340.7	6.3	0.0	626.4	139.7	151.4	9.1	1420.0	1720.3
7-7.5	139.7	378.5	2.9	0.0	521.1	310.8	378.5	6.9	0.0	696.2	171.1	151.4	9.7	1420.0	1752.2
7.5-8	139.7	378.5	2.9	0.0	521.1	367.4	378.5	7.4	0.0	753.4	227.7	151.4	10.3	1420.0	1809.4
8-8.5	139.7	378.5	2.9	0.0	521.1	398.4	378.5	10.3	0.0	787.2	258.7	151.4	13.1	1420.0	1843.3
8.5-9	139.7	378.5	2.9	0.0	521.1	419.1	378.5	10.3	0.0	807.9	279.4	151.4	13.1	1420.0	1864.0
9-9.5	139.7	378.5	2.9	0.0	521.1	419.1	378.5	10.3	0.0	807.9	279.4	151.4	13.1	1420.0	1864.0
9.5-10	139.7	378.5	2.9	0.0	521.1	419.1	378.5	10.3	0.0	807.9	279.4	151.4	13.1	1420.0	1864.0
>10	139.7	378.5	2.9	0.0	521.1	419.1	378.5	10.3	0.0	807.9	279.4	151.4	13.1	1420.0	1864.0

Use:	Debris Flow					Debris Flow					Debris Flow				
Residential	1 Floor	Code=			RF1	2_6 Floors	Code=			RF2_6	Fm6	Code=			RFm6
Flow depth	Content	Structure	Clean_up	Garage	Total	Content	Structure	Clean_up	Garage	Total	Content	Structure	Clean_up	Garage	Total
0.0	0.0	0.0	0.0	0.0	0.0	0.0	0.0	0.0	0.0	0.0	0.0	0.0	0.0	0.0	0.0
0-0.5	27.9	37.9	8.1	0.0	73.9	31.4	37.9	8.1	0.0	77.3	0.0	26.5	8.1	0.0	34.6
0.5-1	83.8	151.4	15.6	0.0	250.8	88.0	151.4	15.6	0.0	255.0	0.0	106.0	70.9	1420.0	1596.9
1-1.5	125.7	227.1	25.4	0.0	378.2	119.0	227.1	25.4	0.0	371.5	0.0	159.0	80.7	1420.0	1659.7
1.5-2	139.7	321.8	32.9	0.0	494.3	139.7	321.8	32.9	0.0	494.3	0.0	225.2	88.2	1420.0	1733.4
2-2.5	139.7	340.7	40.4	0.0	520.7	139.7	340.7	40.4	0.0	520.7	0.0	238.5	95.7	1420.0	1754.2
2.5-3	139.7	378.5	47.9	0.0	566.1	139.7	378.5	47.9	0.0	566.1	0.0	265.0	103.2	1420.0	1788.2
3-3.5	139.7	378.5	55.4	0.0	573.6	139.7	378.5	55.4	0.0	573.6	0.0	265.0	110.7	1420.0	1795.7
3.5-4	139.7	378.5	55.4	0.0	573.6	171.1	378.5	63.4	0.0	613.1	31.4	265.0	118.8	1420.0	1835.2
4-4.5	139.7	378.5	55.4	0.0	573.6	227.7	378.5	70.9	0.0	677.2	88.0	265.0	126.3	1420.0	1899.3
4.5-5	139.7	378.5	55.4	0.0	573.6	258.7	378.5	81.3	0.0	718.5	119.0	265.0	136.6	1420.0	1940.6
5-5.5	139.7	378.5	55.4	0.0	573.6	279.4	378.5	88.8	0.0	746.7	139.7	265.0	144.1	1420.0	1968.8
5.5-6	139.7	378.5	55.4	0.0	573.6	279.4	378.5	96.3	0.0	754.2	139.7	265.0	151.6	1420.0	1976.3
6-6.5	139.7	378.5	55.4	0.0	573.6	279.4	378.5	103.8	0.0	761.7	139.7	265.0	159.1	1420.0	1983.8
6.5-7	139.7	378.5	55.4	0.0	573.6	279.4	378.5	111.3	0.0	769.2	139.7	265.0	166.6	1420.0	1991.3
7-7.5	139.7	378.5	55.4	0.0	573.6	310.8	378.5	119.4	0.0	808.7	171.1	265.0	174.7	1420.0	2030.8
7.5-8	139.7	378.5	55.4	0.0	573.6	367.4	378.5	127.4	0.0	873.4	227.7	265.0	182.8	1420.0	2095.5
8-8.5	139.7	378.5	55.4	0.0	573.6	398.4	378.5	137.8	0.0	914.7	258.7	265.0	193.1	1420.0	2136.8
8.5-9	139.7	378.5	55.4	0.0	573.6	419.1	378.5	145.3	0.0	942.9	279.4	265.0	200.6	1420.0	2165.0
9-9.5	139.7	378.5	55.4	0.0	573.6	419.1	378.5	152.8	0.0	950.4	279.4	265.0	208.1	1420.0	2172.5
9.5-10	139.7	378.5	55.4	0.0	573.6	419.1	378.5	160.3	0.0	957.9	279.4	265.0	215.6	1420.0	2180.0
>10	139.7	378.5	55.4	0.0	573.6	419.1	378.5	160.3	0.0	957.9	279.4	265.0	215.6	1420.0	2180.0

Annex 7. Absolute vulnerability tables - Educational

Use:	Flood					Flood					Flood				
Educational	1 Floor	Code=			EF1	2_6 Floors	Code=			EF2_6	FM6	Code=			EFm6
Flow depth	Content	Structure	Clean_up	Garage	Total	Content	Structure	Clean_up	Garage	Total	Content	Structure	Clean_up	Garage	Total
0.0	0.0	0.0	0.0	0.0	0.0	0.0				0.0	0.0				0.0
0-0.5	104.6	9.3	0.6	0.0	114.5	104.6	9.3	0.6	0.0	114.5	104.6	9.3	0.6	0.0	105.2
0.5-1	292.9	69.8	0.6	0.0	363.2	292.9	23.3	0.6	0.0	316.7	292.9	9.3	0.6	0.0	302.8
1-1.5	396.1	186.0	2.9	0.0	585.0	396.1	69.8	2.9	0.0	468.7	396.1	32.6	2.9	0.0	431.5
1.5-2	465.0	325.5	2.9	0.0	793.4	465.0	116.3	2.9	0.0	584.1	465.0	74.4	2.9	0.0	542.3
2-2.5	465.0	418.5	2.9	0.0	886.4	465.0	139.5	2.9	0.0	607.4	465.0	88.4	2.9	0.0	556.2
2.5-3	465.0	441.8	2.9	0.0	909.6	465.0	153.5	2.9	0.0	621.3	465.0	93.0	2.9	0.0	560.9
3-3.5	465.0	465.0	2.9	0.0	932.9	465.0	162.8	2.9	0.0	630.6	465.0	97.7	2.9	0.0	565.5
3.5-4	465.0	465.0	2.9	0.0	932.9	569.6	190.7	3.4	0.0	763.7	569.6	107.0	3.4	0.0	680.0
4-4.5	465.0	465.0	2.9	0.0	932.9	757.9	237.2	3.4	0.0	998.5	757.9	139.5	3.4	0.0	900.8
4.5-5	465.0	465.0	2.9	0.0	932.9	861.1	279.0	6.3	0.0	1146.4	861.1	176.7	6.3	0.0	1044.1
5-5.5	465.0	465.0	2.9	0.0	932.9	930.0	306.9	6.3	0.0	1243.2	930.0	186.0	6.3	0.0	1122.3
5.5-6	465.0	465.0	2.9	0.0	932.9	930.0	325.5	6.3	0.0	1261.8	930.0	186.0	6.3	0.0	1122.3
6-6.5	465.0	465.0	2.9	0.0	932.9	930.0	372.0	6.3	0.0	1308.3	930.0	186.0	6.3	0.0	1122.3
6.5-7	465.0	465.0	2.9	0.0	932.9	930.0	418.5	6.3	0.0	1354.8	930.0	186.0	6.3	0.0	1122.3
7-7.5	465.0	465.0	2.9	0.0	932.9	1034.6	465.0	6.9	0.0	1506.4	1034.6	186.0	6.9	0.0	1227.4
7.5-8	465.0	465.0	2.9	0.0	932.9	1222.9	465.0	7.4	0.0	1695.3	1222.9	186.0	7.4	0.0	1416.3
8-8.5	465.0	465.0	2.9	0.0	932.9	1326.1	465.0	10.3	0.0	1801.4	1326.1	186.0	10.3	0.0	1522.4
8.5-9	465.0	465.0	2.9	0.0	932.9	1395.0	465.0	10.3	0.0	1870.3	1395.0	186.0	10.3	0.0	1591.3
9-9.5	465.0	465.0	2.9	0.0	932.9	1395.0	465.0	10.3	0.0	1870.3	1395.0	186.0	10.3	0.0	1591.3
9.5-10	465.0	465.0	2.9	0.0	932.9	1395.0	465.0	10.3	0.0	1870.3	1395.0	186.0	10.3	0.0	1591.3
>10	465.0	465.0	2.9	0.0	932.9	1395.0	465.0	10.3	0.0	1870.3	1395.0	186.0	10.3	0.0	1591.3

Use:	Debris Flow					Debris Flow					Debris Flow				
Educational	1 Floor	Code=			EF1	2_6 Floors	Code=			EF2_6	FM6	Code=			EFm6
Flow depth	Content	Structure	Clean_up	Garage	Total	Content	Structure	Clean_up	Garage	Total	Content	Structure	Clean_up	Garage	Total
0.0	0.0	0.0	0.0	0.0	0.0	0.0				0.0	0.0				0.0
0-0.5	104.6	46.5	8.1	0.0	159.2	104.6	46.5	8.1	0.0	159.2	104.6	32.6	8.1	0.0	145.2
0.5-1	292.9	186.0	15.6	0.0	494.5	292.9	186.0	15.6	0.0	494.5	292.9	130.2	15.6	0.0	438.7
1-1.5	396.1	279.0	25.4	0.0	700.5	396.1	279.0	25.4	0.0	700.5	396.1	195.3	25.4	0.0	616.8
1.5-2	465.0	395.3	32.9	0.0	893.1	465.0	395.3	32.9	0.0	893.1	465.0	276.7	32.9	0.0	774.5
2-2.5	465.0	418.5	40.4	0.0	923.9	465.0	418.5	40.4	0.0	923.9	465.0	293.0	40.4	0.0	798.3
2.5-3	465.0	465.0	47.9	0.0	977.9	465.0	465.0	47.9	0.0	977.9	465.0	325.5	47.9	0.0	838.4
3-3.5	465.0	465.0	55.4	0.0	985.4	465.0	465.0	55.4	0.0	985.4	465.0	325.5	55.4	0.0	845.9
3.5-4	465.0	465.0	55.4	0.0	985.4	569.6	465.0	63.4	0.0	1098.0	569.6	325.5	63.4	0.0	958.5
4-4.5	465.0	465.0	55.4	0.0	985.4	757.9	465.0	70.9	0.0	1293.8	757.9	325.5	70.9	0.0	1154.3
4.5-5	465.0	465.0	55.4	0.0	985.4	861.1	465.0	81.3	0.0	1407.4	861.1	325.5	81.3	0.0	1267.9
5-5.5	465.0	465.0	55.4	0.0	985.4	930.0	465.0	88.8	0.0	1483.8	930.0	325.5	88.8	0.0	1344.3
5.5-6	465.0	465.0	55.4	0.0	985.4	930.0	465.0	96.3	0.0	1491.3	930.0	325.5	96.3	0.0	1351.8
6-6.5	465.0	465.0	55.4	0.0	985.4	930.0	465.0	103.8	0.0	1498.8	930.0	325.5	103.8	0.0	1359.3
6.5-7	465.0	465.0	55.4	0.0	985.4	930.0	465.0	111.3	0.0	1506.3	930.0	325.5	111.3	0.0	1366.8
7-7.5	465.0	465.0	55.4	0.0	985.4	1034.6	465.0	119.4	0.0	1618.9	1034.6	325.5	119.4	0.0	1479.4
7.5-8	465.0	465.0	55.4	0.0	985.4	1222.9	465.0	127.4	0.0	1815.3	1222.9	325.5	127.4	0.0	1675.8
8-8.5	465.0	465.0	55.4	0.0	985.4	1326.1	465.0	137.8	0.0	1928.9	1326.1	325.5	137.8	0.0	1789.4
8.5-9	465.0	465.0	55.4	0.0	985.4	1395.0	465.0	145.3	0.0	2005.3	1395.0	325.5	145.3	0.0	1865.8
9-9.5	465.0	465.0	55.4	0.0	985.4	1395.0	465.0	152.8	0.0	2012.8	1395.0	325.5	152.8	0.0	1873.3
9.5-10	465.0	465.0	55.4	0.0	985.4	1395.0	465.0	160.3	0.0	2020.3	1395.0	325.5	160.3	0.0	1880.8
>10	465.0	465.0	55.4	0.0	985.4	1395.0	465.0	160.3	0.0	2020.3	1395.0	325.5	160.3	0.0	1880.8

Annex 7. Absolute vulnerability tables - Commercial

Use:	Flood					Flood					Flood				
Commercial	1 Floor	Code=			CF1	2_6 Floors	Code=			CF2_6	FM6	Code=			CFm6
Flow depth	Content	Structure	Clean_up	Garage	Total	Content	Structure	Clean_up	Garage	Total	Content	Structure	Clean_up	Garage	Total
0.0	0	0	0	0	0	0	0	0	0	0	0	0	0	0	0
0-0.5	104.6	9.3	0.6	0.0	114.5	104.6	9.3	0.6	0.0	114.5	104.6	0.0	0.6	0.0	105.2
0.5-1	292.9	69.8	0.6	0.0	363.2	292.9	23.3	0.6	23.0	339.7	292.9	9.3	3.4	1420.0	1725.6
1-1.5	396.1	186.0	2.9	0.0	585.0	396.1	69.8	2.9	0.0	468.7	396.1	32.6	5.7	1420.0	1854.4
1.5-2	465.0	276.7	2.9	0.0	744.5	465.0	116.3	2.9	0.0	584.1	465.0	74.4	5.7	1420.0	1965.1
2-2.5	465.0	376.7	2.9	0.0	844.5	465.0	139.5	2.9	0.0	607.4	465.0	88.4	5.7	1420.0	1979.1
2.5-3	465.0	441.8	2.9	0.0	909.6	465.0	153.5	2.9	0.0	621.3	465.0	93.0	5.7	1420.0	1983.7
3-3.5	465.0	465.0	2.9	0.0	932.9	465.0	162.8	2.9	0.0	630.6	465.0	97.7	5.7	1420.0	1988.4
3.5-4	465.0	465.0	2.9	0.0	932.9	569.6	190.7	3.4	0.0	763.7	569.6	107.0	6.3	1420.0	2102.8
4-4.5	465.0	465.0	2.9	0.0	932.9	757.9	237.2	3.4	0.0	998.5	757.9	139.5	6.3	1420.0	2323.7
4.5-5	465.0	465.0	2.9	0.0	932.9	861.1	279.0	6.3	0.0	1146.4	861.1	176.7	9.1	1420.0	2466.9
5-5.5	465.0	465.0	2.9	0.0	932.9	930.0	306.9	6.3	0.0	1243.2	930.0	186.0	9.1	1420.0	2545.1
5.5-6	465.0	465.0	2.9	0.0	932.9	930.0	325.5	6.3	0.0	1261.8	930.0	186.0	9.1	1420.0	2545.1
6-6.5	465.0	465.0	2.9	0.0	932.9	930.0	372.0	6.3	0.0	1308.3	930.0	186.0	9.1	1420.0	2545.1
6.5-7	465.0	465.0	2.9	0.0	932.9	930.0	418.5	6.3	0.0	1354.8	930.0	186.0	9.1	1420.0	2545.1
7-7.5	465.0	465.0	2.9	0.0	932.9	1034.6	465.0	6.9	0.0	1506.4	1034.6	186.0	9.7	1420.0	2650.3
7.5-8	465.0	465.0	2.9	0.0	932.9	1222.9	465.0	7.4	0.0	1695.3	1222.9	186.0	10.3	1420.0	2839.2
8-8.5	465.0	465.0	2.9	0.0	932.9	1326.1	465.0	10.3	0.0	1801.4	1326.1	186.0	13.1	1420.0	2945.2
8.5-9	465.0	465.0	2.9	0.0	932.9	1395.0	465.0	10.3	0.0	1870.3	1395.0	186.0	13.1	1420.0	3014.1
9-9.5	465.0	465.0	2.9	0.0	932.9	1395.0	465.0	10.3	0.0	1870.3	1395.0	186.0	13.1	1420.0	3014.1
9.5-10	465.0	465.0	2.9	0.0	932.9	1395.0	465.0	10.3	0.0	1870.3	1395.0	186.0	13.1	1420.0	3014.1
>10	465.0	465.0	2.9	0.0	932.9	1395.0	465.0	10.3	0.0	1870.3	1395.0	186.0	13.1	1420.0	3014.1

Use:	Debris Flow					Debris Flow					Debris Flow				
Commercial	1 Floor	Code=			CF1	2_6 Floors	Code=			CF2_6	FM6	Code=			CFm6
Flow depth	Content	Structure	Clean_up	Garage	Total	Content	Structure	Clean_up	Garage	Total	Content	Structure	Clean_up	Garage	Total
0.0	0	0	0	0.0	0	0	0	0	0	0	0	0	0	0	0
0-0.5	104.6	46.5	8.1	0.0	159.2	104.6	46.5	8.1	0.0	159.2	104.6	32.6	8.1	0.0	145.2
0.5-1	292.9	186.0	15.6	0.0	494.5	292.9	186.0	15.6	0.0	494.5	292.9	130.2	70.9	1420.0	1914.0
1-1.5	396.1	279.0	25.4	0.0	700.5	396.1	279.0	25.4	0.0	700.5	396.1	195.3	80.7	1420.0	2092.1
1.5-2	465.0	395.3	32.9	0.0	893.1	465.0	395.3	32.9	0.0	893.1	465.0	276.7	88.2	1420.0	2249.9
2-2.5	465.0	418.5	40.4	0.0	923.9	465.0	418.5	40.4	0.0	923.9	465.0	293.0	95.7	1420.0	2273.7
2.5-3	465.0	465.0	47.9	0.0	977.9	465.0	465.0	47.9	0.0	977.9	465.0	325.5	103.2	1420.0	2313.7
3-3.5	465.0	465.0	55.4	0.0	985.4	465.0	465.0	55.4	0.0	985.4	465.0	325.5	110.7	1420.0	2321.2
3.5-4	465.0	465.0	55.4	0.0	985.4	569.6	465.0	63.4	0.0	1098.0	569.6	325.5	118.8	1420.0	2433.9
4-4.5	465.0	465.0	55.4	0.0	985.4	757.9	465.0	70.9	0.0	1293.8	757.9	325.5	126.3	1420.0	2629.7
4.5-5	465.0	465.0	55.4	0.0	985.4	861.1	465.0	81.3	0.0	1407.4	861.1	325.5	81.3	1420.0	2687.9
5-5.5	465.0	465.0	55.4	0.0	985.4	930.0	465.0	88.8	0.0	1483.8	930.0	325.5	88.8	1420.0	2764.3
5.5-6	465.0	465.0	55.4	0.0	985.4	930.0	465.0	96.3	0.0	1491.3	930.0	325.5	96.3	1420.0	2771.8
6-6.5	465.0	465.0	55.4	0.0	985.4	930.0	465.0	103.8	0.0	1498.8	930.0	325.5	103.8	1420.0	2779.3
6.5-7	465.0	465.0	55.4	0.0	985.4	930.0	465.0	111.3	0.0	1506.3	930.0	325.5	111.3	1420.0	2786.8
7-7.5	465.0	465.0	55.4	0.0	985.4	1034.6	465.0	119.4	0.0	1618.9	1034.6	325.5	119.4	1420.0	2899.4
7.5-8	465.0	465.0	55.4	0.0	985.4	1222.9	465.0	127.4	0.0	1815.3	1222.9	325.5	127.4	1420.0	3095.8
8-8.5	465.0	465.0	55.4	0.0	985.4	1326.1	465.0	137.8	0.0	1928.9	1326.1	325.5	137.8	1420.0	3209.4
8.5-9	465.0	465.0	55.4	0.0	985.4	1395.0	465.0	145.3	0.0	2005.3	1395.0	325.5	145.3	1420.0	3285.8
9-9.5	465.0	465.0	55.4	0.0	985.4	1395.0	465.0	152.8	0.0	2012.8	1395.0	325.5	152.8	1420.0	3293.3
9.5-10	465.0	465.0	55.4	0.0	985.4	1395.0	465.0	160.3	0.0	2020.3	1395.0	325.5	160.3	1420.0	3300.8
>10	465.0	465.0	55.4	0.0	985.4	1395.0	465.0	160.3	0.0	2020.3	1395.0	325.5	160.3	1420.0	3300.8

Annex 7. Absolute vulnerability tables – Healthcare

Use: Healthcare	Flood					Flood					Flood				
	1 Floor	Code=			HF1	2_6 Floors	Code=			HF2_6	2_6 Floors	Code=			HFm6
Flow depth	Content	Structure	Clean_up	Garage	Total	Content	Structure	Clean_up	Garage	Total	Content	Structure	Clean_up	Garage	Total
0.0	0	0	0	0	0	0	0	0	0	0	0	0	0	0	0
0-0.5	156.9	9.3	2.9	0.0	169.0	117.7	0.0	2.9	0.0	120.5	117.7	0.0	2.9	0.0	120.5
0.5-1	439.4	69.8	2.9	0.0	512.0	439.4	9.3	2.9	0.0	451.5	439.4	9.3	2.9	0.0	451.5
1-1.5	523.1	186.0	14.3	0.0	723.4	523.1	32.6	14.3	0.0	570.0	523.1	32.6	14.3	0.0	570.0
1.5-2	697.5	325.5	14.3	0.0	1037.3	697.5	74.4	14.3	0.0	786.2	697.5	74.4	14.3	0.0	786.2
2-2.5	697.5	418.5	14.3	0.0	1130.3	697.5	88.4	14.3	0.0	800.1	697.5	88.4	14.3	0.0	800.1
2.5-3	697.5	441.8	14.3	0.0	1153.5	697.5	93.0	14.3	0.0	804.8	697.5	93.0	14.3	0.0	804.8
3-3.5	697.5	465.0	14.3	0.0	1176.8	697.5	97.7	14.3	0.0	809.4	697.5	97.7	14.3	0.0	809.4
3.5-4	697.5	465.0	14.3	0.0	1176.8	815.2	107.0	17.1	0.0	939.2	815.2	107.0	17.1	0.0	939.2
4-4.5	697.5	465.0	14.3	0.0	1176.8	1136.9	139.5	17.1	0.0	1293.5	1136.9	139.5	17.1	0.0	1293.5
4.5-5	697.5	465.0	14.3	0.0	1176.8	1220.6	176.7	31.4	0.0	1428.8	1220.6	176.7	31.4	0.0	1428.8
5-5.5	697.5	465.0	14.3	0.0	1176.8	1395.0	186.0	31.4	0.0	1612.4	1395.0	186.0	31.4	0.0	1612.4
5.5-6	697.5	465.0	14.3	0.0	1176.8	1395.0	186.0	31.4	0.0	1612.4	1395.0	186.0	31.4	0.0	1612.4
6-6.5	697.5	465.0	14.3	0.0	1176.8	1395.0	186.0	31.4	0.0	1612.4	1395.0	186.0	31.4	0.0	1612.4
6.5-7	697.5	465.0	14.3	0.0	1176.8	1395.0	186.0	31.4	0.0	1612.4	1395.0	186.0	31.4	0.0	1612.4
7-7.5	697.5	465.0	14.3	0.0	1176.8	1512.7	186.0	34.3	0.0	1732.9	1512.7	186.0	34.3	0.0	1732.9
7.5-8	697.5	465.0	14.3	0.0	1176.8	1834.4	186.0	37.1	0.0	2057.5	1834.4	186.0	37.1	0.0	2057.5
8-8.5	697.5	465.0	14.3	0.0	1176.8	1918.1	186.0	51.4	0.0	2155.6	1918.1	186.0	51.4	0.0	2155.6
8.5-9	697.5	465.0	14.3	0.0	1176.8	2092.5	186.0	51.4	0.0	2329.9	2092.5	186.0	51.4	0.0	2329.9
9-9.5	697.5	465.0	14.3	0.0	1176.8	2092.5	186.0	51.4	0.0	2329.9	2092.5	186.0	51.4	0.0	2329.9
9.5-10	697.5	465.0	14.3	0.0	1176.8	2092.5	186.0	51.4	0.0	2329.9	2092.5	186.0	51.4	0.0	2329.9
>10	697.5	465.0	14.3	0.0	1176.8	2092.5	186.0	51.4	0.0	2329.9	2092.5	186.0	51.4	0.0	2329.9

Use: Healthcare	Debris Flow					Debris Flow					Debris Flow				
	1 Floor	Code=			HF1	2_6 Floors	Code=			H2_6	FM6	Code=			HFm6
Flow depth	Content	Structure	Clean_up	Garage	Total	Content	Structure	Clean_up	Garage	Total	Content	Structure	Clean_up	Garage	Total
0.0	0	0	0	0	0	0.00	0	0	0	0	0	0	0	0	0
0-0.5	117.7	46.5	10.9	0.0	175.1	117.66	32.6	10.9	0.0	161.1	117.7	32.6	10.9	0.0	161.1
0.5-1	439.4	186.0	18.4	0.0	643.8	439.37	130.2	18.4	0.0	588.0	439.4	130.2	18.4	0.0	588.0
1-1.5	523.1	279.0	39.6	0.0	841.8	523.13	195.3	39.6	0.0	758.1	523.1	195.3	39.6	0.0	758.1
1.5-2	697.5	395.3	47.1	0.0	1139.9	697.50	276.7	47.1	0.0	1021.3	697.5	276.7	47.1	0.0	1021.3
2-2.5	697.5	418.5	54.6	0.0	1170.6	697.50	293.0	54.6	0.0	1045.1	697.5	293.0	54.6	0.0	1045.1
2.5-3	697.5	465.0	62.1	0.0	1224.6	697.50	325.5	62.1	0.0	1085.1	697.5	325.5	62.1	0.0	1085.1
3-3.5	697.5	465.0	69.6	0.0	1232.1	697.50	325.5	69.6	0.0	1092.6	697.5	325.5	69.6	0.0	1092.6
3.5-4	697.5	465.0	69.6	0.0	1232.1	815.16	325.5	77.7	0.0	1218.4	815.2	325.5	77.7	0.0	1218.4
4-4.5	697.5	465.0	69.6	0.0	1232.1	1136.87	325.5	85.2	0.0	1547.6	1136.9	325.5	85.2	0.0	1547.6
4.5-5	697.5	465.0	69.6	0.0	1232.1	1220.63	325.5	95.6	0.0	1641.7	1220.6	325.5	95.6	0.0	1641.7
5-5.5	697.5	465.0	69.6	0.0	1232.1	1395.00	325.5	103.1	0.0	1823.6	1395.0	325.5	103.1	0.0	1823.6
5.5-6	697.5	465.0	69.6	0.0	1232.1	1395.00	325.5	110.6	0.0	1831.1	1395.0	325.5	110.6	0.0	1831.1
6-6.5	697.5	465.0	69.6	0.0	1232.1	1395.00	325.5	118.1	0.0	1838.6	1395.0	325.5	118.1	0.0	1838.6
6.5-7	697.5	465.0	69.6	0.0	1232.1	1395.00	325.5	125.6	0.0	1846.1	1395.0	325.5	125.6	0.0	1846.1
7-7.5	697.5	465.0	69.6	0.0	1232.1	1512.66	325.5	133.6	0.0	1971.8	1512.7	325.5	133.6	0.0	1971.8
7.5-8	697.5	465.0	69.6	0.0	1232.1	1834.37	325.5	141.7	0.0	2301.6	1834.4	325.5	141.7	0.0	2301.6
8-8.5	697.5	465.0	69.6	0.0	1232.1	1918.13	325.5	152.1	0.0	2395.7	1918.1	325.5	152.1	0.0	2395.7
8.5-9	697.5	465.0	69.6	0.0	1232.1	2092.50	325.5	159.6	0.0	2577.6	2092.5	325.5	159.6	0.0	2577.6
9-9.5	697.5	465.0	69.6	0.0	1232.1	2092.50	325.5	167.1	0.0	2585.1	2092.5	325.5	167.1	0.0	2585.1
9.5-10	697.5	465.0	69.6	0.0	1232.1	2092.50	325.5	174.6	0.0	2592.6	2092.5	325.5	174.6	0.0	2592.6
>10	697.5	465.0	69.6	0.0	1232.1	2092.50	325.5	174.6	0.0	2592.6	2092.5	325.5	174.6	0.0	2592.6

Annex 7. Absolute vulnerability tables – Industry

Use:	Flood					Flood					Flood				
Industry	1 Floor	Code=			IF1	2_6 Floors	Code=			IF2_6	FM6	Code=			IFm6
Flow depth	Content	Structure	Clean_up	Garage	Total	Content	Structure	Clean_up	Garage	Total	Content	Structure	Clean_up	Garage	Total
0.0	0	0	0	0	0	0.0	0.0	0.0	0.0	0.0	0.0	0	0	0	0
0-0.5	146.8	8.7	0.6	0.0	156.0	69.3	0.0	0.6	0.0	69.9	69.3	0.0	0.6	0.0	69.9
0.5-1	411.0	65.3	0.6	0.0	476.9	308.3	21.8	0.6	0.0	330.6	308.3	8.7	0.6	0.0	317.5
1-1.5	489.4	174.0	2.9	0.0	666.2	489.4	65.3	2.9	0.0	557.5	489.4	30.5	2.9	0.0	522.7
1.5-2	652.5	304.5	2.9	0.0	959.9	652.5	108.8	2.9	0.0	764.1	652.5	69.6	2.9	0.0	725.0
2-2.5	652.5	391.5	2.9	0.0	1046.9	652.5	130.5	2.9	0.0	785.9	652.5	82.7	2.9	0.0	738.0
2.5-3	652.5	413.3	2.9	0.0	1068.6	652.5	143.6	2.9	0.0	798.9	652.5	87.0	2.9	0.0	742.4
3-3.5	652.5	435.0	2.9	0.0	1090.4	652.5	152.3	2.9	0.0	807.6	652.5	91.4	2.9	0.0	746.7
3.5-4	652.5	435.0	2.9	0.0	1090.4	721.8	178.4	3.4	0.0	903.6	721.8	100.1	3.4	0.0	825.3
4-4.5	652.5	435.0	2.9	0.0	1090.4	960.8	221.9	3.4	0.0	1186.1	960.8	130.5	3.4	0.0	1094.7
4.5-5	652.5	435.0	2.9	0.0	1090.4	1141.9	261.0	6.3	0.0	1409.2	1141.9	165.3	6.3	0.0	1313.5
5-5.5	652.5	435.0	2.9	0.0	1090.4	1305.0	287.1	6.3	0.0	1598.4	1305.0	174.0	6.3	0.0	1485.3
5.5-6	652.5	435.0	2.9	0.0	1090.4	1305.0	304.5	6.3	0.0	1615.8	1305.0	174.0	6.3	0.0	1485.3
6-6.5	652.5	435.0	2.9	0.0	1090.4	1305.0	348.0	6.3	0.0	1659.3	1305.0	174.0	6.3	0.0	1485.3
6.5-7	652.5	435.0	2.9	0.0	1090.4	1305.0	391.5	6.3	0.0	1702.8	1305.0	174.0	6.3	0.0	1485.3
7-7.5	652.5	435.0	2.9	0.0	1090.4	1374.4	435.0	6.9	0.0	1816.2	1374.4	174.0	6.9	0.0	1555.2
7.5-8	652.5	435.0	2.9	0.0	1090.4	1613.3	435.0	7.4	0.0	2055.7	1613.3	174.0	7.4	0.0	1794.7
8-8.5	652.5	435.0	2.9	0.0	1090.4	1794.4	435.0	10.3	0.0	2239.7	1794.4	174.0	10.3	0.0	1978.7
8.5-9	652.5	435.0	2.9	0.0	1090.4	1957.5	435.0	10.3	0.0	2402.8	1957.5	174.0	10.3	0.0	2141.8
9-9.5	652.5	435.0	2.9	0.0	1090.4	1957.5	435.0	10.3	0.0	2402.8	1957.5	174.0	10.3	0.0	2141.8
9.5-10	652.5	435.0	2.9	0.0	1090.4	1957.5	435.0	10.3	0.0	2402.8	1957.5	174.0	10.3	0.0	2141.8
>10	652.5	435.0	2.9	0.0	1090.4	1957.5	435.0	10.3	0.0	2402.8	1957.5	174.0	10.3	0.0	2141.8

Use:	Debris Flow					Debris Flow					Debris Flow				
Industry	1 Floor	Structure	Clean_up	Garage	IF1	2_6 Floors	Structure	Clean_up	Garage	IF2_6	FM6	Structure	Clean_up	Garage	IFm6
Flow depth	Content	Structure	Clean_up	Garage	Total	Content	Structure	Clean_up	Garage	Total	Content	Structure	Clean_up	Garage	Total
0.0	0	0	0	0	0	0	0	0	0	0	0	0	0	0	0
0-0.5	69.3	43.5	8.1	0.0	120.9	69.3	43.5	8.1	0.0	120.9	69.3	30.5	8.1	0.0	107.9
0.5-1	308.3	174.0	15.6	0.0	497.8	308.3	174.0	15.6	0.0	497.8	308.3	121.8	15.6	0.0	445.6
1-1.5	489.4	261.0	25.4	0.0	775.7	489.3	261.0	25.4	0.0	775.7	489.4	182.7	25.4	0.0	697.4
1.5-2	652.5	369.8	32.9	0.0	1055.1	652.5	369.8	32.9	0.0	1055.1	652.5	258.8	32.9	0.0	944.2
2-2.5	652.5	391.5	40.4	0.0	1084.4	652.5	391.5	40.4	0.0	1084.4	652.5	274.1	40.4	0.0	966.9
2.5-3	652.5	435.0	47.9	0.0	1135.4	652.5	435.0	47.9	0.0	1135.4	652.5	304.5	47.9	0.0	1004.9
3-3.5	652.5	435.0	55.4	0.0	1142.9	652.5	435.0	55.4	0.0	1142.9	652.5	304.5	55.4	0.0	1012.4
3.5-4	652.5	435.0	55.4	0.0	1142.9	721.8	435.0	63.4	0.0	1220.3	721.8	304.5	63.4	0.0	1089.8
4-4.5	652.5	435.0	55.4	0.0	1142.9	960.7	435.0	70.9	0.0	1466.7	960.8	304.5	70.9	0.0	1336.2
4.5-5	652.5	435.0	55.4	0.0	1142.9	1141.9	435.0	81.3	0.0	1658.2	1141.9	304.5	81.3	0.0	1527.7
5-5.5	652.5	435.0	55.4	0.0	1142.9	1305.0	435.0	88.8	0.0	1828.8	1305.0	304.5	88.8	0.0	1698.3
5.5-6	652.5	435.0	55.4	0.0	1142.9	1305.0	435.0	96.3	0.0	1836.3	1305.0	304.5	96.3	0.0	1705.8
6-6.5	652.5	435.0	55.4	0.0	1142.9	1305.0	435.0	103.8	0.0	1843.8	1305.0	304.5	103.8	0.0	1713.3
6.5-7	652.5	435.0	55.4	0.0	1142.9	1305.0	435.0	111.3	0.0	1851.3	1305.0	304.5	111.3	0.0	1720.8
7-7.5	652.5	435.0	55.4	0.0	1142.9	1374.3	435.0	119.4	0.0	1928.7	1374.4	304.5	119.4	0.0	1798.2
7.5-8	652.5	435.0	55.4	0.0	1142.9	1613.3	435.0	127.4	0.0	2175.7	1613.3	304.5	127.4	0.0	2045.2
8-8.5	652.5	435.0	55.4	0.0	1142.9	1794.4	435.0	137.8	0.0	2367.2	1794.4	304.5	137.8	0.0	2236.7
8.5-9	652.5	435.0	55.4	0.0	1142.9	1957.5	435.0	145.3	0.0	2537.8	1957.5	304.5	145.3	0.0	2407.3
9-9.5	652.5	435.0	55.4	0.0	1142.9	1957.5	435.0	152.8	0.0	2545.3	1957.5	304.5	152.8	0.0	2414.8
9.5-10	652.5	435.0	55.4	0.0	1142.9	1957.5	435.0	160.3	0.0	2552.8	1957.5	304.5	160.3	0.0	2422.3
>10	652.5	435.0	55.4	0.0	1142.9	1957.5	435.0	160.3	0.0	2552.8	1957.5	304.5	160.3	0.0	2422.3

Annex 8. ILWIS Script for loss calculation in the Ayura catchment

```

/////////////////////////////////////////////////////////////////
//SCRIPT FOR CALCULATING EXPOSURE, VULNERABILITY AND LOSSES.
/////////////////////////////////////////////////////////////////
//THIS SCRIPT IS ONLY FOR BUILDING FOOTPRINTS AS ELEMENTS-AT_RISK
//THE SCRIPT USES THE FOLLOWING VARIABLES
//%1 = Hazard Type (e.g. FL, DF, LS)
//%2 = Intensity measure (e.g. DE, IP)
//%3 = Return period (e.g. 020)
//%4 = Future Year (2018,2050)
//%5 = Risk reduction alternative (A0, A1, A2,A3)
//%6 = Scenario (S1, S2, S3, S4)
//%7 = Physical Risk (PH)

//First rasterize the element-at-risk map
//BU_%4_%5_%6.mpr := MapRasterizePolygon(BU_%4_%5_%6.mpa,Ayura.grf)

//Delete the cross table if it is already there
Del CTemp.* -force
Del RTemp.* -force
Crtbl RTemp BU_%4

//Then overlay the element at risk map with the hazard intensity map
TabCalc Ctemp.tbt := TableCross(BU_%4_%5_%6, %1_%2_%3_%5_%6, IgnoreUndefs)

//Make sure the cross table is calculated
Calc CTemp.tbt

//We now calculate the average flood depth per building and store results in a table starting with R_
Tabcalc RTemp.tbt Depth:=ColumnJoinAVG(CTemp.tbt,%1_%2_%3_%5_%6,BU_%4_%5_%6,1)

//Classify the results.
TabCalc RTemp.tbt DepthCL:=CLFY(Depth,FL_DE_T)

//We need to know the area of the building footprint
TabCalc RTemp.tbt Area:= ColumnJoin(BU_%4_%5_%6.tbt,Area)

//We the also read in Building types
TabCalc RTemp.tbt Type := ColumnJoin(BU_%4_%5_%6.tbt,New_Type)

//Now we start bringing in the vulnerability values for the building contents.

TabCalc RTemp.tbt RF1 := ColumnJoin(VULN_%1_%2_BU_%5.tbt,RF1, DepthCL )
TabCalc RTemp.tbt RF2_6 := ColumnJoin(VULN_%1_%2_BU_%5.tbt,RF2_6, DepthCL )
TabCalc RTemp.tbt RFm6 := ColumnJoin(VULN_%1_%2_BU_%5.tbt,RFm6, DepthCL )

```

```

TabCalc RTemp.tbt CF1 := ColumnJoin(VULN_%1_%2_BU_%5.tbt,CF1, DepthCL )
TabCalc RTemp.tbt CF2_6 := ColumnJoin(VULN_%1_%2_BU_%5.tbt,CF2_6, DepthCL )
TabCalc RTemp.tbt CFm6 := ColumnJoin(VULN_%1_%2_BU_%5.tbt,CFm6, DepthCL )

TabCalc RTemp.tbt IF1 := ColumnJoin(VULN_%1_%2_BU_%5.tbt,IF1, DepthCL )
TabCalc RTemp.tbt IF2_6 := ColumnJoin(VULN_%1_%2_BU_%5.tbt,IF2_6, DepthCL )
TabCalc RTemp.tbt IFm6 := ColumnJoin(VULN_%1_%2_BU_%5.tbt,IFm6, DepthCL )

TabCalc RTemp.tbt EF1 := ColumnJoin(VULN_%1_%2_BU_%5.tbt,EF1, DepthCL )
TabCalc RTemp.tbt EF2_6 := ColumnJoin(VULN_%1_%2_BU_%5.tbt,EF2_6, DepthCL )
TabCalc RTemp.tbt EFm6 := ColumnJoin(VULN_%1_%2_BU_%5.tbt,EFm6, DepthCL )

TabCalc RTemp.tbt HF1 := ColumnJoin(VULN_%1_%2_BU_%5.tbt,HF1, DepthCL )
TabCalc RTemp.tbt HF2_6 := ColumnJoin(VULN_%1_%2_BU_%5.tbt,HF2_6, DepthCL )
TabCalc RTemp.tbt HFm6 := ColumnJoin(VULN_%1_%2_BU_%5.tbt,HFm6, DepthCL )

TabCalc RTemp.tbt VULN1 :=
iff(Type="RF1",RF1,iff(Type="CF1",CF1,Iff(type="IF1",IF1,iff(Type="HF1",HF1,iff(Type="EF1",EF1
,0))))))
TabCalc RTemp.tbt VULN2 :=
iff(Type="RF2_6",RF2_6,iff(Type="CF2_6",CF2_6,Iff(type="IF2_6",IF2_6,iff(Type="HF2_6",HF2_6,if
f(Type="EF2_6",EF2_6,0))))))
TabCalc RTemp.tbt VULN3 :=
iff(Type="RFm6",RFm6,iff(Type="CFm6",CFm6,Iff(type="IFm6",IFm6,iff(Type="HFm6",HFm6,iff(T
ype="EFm6",EFm6,0))))))
TabCalc RTemp.tbt VULNERABILITY := Max(VULN1,VULN2,VULN3)

//Calculating Loss
TabCalc RTemp.tbt LOSS_%1_%3_%4_%5_%6_%7 {dom=value; vr=0: 1000000000 :1} :=
VULNERABILITY*Area

//Aggregate loss for the buildings and put the results in the table Results_BU_%4
TabCalc Results_BU_%4.tbt %1_%3_%4_%5_%6_%7:= ColumnJoin(RTemp.tbt,
LOSS_%1_%3_%4_%5_%6_%7)

//Aggregate loss for the administrative Units and put the results in the Table Results_Admin_units
TabCalc Results_Admin_units.tbt %1_%3_%4_%5_%6_%7:= ColumnJoinSum(Results_BU_%4.tbt,
%1_%3_%4_%5_%6_%7,Admin_Units,1)

//Deleting the intermediate files
//Del RTemp*.* -force
//Del CTemp*.* -force

//Message The calculation of the %7 losses for the combination of hazard type %1 , Return Period %3,
Possible scenario %6, Future year %4 and risk Reduction Alternative %5 is finished.

```

Annex 9. ILWIS Script to calculate the risk (Area under the risk curve)

```

////////////////////////////////////
//SCRIPT FOR RISK CALCULATION
////////////////////////////////////

//parameters
//%1 = Year
//%2 = Alternativer
//%3 = Scenario
//%4 = First return period
//%5 = Second return period
//%6 = Third return period
//%7 = Fourth return period

//We assume that flooding and debrisflows are depending on the same trigger, so we take the maximum
//First we calculate the losses per administrative unit taken into account the interdependency of the hazard

TabCalc Results_Admin_Units Loss_%1_%2_%3_25:=Max(FL_25_%1_%2_%3_PH,DF_25_%1_%2_%3_PH)
TabCalc Results_Admin_Units Loss_%1_%2_%3_50:=Max(FL_50_%1_%2_%3_PH,DF_50_%1_%2_%3_PH)
TabCalc Results_Admin_Units
Loss_%1_%2_%3_100:=Max(FL_100_%1_%2_%3_PH,DF_100_%1_%2_%3_PH)
TabCalc Results_Admin_Units
Loss_%1_%2_%3_200:=Max(FL_200_%1_%2_%3_PH,DF_200_%1_%2_%3_PH)

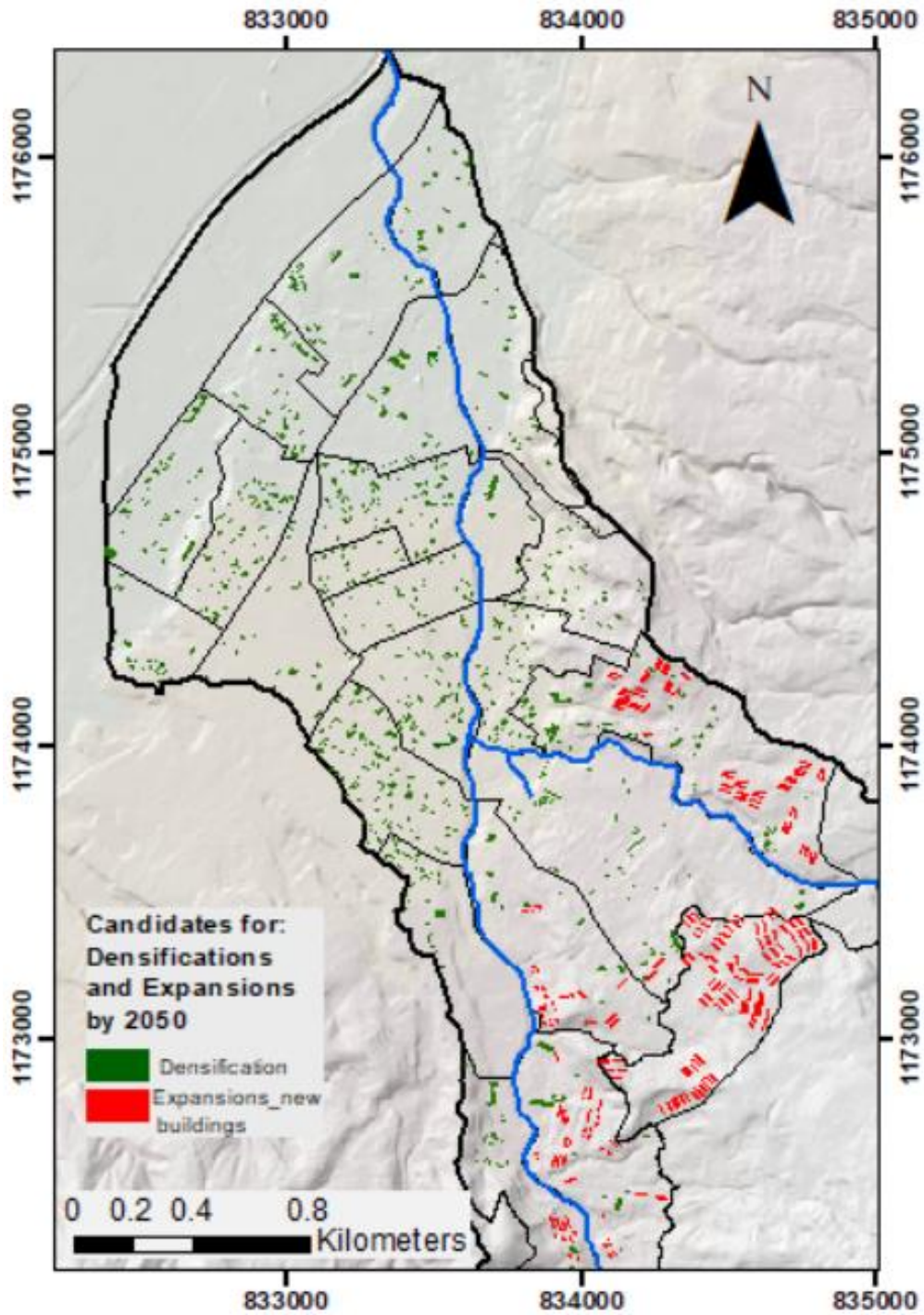
//then we sum up all the losses for the entire area
TabCalc Risk_results
Loss_%1_%2_%3_25:=ColumnJoinSum(Results_Admin_Units.tbt,Loss_%1_%2_%3_25,admin_units,1)
TabCalc Risk_results
Loss_%1_%2_%3_50:=ColumnJoinSum(Results_Admin_Units.tbt,Loss_%1_%2_%3_50,admin_units,1)
TabCalc Risk_results
Loss_%1_%2_%3_100:=ColumnJoinSum(Results_Admin_Units.tbt,Loss_%1_%2_%3_100,admin_units,1)
TabCalc Risk_results
Loss_%1_%2_%3_200:=ColumnJoinSum(Results_Admin_Units.tbt,Loss_%1_%2_%3_200,admin_units,1)

//Then we calculate the annualized risk
TabCalc Risk_results AR_%1_%2_%3:=Loss_%1_%2_%3_200*(1/%7)+(((1/%6)-
(1/%7))*(Loss_%1_%2_%3_200+Loss_%1_%2_%3_100)/2)+(((1/%5)-(1/%6))*(Loss_%1_%2_%3_100+
Loss_%1_%2_%3_50)/2)+(((1/%4)-(1/%5))*(Loss_%1_%2_%3_50+ Loss_%1_%2_%3_25)/2)

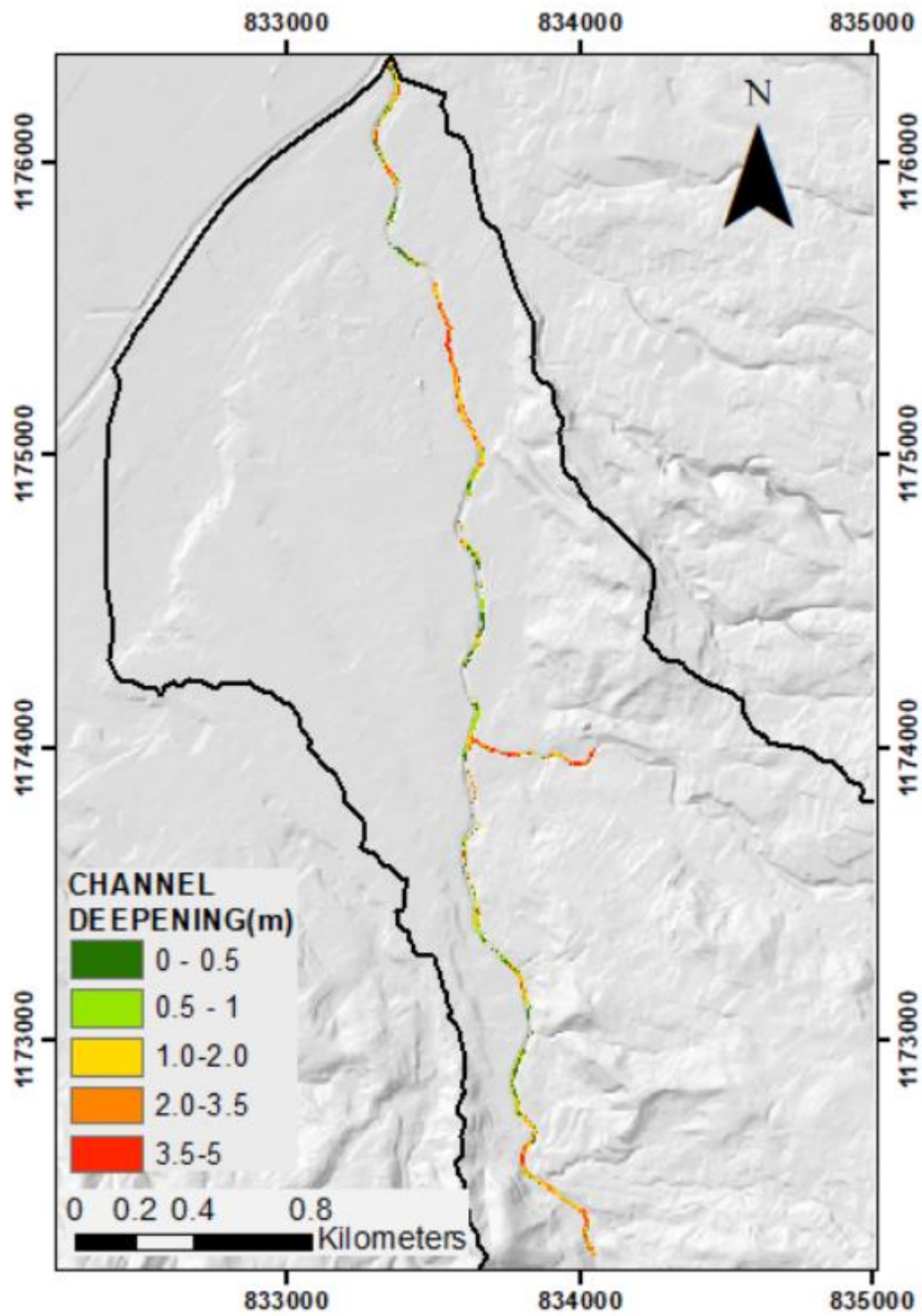
//we delete the three loss columns again
delcol Risk_results.tbt.Loss_%1_%2_%3_25
delcol Risk_results.tbt.Loss_%1_%2_%3_50
delcol Risk_results.tbt.Loss_%1_%2_%3_100
delcol Risk_results.tbt.Loss_%1_%2_%3_200

```

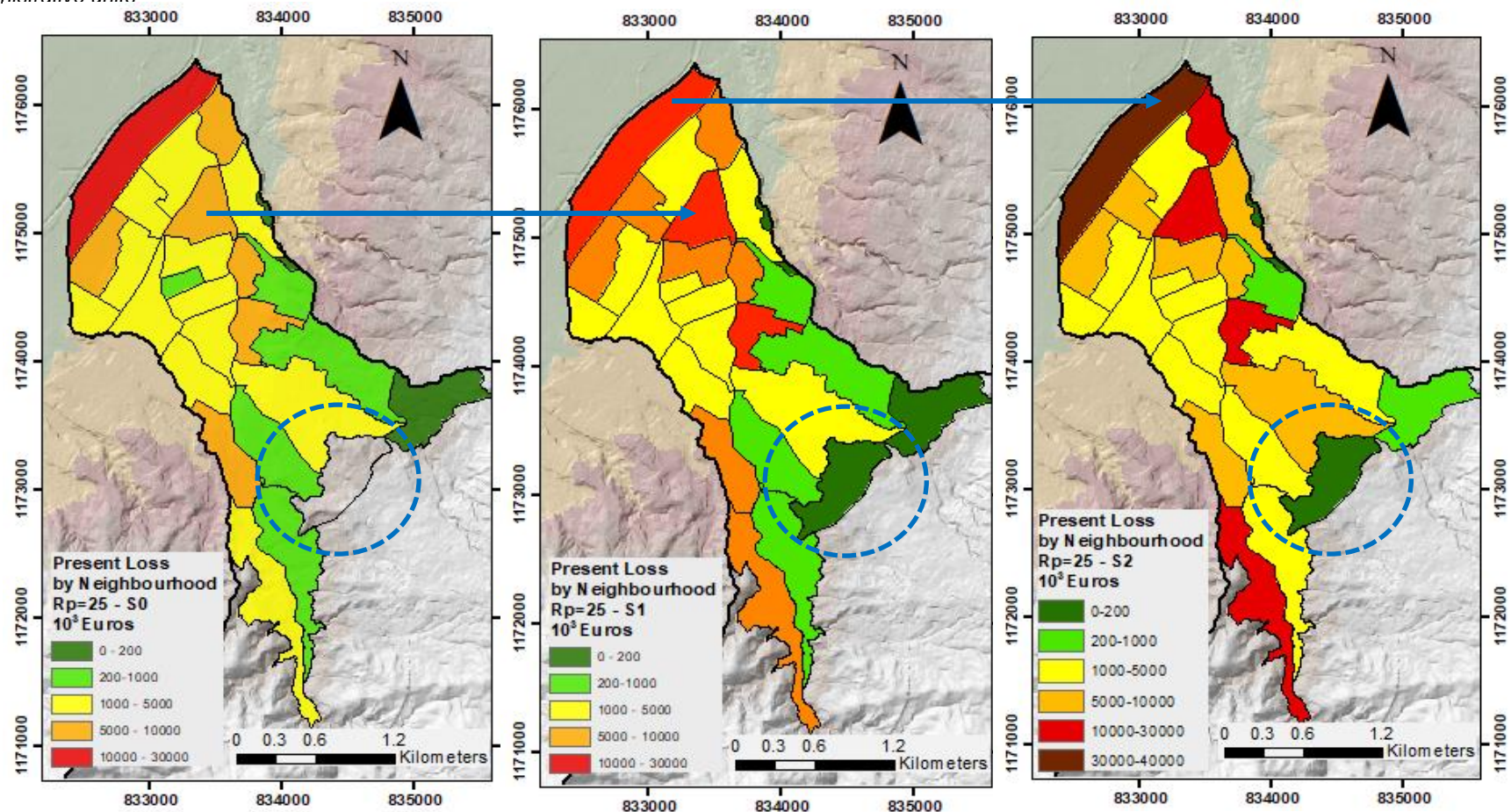
Annex 10. Map indicating possible areas that have changed for scenario 1, including densification area and urban expansion areas.



Annex 11. Map indicating the channel intervention



Annex 12. Maps indicating changes in losses between scenarios (S0, S1, S2) for the occurrence of multi-hazards in the return period of 25 years and aggregated by administrative units



In the maps, the changes in losses per neighbourhood can be noticed in examples as shown by the blue arrows. As mentioned in the research S0(2018) and S1(2050) are affected by the same hazard intensity (because climate change does not take place in S1) but differentiate in the number of elements at risk. One example of this is the creation of a new neighbourhood for the necessity of the construction of new buildings. On the other side is S2 which has increases in the EaR and in hazard for the influence of climate change.

Annex 13. Cost-Benefit Analysis

Maximum investment for the implementation of alternatives

To assess the efficiency of the planning alternatives in the AC, the approach used was the known cost-benefit analysis (CBA). According to Newman et al., (2014) and CHARIM (2014), the CBA allows comparing the cost of the implementation of structural measures with the benefits they provide (risk reduction) taking into account the variation of risk time. The aim of applying this method was to evaluate the economic feasibility of the implementation of the proposed alternatives.

For this work, not all the alternatives were evaluated with CBA but only those ones that provided the highest risk reduction (see section 7.4) and under the most critical scenario (S2-Climate change). In this way, the alternative with the highest net present value (NPV) and with an internal rate of return (IRR) above the 12% was considered as the most suitable in economic terms to be undertaken. The reason to select the 12% as minimum IRR was based on Bonzanigo & Kalra (2014) who mention that this rate is usually used as a reference by the World Bank.

On the other hand, owing to it was not possible to calculate the detailed investment that would require the execution of the alternatives, an alternative approach was taken. The investment required to produce the desired NPV and IRR indicators was found by a trial and error procedure. As a conclusion, the investment stood for the maximum expense to guarantee the feasibility of the project.

CBA for combined alternatives (A1, A2, A3)

A realistic investment scenario was tried to be achieved in a trial and error procedure. This was based on:

- 1) The investments for channel intervention (A1) and for solid retention systems (A2) can be done in 2 years starting from 2019. This was considered a reasonable time to develop the adequations and constructions works. Additionally, it was considered that each alternative would require approximately 33.3% of the investment and maintenance was included. Also, the risk reduction starts once the measures are completed.
- 2) For flood gates, it was assumed that the adequations and constructions would be done each 5 years. This was selected because it was assumed that the most probable scenario would be the progressive construction of new high-rise buildings through the years and according to the demand of the new population.

Year	ALL(A)			Investment	Risk reduction	Incr. Benefit	Variation of Risk reduction	NPV	Interest
	COST A1	COST A2	COST A3						
1				0	0		0	€ 16,362,317.52	5%
2	€ 3,500,000.00	€ 3,400,000.00		€ 6,900,000.00	€ -	€ 6,900,000.00	2019	€ 2,633,695.33	10%
3	€ 3,500,000.00	€ 3,400,000.00	€ 1,750,000.00	€ 8,650,000.00	€ -	€ 8,650,000.00	2020	€ -4,257,439.13	20%
4				€ -	€ 1,874,613.53	€ 1,874,613.53	2021	IRR	12.1%
5				€ -	€ 1,929,803.79	€ 1,929,803.79	2022		
6				€ -	€ 1,984,994.05	€ 1,984,994.05	2023		
7				€ -	€ 2,040,184.30	€ 2,040,184.30	2024		
8			€ 1,750,000.00	€ 1,750,000.00	€ 2,095,374.56	€ 345,374.56	2025		
9				€ -	€ 2,150,564.82	€ 2,150,564.82	2026		
10				€ -	€ 2,205,755.08	€ 2,205,755.08	2027		
11				€ -	€ 2,260,945.33	€ 2,260,945.33	2028		
12				€ -	€ 2,316,135.59	€ 2,316,135.59	2029		
13			€ 1,750,000.00	€ 1,750,000.00	€ 2,371,325.85	€ 621,325.85	2030		
14				€ -	€ 2,426,516.11	€ 2,426,516.11	2031		
15				€ -	€ 2,481,706.36	€ 2,481,706.36	2032		
16				€ -	€ 2,536,896.62	€ 2,536,896.62	2033		
17				€ -	€ 2,592,086.88	€ 2,592,086.88	2034		
18			€ 1,750,000.00	€ 1,750,000.00	€ 2,647,277.14	€ 897,277.14	2035		
19				€ -	€ 2,702,467.39	€ 2,702,467.39	2036		
20				€ -	€ 2,757,657.65	€ 2,757,657.65	2037		
21				€ -	€ 2,812,847.91	€ 2,812,847.91	2038		
22				€ -	€ 2,868,038.17	€ 2,868,038.17	2039		
23				€ -	€ 2,923,228.42	€ 2,923,228.42	2040		
24				€ -	€ 2,978,418.68	€ 2,978,418.68	2041		
25				€ -	€ 3,033,608.94	€ 3,033,608.94	2042		
26				€ -	€ 3,088,799.20	€ 3,088,799.20	2043		
27				€ -	€ 3,143,989.45	€ 3,143,989.45	2044		
28				€ -	€ 3,199,179.71	€ 3,199,179.71	2045		
29				€ -	€ 3,254,369.97	€ 3,254,369.97	2046		
30				€ -	€ 3,309,560.23	€ 3,309,560.23	2047		
31				€ -	€ 3,364,750.48	€ 3,364,750.48	2048		
32				€ -	€ 3,419,940.74	€ 3,419,940.74	2049		
33				€ -	€ 3,475,131.00	€ 3,475,131.00	2050		
Total Investment				€ 20,800,000.00					

Table A-13 Cost-benefit analysis of the combination of alternatives (A1+A2+A3)

As result, it was obtained that the maximum probable investment required to maintain the profitability of the project was 20.8 million euros. The calculation is shown in the following table:

As can be seen in the tables above, the project is profitable even under the investment estimated and even interest rates of 10%.

CBA for consequence reduction or intervention of the vulnerability(A3)

By applying the same investment for the alternative A3, as shown in and **Table A-13** and considering the specific risk reduction for the scenario S2(climate change +population growth), the results of applying the CBA were:

NPV	Interest
€ 28,581,300.35	5%
€ 14,919,196.68	10%
€ 4,598,244.29	20%
IRR	107.18%

As it can be noticed, the NPV and IRR indicate that the investment in alternative 3 is highly profitable for the municipality.

CBA for hazard reduction

To check the economic suitability of the alternatives for hazard reduction (A1+A2). The investment program already exposed was used with the risk reduction produced by the implementation of both measures. In this way, from the application of CBA analysis it was obtained:

NPV	Interest
€ 7,423,388.07	5%
-€ 1,387,562.30	10%
-€ 5,405,773.84	20%
IRR	8.8%

In conclusion, only the application of hazard reduction alternatives under the investment program proposed was not economically profitable.

In the light of the results if the CBA and risk reduction were taken into account the best planning alternative would be A3. However, the fact that the hazard measures did not perform well in the present research does not imply that the alternative A3 will be necessarily selected. Before other criteria need to be taken into account as the acceptance of the alternative A3, the proposal of new alternatives proposed by stakeholders,

the technical feasibility, etc. All these criteria need to be taken inside SDSS to perform a multicriteria evaluation.